FINAL REPORT

Abiotic Reductive Dechlorination of Tetrachloroethylene and Trichloroethylene in Anaerobic Environments

SERDP Project ER-1368

JANUARY 2009

Elizabeth Butler
Yiran Dong
Xiaoming Liang
School of Civil Engineering and Environmental Science

Tomasz Kuder
R. Paul Philp
School of Geology and Geophysics

Lee R. Krumholz
Department of Botany and Microbiology

This document has been approved for public release.

DoD EPA DOE SERDP
Strategic Environmental Research and Development Program

This report was prepared under contract to the Department of Defense Strategic Environmental Research and Development Program (SERDP). The publication of this report does not indicate endorsement by the Department of Defense, nor should the contents be construed as reflecting the official policy or position of the Department of Defense. Reference herein to any specific commercial product, process, or service by trade name, trademark, manufacturer, or otherwise, does not necessarily constitute or imply its endorsement, recommendation, or favoring by the Department of Defense.

Final Technical Report

Abiotic Reductive Dechlorination of Tetrachloroethylene and Trichloroethylene in Anaerobic Environments

ER-1368

Performing Organization: University of Oklahoma

Lead Principal Investigator: Elizabeth C. Butler
Co-Principal Investigators: Lee R. Krumholz and R. Paul Philp

Report Authors

Elizabeth Butler[1], Yiran Dong[1], Xiaoming Liang[1], Tomasz Kuder[2], Lee R. Krumholz[3], and R. Paul Philp[2]

University of Oklahoma

January 15, 2009

[1] School of Civil Engineering and Environmental Science
[2] School of Geology and Geophysics
[3] Department of Botany and Microbiology

Table of Contents

Section	Page
List of Acronyms	iv
List of Figures and Tables	v
Acknowledgments	viii
Executive Summary	1
Objective	3
Background	4
Materials and Methods	7
Quantification of Reactants and Products	8
Isotope Measurements	9
Task 1 Details	10
Experiments with Minerals	10
Treatment of Kinetic Data	10
Experiments with Pure and Mixed Cultures	11
Task 2 and 3 Details	11
Microcosm Setup	11
Geochemical Analysis	14
Calculation of Total Concentrations	15
Calculation of Observed Product Recoveries	16
Correction of Rate Constants for Partitioning among the Gas, Aqueous, and Solid Phases	17
Results and Accomplishments	18
Distinguishing Abiotic and Biotic Transformation by Stable Carbon	

Isotope Fractionation (Task 1) 18

Abiotic Reductive Dechlorination and Isotope Fractionation 18

Biotic Reductive Dechlorination and Isotope Fractionation 19

Comparison of Abiotic Versus Biotic Microcosms 20

Measurement of Kinetic and Isotope Parameters for Other Reactive Minerals 22

Correlation of Geochemical Parameters with Abiotic Reductive Dechlorination; Validation at DoD Field Sites (Tasks 2 and 3) 25

Relative Importance of Abiotic and Biotic Reductive Dechlorination 25

Isotope Fractionation during Reductive Dechlorination 27

Influence of Geochemical Parameters on Abiotic Reductive Dechlorination 26

Conclusions 30

References 32

Tables 40

Figures 47

Appendix 62

List of Acronyms

AAFB	Altus Air Force Base
$AKIE_C$	apparent kinetic isotope effect for carbon
BB1	*Desulfuromonas michiganensis strain* BB1
BDI	BioDechlor INOCULUM
CEES	School of Civil Engineering and Environmental Science, University of Oklahoma
CHES	N-cyclohexylaminoethanesulfonic acid
CrES	chromium extractable sulfur
DCE	dichloroethylene
DoD	Department of Defense
DP	Duck Pond
ε_{bulk}	bulk enrichment factor
ECD	electron capture detector
ESTCP	Environmental Security Technology Certification Program
FID	flame ionization detector
GC	gas chromatography
GCIRMS	gas chromatography isotope ratio mass spectrometry
GR-Cl	chloride green rust
$GR\text{-}SO_4$	sulfate green rust
HEPES	N-(2-hydroxyethyl)-piperazine-N'-3-propanesulfonic acid
IR	iron reducing
KIE_C	kinetic isotope effect for carbon
L	Norman Landfill
NOM	natural organic matter
OU	University of Oklahoma
PCE	tetrachloroethylene
PT	purge and trap
SEM	scanning electron microscopy
SERDP	Strategic Environmental Research and Development Plan
Sm	*Sulfurospirillum multivorans*
SR	sulfate reducing
TAPS	[(2-Hydroxy-1,1-bis(hydroxymethyl)ethyl)amino]-1-propanesulfonic acid
TCE	trichloroethylene
TOC	total organic carbon
USEPA	United States Environmental Protection Agency
VC	vinyl chloride
XRD	x-ray diffraction

List of Figures

Title	Page
Figure 1. Pathways for Reductive Dechlorination of PCE and TCE.	47
Figure 2. SEM Photomicrographs of Sediment from Sample DP-SR-pH 8.2. Cells Attached to the Surface of the Minerals are Indicated by Arrows. Crystalline Mineral Precipitates are Visible on the Right Side of Panel (b).	48
Figure 3. Normalized Concentrations of PCE and Reaction Products in Live AAFB Microcosms. Reactants and Products were Normalized by Dividing the Concentration at Any Time by the Concentration of the Reactant at Time Zero. The Insets Show Reaction Products with Low Concentrations. Error Bars are Standard Deviations of Triplicate Microcosms.	49
Figure 4. Abiotic Reductive Degradation of PCE and TCE in the Presence of FeS at Different pH Values. Lines Represent a Pseudo First-order Model Fit.	50
Figure 5. Isotope Fractionation During the Reductive Dechlorination of PCE and TCE by Abiotic and Biotic Microcosms. Lines Represent a Rayleigh Model Fit.	51
Figure 6. Microbial Reductive Degradation of PCE by (A) BB1, (B) *Sm*, and (C) BDI and TCE by (D) BB1, (E) *Sm*, and (F) BDI. Error Bars Represent 95 % Confidence Intervals for Mean Values from Three Microcosms.	52
Figure 7. Abiotic Transformation of PCE in the Presence of Chloride Green Rust (GR-Cl), pyrite, Sulfate Green Rust (GR-SO_4), and Magnetite at pH 8. Lines Represent a Pseudo first-order Model Fit. The Insets Show Reaction Products with Low Concentrations.	53
Figure 8. Abiotic Transformation of TCE in the Presence of Chloride Green Rust (GR-Cl), Pyrite, Sulfate Green Rust (GR-SO_4), and Magnetite at pH 8. Lines Represent a Pseudo first-order Model fit. The Insets Show Reaction Products with Low Concentrations.	54
Figure 9. Carbon Isotope Fractionation During Abiotic Reductive Dechlorination of TCE by Chloride Green Rust (GR-Cl) and Pyrite at pH 8. Lines Represent a Rayleigh Model Fit. Uncertainties are 95% Confidence Intervals Calculated by Nonlinear Regression.	55
Figure 10. PCE Reductive Dechlorination in the Duck Pond (DP) (a), Landfill (L) (b), and Altus AFB (AAFB) (c) Microcosms and TCE Reductive Dechlorination in Selected DP and L Microcosms (d), Under Iron Reducing (IR), Sulfate Reducing (SR), and Methanogenic (Meth) Conditions. Data Points are Averages of Samples from Duplicate or Triplicate Microcosms.	56

List of Figures (continued)

Page

Figure 11. Normalized concentrations of PCE (a-d), TCE (e-f), and Reaction Products in Representative Microcosms. Reactants and Products were Normalized by Dividing the Concentration at Any Time by the Concentration of the Reactant at Time Zero. The Insets Show Reaction Products with Low Concentrations. Error Bars are Standard Deviations of Triplicate Microcosms. To Better Show the Data Points, Parts of the Error Bars were Cut off in the Insets for (a) and (e). In the Inset for (e), the Symbols for 1,1-DCE (closed hexagons) are Partially Covered with ethylene (open circles) and acetylene (open triangles). 57

Figure 12. PCE Reductive Dechlorination in the Microcosms with (gray symbols) and without (black symbols) Antibiotic and Heat Treatments. 58

Figure 13. Acetylene Transformation in the Microcosms. Error Bars are Standard Deviations of the Means for Duplicate Measurements from the Same Microcosm. 59

Figure 14. Isotope Fractionation of PCE (a) and TCE (b) in the Microcosms where PCE and TCE were Below Detection Limits at the End of Experiment. The Values in Parentheses are Bulk Enrichment Factors (ε_{bulk} values). Data Points are Experimentally Measured Values, and Lines Represent a Fit to the Rayleigh Model. Uncertainties are 95 % Confidence Intervals. 60

Figure 15. Geochemical Analyses of the Microcosms, Including FeS (a), weakly bound Fe(II) (b), strongly bound Fe(II) (c), chromium extractable sulfur (CrES) (d) and TOC (e), under unamended, iron reducing (Fe(III) Red.), sulfate reducing (SO_4^{2-} Red.) or methanogenic (Meth) conditions. Arrows Indicate the Microcosms where Neither PCE nor TCE abiotic Reductive Dechlorination Products were Detected. Error Bars are Standard Deviations of Triplicate Samples from the Same Microcosm. 61

List of Tables

	Page
Table 1. Surface Area Normalized Pseudo first-order Rate Constants, Products, and Mass Recoveries, for PCE Transformation by Chloride Green Rust (GR-Cl), Pyrite, Sulfate Green Rust (GR-SO_4), Magnetite, Fe(II)-treated Goethite, and S(-II)-treated Goethite at pH 8.	40
Table 2. Surface Area Normalized Pseudo first-order Rate Constants, Products, and Mass Recoveries, for TCE Transformation by Chloride Green Rust (GR-Cl), Pyrite, Sulfate Green Rust (GR-SO_4), Magnetite, Fe(II)-treated Goethite, and S(-II)-treated Goethite at pH 8.	41
Table 3. Summary of Results for the Microcosm Experiments.	42
Table 4. Geochemical Properties of the Microcosms.	43
Table 5. Results of Geochemical Analyses Before and After Heat Treatment.	44
Table 6. Physical-chemical and Kinetic Properties of Reactants and Products.	45
Table 7. Rate Constants, ε_{bulk} Values, and Apparent Kinetic Isotope Effects for Carbon ($AKIE_C$ values).	46

Acknowledgments

This research was supported wholly by the U. S. Department of Defense (DoD) through the Strategic Environmental Research and Development Program (SERDP). The Co-Principal Investigators were Lee Krumholz (Department of Botany and Microbiology, University of Oklahoma [OU]) and Paul Philp (School of Geology and Geophysics, OU). The graduate student and postdoctoral collaborators were Yiran Dong and Xiaoming Liang (School of Civil Engineering and Environmental Science [CEES], OU) and Tomasz Kuder (School of Geology and Geophysics, OU). We are grateful to many people for providing invaluable help with this project. Scott Christenson, Ernie Smith, and Jason Masoner from the U.S. Geological Survey in Oklahoma City provided the Geoprobe and collected soil samples from the Norman Landfill. Tohren Kibbey, Xingdong Zhu, and Hongbo Shao from OU CEES helped with sampling at the Norman Landfill and Duck Pond. Hongbo Shao assisted with geochemical analyses. John Wilson, Yongtian He, Ken Jewell, Brad Scroggins, and Kevin Smith from the U.S. Environmental Protection Agency (USEPA) Robert S. Kerr Environmental Research Center in Ada, Oklahoma collected and provided solid and ground water samples from the biowalls at Altus Air Force Base in Altus, Oklahoma. Jon Allen, Evelyn Cortez, and Janel McMahon from the OU School of Geology and Geophysics performed isotope analyses. Preston Larson from the Samuel Roberts Noble Electron Microscopy Laboratory at OU performed SEM analysis. John Senko and Anne Spain from the Department of Botany and Microbiology at OU helped with the microbial experiments. Finally, Frank Loeffler from the Georgia Institute of Technology kindly provided several microbial cultures used in these experiments.

Executive Summary

Summary of the Environmental Problem

Tetrachloroethylene (PCE) and trichloroethylene (TCE) are among the most frequently detected ground water contaminants at industrial sites, including many DoD facilities. Due to the high cost and uneven performance of traditional remediation technologies, monitored natural attenuation is emerging as a new technology for ground water remediation of pollutants such as these. In addition, there is growing interest in active remediation technologies that employ abiotic minerals. PCE and TCE are susceptible to reductive dechlorination by microorganisms as well as reduced minerals such as iron sulfide (FeS). Unlike biological reductive dechlorination, which often results in accumulation of harmful intermediates such as *cis* 1,2-dichloroethylene (*cis*-DCE) and vinyl chloride (VC), abiotic mineral-mediated dechlorination of PCE and TCE tends to result in complete transformation to non-toxic products such as acetylene. To more accurately apply natural attenuation and other remediation technologies, a greater understanding of the geochemical factors affecting the rates of purely abiotic reductive dechlorination of PCE and TCE is needed. Additional tools are also needed to determine whether or not abiotic reductive dechlorination is occurring at a particular site, and its relative importance compared to microbial dechlorination under a variety of geochemical conditions.

Research Objectives

The overall objective of this project was to develop and apply methods to quantify the rates of abiotic natural attenuation at sites contaminated with PCE and TCE in order to allow a quantitative estimate of the potential for abiotic transformation of these compounds based on analysis of subsurface geochemistry. Specific project objectives were: (1) to assess whether stable (i.e., non-radioactive) carbon (C) isotope fractionation can be used to distinguish between abiotic and biotic reductive dechlorination of TCE and PCE (Task 1); (2) to identify the geochemical conditions most strongly correlated with high rates of abiotic PCE and TCE reductive dechlorination in well-defined microcosm studies (Task 2); and (3) to validate and apply our findings at a series of DoD field sites contaminated with PCE or TCE (Task 3). This report summarizes our research approach, findings, and recommendations.

Results and Potential Applications

In Task 1, we conducted PCE and TCE reductive dechlorination experiments using pure minerals and well characterized pure and mixed cultures of bacteria. Significant carbon isotope fractionation was observed during FeS-mediated reductive dechlorination of PCE and TCE as well as during transformation of TCE by chloride green rust (GR-Cl) and pyrite. Bulk enrichment factors (ε_{bulk}) for PCE transformation by FeS were -30.2 ± 4.3‰ (pH 7), -29.54 ± 0.83‰ (pH 8), and -24.6 ± 1.1‰ (pH 9). For TCE, ε_{bulk} values were -33.4 ± 1.5‰ (pH 8) and -27.9 ± 1.3‰ (pH 9). Bulk enrichment factors (ε_{bulk}) for TCE transformation by GR-Cl and pyrite at pH 8 were -23.0 ± 1.8‰ and -21.7 ± 1.0‰, respectively.

A smaller magnitude of carbon isotope fractionation resulted from microbial reductive dechlorination by two isolated pure cultures (*Desulfuromonas michiganensis strain* BB1 (BB1) and *Sulfurospirillum multivorans* (*Sm*) and a bacterial consortium (BioDechlor INOCULUM (BDI). The ε_{bulk} values for biological PCE microbial dechlorination were -1.39 ± 0.21‰ (BB1), -1.33 ± 0.13‰ (*Sm*), and -7.12 ± 0.72‰ (BDI), while those for TCE were -4.07 ± 0.48‰ (BB1), -12.8 ± 1.6‰ (*Sm*), and -15.27 ± 0.79‰ (BDI). We interpreted our results by calculating the apparent kinetic isotope effect for carbon ($AKIE_C$) and the results suggest that differences in isotope fractionation for abiotic and microbial dechlorination resulted from differences in rate limiting steps during the dechlorination reaction.

Task 1 results suggest that isotope fractionation is one tool that can be used, in conjunction with other tools such as microbial, geochemical, and reaction product analysis, to provide evidence about the predominant PCE or TCE transformation pathway at a contaminated site, i.e., abiotic or biotic. (Interpretation of ε_{bulk} values measured in the field must always account for contaminant dispersion and dilution effects in flow-through systems [e.g., van Breukelen, 2007]). There is too much variability and overlap in ε_{bulk} values for different minerals and different microbial cultures, however, for isotope fractionation to be a stand alone tool for distinguishing abiotic and microbial reductive dechlorination of PCE or TCE.

In Tasks 2 and 3, we studied PCE and TCE reductive dechlorination in well defined microcosms prepared with aquifer materials from three locations. We added electron donors and terminal electron acceptors to both stimulate microbial activity and to generate reactive minerals via microbial iron and sulfate reduction. We assessed the relative importance of abiotic and biotic PCE and TCE reductive dechlorination by analysis of reaction products, reaction kinetics, and stable carbon isotope fractionation. Based on these analyses, the predominant PCE and TCE transformation pathway in most microcosms was microbial reductive dechlorination. Rates of abiotic transformation were similar in magnitude to those for microbial reductive dechlorination only in a few microcosms, most of which were prepared at slightly elevated pH (pH 8.2 versus 7.2), which may have inhibited dechlorinating bacteria.

Microbial PCE and TCE transformation was typically faster than abiotic transformation in the microcosms, which contained 20 g wet soil, 100 mL water, and 50 mL headspace. Under field conditions, the higher mass loading of soils compared to the microcosm conditions would potentially result in higher mass loadings of reactive minerals as well as higher activities of bacteria capable of transforming PCE and TCE, both of which could affect the relative contributions of abiotic and microbial PCE and TCE reductive dechlorination. While microbial processes have the potential for rapid transformation of PCE and TCE, abiotic processes also have the potential to contribute to the transformation of PCE and TCE in cases where high mass loadings of reactive minerals are generated in situ as part of a remediation technology, where the activity of dechlorinating bacteria is low, and/or where bacteria of complete dechlorination of PCE or TCE to ethene are not present.

Objective

Unlike biological reductive dechlorination, which often results in accumulation of harmful intermediates such as *cis* 1,2-dichloroethylene (*cis*-DCE) and VC, abiotic dechlorination of PCE and TCE tends to result in complete transformation to non-toxic products such as acetylene. Thus, it is imperative to develop the knowledge and tools needed to identify contaminated sites with the greatest potential for abiotic reductive dechlorination of PCE and TCE. The overall objective of this project was to develop and apply methods to quantify the rates of abiotic natural attenuation at sites contaminated with PCE and TCE. Specific project objectives were: (1) to assess whether stable (i.e., non-radioactive) carbon (C) isotope fractionation can be used to distinguish between abiotic and biotic reductive dechlorination of TCE and PCE (Task 1); (2) to identify the geochemical conditions most strongly correlated with high rates of abiotic PCE and TCE reductive dechlorination in well-defined microcosm studies (Task 2); and (3) to validate and apply our findings at DoD field sites contaminated with PCE or TCE (Task 3).

Background

Abiotic and Biotic Reductive Dechlorination

The fate of contaminants such as PCE and TCE is determined by both abiotic and biotic processes. Abiotic transformation of chlorinated contaminants such as PCE and TCE can occur in the presence of natural Fe(II) and S(-II) containing minerals, such as FeS, greigite (Fe_3S_4), pyrite (FeS_2), magnetite (Fe_3O_4), and various green rusts (Kriegman-King and Reinhard, 1991; Sivavec et al. 1995, 1996, Sivavec and Horney 1997, Erbs et al. 1999, Butler and Hayes 1999, 2001, Weerasooriya and Dharmasena 2001, Hwang and Batchelor, 2001, Lee and Batchelor, 2002a, 2002b). In addition, Fe(II) adsorbed to iron oxides has been shown to cause reductive dechlorination (Pecher et al., 2002, Elsner et al., 2004a).

Microbial reductive dechlorination of PCE and TCE also occurs via dehalorespiration, in which chlorinated aliphatics act as terminal electron acceptors (e.g., Bouwer and McCarty, 1983; Bagley and Gossett, 1990). Iron reducing bacteria, methanogens, acetogens, nitrate reducing bacteria, and sulfate reducing bacteria are the major microorganisms involved in microbial reductive dechlorination (Bossert et al., 2003). Microbial process such as dissimilatory iron reduction and sulfate reduction also indirectly influence rates of abiotic reductive dechlorination because they lead to formation of the reactive Fe(II) and S(-II) minerals listed above. For example, biogenic magnetite (Fe_3O_4), created by the iron reducing bacterium *Geobacter metallireducens*, caused the abiotic reductive dechlorination of carbon tetrachloride (McCormick et al., 2001), and carbonate green rust formed by the iron reducing bacteria *Shewanella putrefaciens* CN32 caused *cis*-DCE reductive dechlorination (Pasakamis et al., 2006).

Abiotic and biotic reductive dechlorination of PCE and TCE take place via different pathways: reductive β-elimination (abiotic) and hydrogenolysis (biotic), each leading to different reaction products, as illustrated in Figure 1. Because both reactive minerals and microorganisms are present at contaminated sites, both abiotic and biotic reductive dechlorination have the potential to occur simultaneously. Thus the relative abundance of the products of abiotic and biotic reductive dechlorination of PCE and TCE can indicate the predominant transformation process, i.e., abiotic or biotic.

The geochemical properties of soil and groundwater have the potential to influence the rate and thus the relative contribution of abiotic reductive dechlorination at contaminated sites. For example, for a given mass of reactive mineral, increasing pH generally leads to higher rates of abiotic reductive dechlorination and related reactions such as nitroaromatic reduction (Klausen et al., 1995; Butler and Hayes, 1998, 2001; Pecher et al., 2002; Danielsen and Hayes, 2004), perhaps due to a greater abundance of deprotonated iron species at higher pH values. The abundance of sorbed or other surface associated Fe(II) species also influences abiotic degradation rates by reactive mineral surfaces (Pecher et al., 2002, Elsner et al., 2004a). The available surface area of reactive minerals such as FeS also influences dechlorination rates (e.g., Sivavec et al., 1995). In addition, depending on its structure, NOM has been found to either enhance dechlorination rates, possibly by facilitating electron transfer (Butler and Hayes, 1998; Doong and Chiang, 2005), decrease dechlorination rates by blocking reactive mineral sites (Butler and

Hayes, 1998), or have no influence on rates (Hanoch et al., 2006). NOM also has the potential to increase the rates of microbial reductive dechlorination by acting as an electron donor, thus indirectly causing the formation of reactive minerals.

Stable Carbon Isotope Fractionation

Stable carbon isotope analysis is a relatively new tool to assess the fate of PCE and TCE in contaminated ground waters (Dayan et al., 1999; Hunkeler et al., 1999; Sherwood Lollar et al., 1999; Bloom et al., 2000; Slater et al., 2001, 2002, 2003; Schüth et al., 2003; Vieth et al., 2003; VanStone et al., 2004; Zwank, 2004; Elsner et al., 2005; Nijenhuis, et al., 2005; Lee et al., 2007). Because the rate constant for cleavage of a chemical bond containing ^{12}C is greater than that for an otherwise equivalent bond containing ^{13}C, reactions for which bond cleavage is the rate limiting step can result in the enrichment of the heavier isotope (^{13}C) in the remaining parent compound (Elsner et al., 2005). The magnitude of isotope fractionation can be described by the bulk enrichment factor, ε_{bulk}, derived from the Rayleigh model (Mariotti et al., 1981). Previously reported ε_{bulk} values for abiotic PCE reductive dechlorination (in‰) include -15.5 to -5.7 for Peerless and Connelly irons (VanStone et al., 2004), -16.5 to -15.8 for Vitamin B_{12} at pH 8.8 (Slater et al., 2003), and -14.7 for FeS at pH 7.3 (Zwank, 2004). For TCE, reported ε_{bulk} values for abiotic dechlorination (in‰) include -10.1 for zerovalent iron filings (Schüth et al., 2003), -16.7 for cast and autoclaved electrolytic iron (Slater et al., 2002), -13.9 to -7.5 for Peerless and Connelly irons (VanStone et al., 2004), -17.2 to -16.6 for Vitamin B_{12} at pH 8.8 (Slater et al., 2003), and -9.6 at pH 7.3 for FeS (Zwank, 2004).

ε_{bulk} values for microbial reductive dechlorination of PCE and TCE are generally smaller in magnitude (less negative) than those for abiotic reductants. The difference between biotic and abiotic ε_{bulk} values is greater for PCE than for TCE (Zwank, 2004). In his dissertation, Zwank (2004) concluded that differences in ε_{bulk} values could be used to distinguish abiotic and biotic reductive dechlorination of PCE, but not TCE, in model sulfate reducing systems. Reported ε_{bulk} values (in‰) for PCE microbial reductive dechlorination include -1.02 ± 0.06 (Zwank, 2004) and -0.42 ± 0.08 (Nijenhuis, et al., 2005) for *Sulfurospirillum multivorans* (*Sm*), and -2, -5.5 to -2.7, and -5.18 for microcosms from a PCE contaminated site (Hunkeler et al., 1999), mixed consortia (Slater et al., 2001), and a pure culture (Nijenhuis et al., 2005), respectively. For TCE microbial reductive dechlorination, ε_{bulk} values (in‰) include -12.6 ± 0.5 (Zwank, 2004) and -16.4 ± 1.5 (Lee et al., 2007) for *Sm*, and -4, -6.6 to -2.5, -7.1, -13.8, and -3.3 to -16 for microcosms from a PCE contaminated site (Hunkeler et al., 1999), microbial consortia (Sherwood Lollar et al., 1999; Bloom et al., 2000; Slater et al., 2001), and two pure cultures (Lee et al., 2007), respectively.

Microbial enzyme-catalyzed generally reactions involve a sequence of steps shown in eq. 1 (O'Leary and Yapp, 1978; Hunkeler and Aravena, 2000; Zwank, 2004; Nijenhuis et al., 2005):

$$\mathbf{S_{out}} \underset{(1)}{\rightleftharpoons} \mathbf{S_{in} + E} \underset{(2)}{\rightleftharpoons} \mathbf{E{\cdot}S_{in}} \underset{(3)}{\longrightarrow} \mathbf{E{\cdot}P_{in}} \underset{(4)}{\rightleftharpoons} \mathbf{E + P_{in}} \underset{(5)}{\rightleftharpoons} \mathbf{P_{out}} \qquad (1)$$

where the numbers refer to: (1) transport of the substrate (S) from outside (S_{out}) to inside (S_{in}) the cell; (2) formation of the enzyme (E)-substrate complex; (3) bond cleavage and formation of enzyme-product (P) complex; (4) dissociation of enzyme-product complex; and (5) transport of the product from inside (P_{in}) to outside (P_{out}) the cell. Similar schemes involving mass transport

of solutes to a mineral surface (step 1), surface complex formation (step 2), electron transfer (step 3), surface complex dissociation (step 4), and mass transport of solutes away from a mineral surface (step 5) have also been proposed for abiotic redox reactions (e.g., Stone, 1986); thus Equation 1 could apply to abiotic reactions as well. Step 3 is the only step in either scheme involving bond cleavage and consequently only step 3 can lead to isotope fractionation (Nijenhuis et al., 2005). Step 3 could, however consist of a series of elementary reaction steps related to bond cleavage, some of which, e.g., reduction of a reactive metal center in a dehalogenase enzyme, do not involve C-Cl cleavage. If such a sub-step were rate limiting, then no isotope fractionation would be observed. In addition, if steps 1, 2, 4, or 5 were rate limiting, little or no isotope fractionation would occur. Nijenhuis et al. (2005) observed an increase in isotope fractionation with a decrease in cell integrity during reductive dechlorination of PCE by *Sm* and *Desulfitobacterium sp*. Strain PCE-S, which suggests that transport of PCE into the cell (e.g., step 1 in equation 1) is the rate limiting step in dechlorination by these bacteria.

Materials and Methods

Chemical Reagents

The following chemicals were obtained from Sigma-Aldrich (St. Louis, Missouri): sodium sulfide nonahydrate, $FeCl_2 \cdot 4H_2O$ (99%), PCE (99%), TCE (99.5%), *cis* 1,2-dichlorethylene (*cis*-DCE), *trans* 1,2-dichlorethylene (*trans*-DCE), 1,1-dichlorethylene (1,1-DCE), N-(2-hydroxyethyl)-piperazine-N'-3-propanesulfonic acid (HEPES), N-cyclohexylaminoethanesulfonic acid (CHES), and [(2-Hydroxy-1,1-bis(hydroxymethyl)ethyl)amino]-1-propanesulfonic acid (TAPS). Methanol, sodium hydroxide, and chemicals used for microbiological medium preparation were purchased from Fisher Scientific (Pittsburgh, Pennsylvania). Ethane (1018 ppm in N_2), ethylene (1026 ppm in N_2), acetylene (1001 ppm in N_2), and VC (1019 ppm in N_2) were obtained from Scott Specialty Gases (Houston, Texas). All aqueous solutions were prepared with Nanopure water (18.0 MΩ cm resistivity, Barnstead Ultrapure Water System, Iowa).

Mineral Preparation

FeS was synthesized using the method described by Rickard (1969). Pyrite from Zacatecas, Mexico was purchased from Ward's (Rochester, Ney York) and processed for 30 minutes in a Shatterbox Laboratory Mill (Model 8500, Spex Industries Inc., Metuchen, New Jersey), then immediately transferred to an anaerobic chamber with an atmosphere of approximately 96% N_2/4% H_2 and a catalytic O_2 removal system (Coy Products, Grass Lake, Michigan). Crushed pyrite was then washed with 1 M N_2-sparged HCl and air-dried in the anaerobic chamber. Chloride green rust (GR-Cl) was synthesized by partial oxidation of ferrous hydroxide according to Refait et al. (1998) except that we used 1 M NaOH and 0.7 M $FeCl_2$. The blue-green precipitate was freeze-dried with a custom vacuum valve to exclude oxygen. Sulfate green rust (GR-SO_4) was synthesized by the method in O'Loughlin et al. (2003). Magnetite was prepared using the method of Kang et al. (1996) because this method produced particles with higher surface area than other methods (Taylor et al., 1987; Schwertmann and Cornell, 1991). Goethite was prepared as described in Atkinson et al. (1967).

All iron minerals were characterized by x-ray diffraction (XRD) (Rigaku DMAX x-ray Diffractometer) after freeze-drying. To prevent oxidation during XRD analysis, GR-Cl and GR-SO_4 samples were prepared in the anaerobic chamber by mixing them with petroleum jelly. Pyrite and magnetite samples were stable with respect to oxidation during the period of XRD analysis. The peak patterns of mineral samples were consistent with those in the Powder Diffraction File (Joint Committee on Powder Diffraction Standards (JCPDS), 1990). All minerals were poorly crystalline. The specific surface areas of FeS, GR-Cl, GR-SO_4, pyrite, magnetite, and goethite were (in $m^2\ g^{-1}$) 2.01, 21, 3.7, 7.5, 90, 74, respectively, determined by BET surface analysis (Autosorb-1, Quantachrome Instruments, Boynton Beach, Florida).

Microbial Cultures

One stimulated mixed culture, BioDechlor INNOCULUM (BDI), and two isolated pure cultures, *Sm* and *Desulfuromonas michiganesis* strain BB1 (BB1), were kindly provided by Prof. Frank E. Loeffler at the Georgia Institute of Technology. (Throughout this report we use the classification *Sulfurospirillum multivorans* (*Sm*), and not *Dehalosprillum multivorans* (Luijten et al., 2003). BDI is an enriched microbial consortium containing several strains of *Dehalococcoides* (Ritalahti et al., 2005). *Sm* was isolated from activated sludge not previously exposed to chlorinated ethylenes (Scholz-Muramatsu et al., 1995; Neumann et al., 1996). BB1 was isolated from unpolluted river sediment (Sung et al., 2003).

Quantification of Reactants and Products

For PCE and TCE analysis in abiotic experiments, a 250 µL aliquot of the supernatant was added to 750 µL isooctane in a 2 mL autosampler vial and 1 µL of the isooctane phase analyzed using a Shimadzu GC-17A gas chromatograph (GC) with an Agilent J&W DB-624 capillary column (30 m × 0.53 mm × 3 µm) and electron capture detector (ECD). The injector temperature was 250°C and the detector temperature was 275°C. The oven temperature was initially 70°C, immediately ramped from 70°C to 90$^{\circ C}$ at 5°C/min, isothermal at 90$^{\circ C}$ for 2 min, ramped to 110°C at 10°C/min, isothermal at 110°C for 1 min, and ramped to 140°C at 15°C/min. External calibration standards for GC/ECD analysis were prepared in isooctane. Relative standard deviations for duplicate injections using this method were typically less than 1 %. Each GC vial was analyzed in duplicate and the peak areas averaged. Relative standard deviations for PCE and TCE between duplicate ampules (measured for selected samples only) were typically less than 1%, which was considered acceptable.

For analysis of *cis*-DCE, VC, acetylene, ethylene, and ethane in abiotic experiments, two-2 mL aliquots of supernatant from each sample ampule were transferred to separate 22 mL vials that were quickly sealed with Teflon-coated septa and aluminum crimp seals for analysis by a Tekmar 7000 headspace autosampler interfaced with a Shimadzu GC-17A/flame ionization detector (FID) and an Agilent GS-GASPRO capillary column (30 m × 0.32 mm). The GC injector temperature was 250°C and the detector temperature was 275°C. The oven temperature was isothermal at 35°C for 3 min, ramped at 20°C/min to 110°C, isothermal at 110°C for 6 min, ramped at 40°C/min to 220°C, and isothermal at 220°C for 14.5 min. Headspace autosampler settings were: sample loop size: 1 mL; loop fill time: 0.25 min; loop, platen, and transfer line temperature: 70°C; sample equilibrium time: 30 min; and inject time: 0.5 min. All standards and samples were run in duplicate. Five point external calibration curves were run daily. Relative standard deviations for duplicate analyses using this method were typically less than 3 %.

In one experiment for the transformation of TCE by pyrite, acetate was quantified in by ion chromatography using the same instrumental setup as in Zhu et al. (2005). Ethanol and acetaldehyde were analyzed for the same experiment by a HP 6890 GC with an Agilent J&W DB-624 capillary column (30 m × 0.53mm × 3 µm) and flame ionization detector (FID). The GC injector temperature was 250°C and the detector temperature was 280°C. The oven temperature was isothermal at 60°C for 6.5 min.

For microbial dechlorination experiments, concentrations of PCE, TCE, *cis*-DCE, VC, ethylene and methane were determined from manual injection headspace analysis with the Shimadzu GC/FID/GS-GASPRO setup. Fifty microliters of headspace were withdrawn with a gas tight syringe (Hamilton Co., Reno, Nevada) and manually injected into the GC/FID using a split ratio of 1:1. The oven temperature was isothermal at 35°C for 5 min, ramped to 190°C at 30°C/min, and isothermal at 190°C for 5 min. The injector temperature and detector temperature were 220°C and 270°C, respectively. Five point external calibration curves were prepared daily. Relative standard deviations for samples and standards using this method were typically less than 5 %. Each microcosm was sampled for concentrations of reactants and products. Isotope analysis was not repeated for duplicate microcosms because there was good agreement in measured ε_{bulk} values between duplicate microcosms (data not shown).

Isotope Measurements

Samples were analyzed by purge and trap (PT) coupled with a GC and isotope ratio mass spectrometer (GCIRMS) for compound-specific isotope ratio analysis. Isotope ratios were measured against a CO_2 standard. PCE and TCE were extracted from water by PT with a Vocarb 3000 or Tenax-silica gel-charcoal trap. The PT transfer line was interfaced to a continuous flow GCIRMS instrument (Finnigan MAT 252 IRMS with a Varian 3400 GC). A combustion reactor installed as part of the GCIRMS interface converted the analytes to carbon dioxide without affecting chromatographic resolution. A Nafion membrane installed prior to the IRMS removed water transferred from PT and from combustion. The PT effluent entered the GC through a 6-port switching valve interface, allowing splitless liquid nitrogen cryofocusing (Smartcryo, Humble Analytical) and complete sample recovery, while maintaining carrier gas flow rates appropriate for PT desorption and GC separation, respectively. A polar pre-column (DB-Carbowax) was installed between the transfer line and the 6-port valve to prevent ice buildup on the cryofocuser.

Samples of 25 mL volume were purged for 12 min at 25°C with a purge flow of 40 mL/min and a sample temperature of 25°C. The trap was desorbed for 5 min. The PT apparatus was baked for 15 min after each run. Desorption and baking temperatures were those specified by the manufacturer. Carrier gas flow during desorption was 8 mL/min. Post-cryo GC separation was done on an Agilent J&W DB-MTBE capillary column (60 m x 0.32 mm x 1.8 µm) at a 1.8 mL/min carrier gas (He) flow rate (measured at 25°C; constant pressure). The GC program was 4 min isothermal at 40°C, followed by a 6°C/min ramp up to the elution of the final compound of interest. The GC was kept at 220°C after each analytical run.

After measurement by GCIRMS, isotope ratios were normalized to an external standard (CO_2) and expressed as $\delta^{13}C$, which is defined as:

$$\delta^{13}\mathrm{C} = \frac{\left(\frac{^{13}\mathrm{C}}{^{12}\mathrm{C}}\right)_{sample} - \left(\frac{^{13}\mathrm{C}}{^{12}\mathrm{C}}\right)_{std}}{\left(\frac{^{13}\mathrm{C}}{^{12}\mathrm{C}}\right)_{std}} \times 1{,}000\,‰ \qquad (2)$$

Using the Rayleigh model (Mariotti et al., 1981), the isotopic composition of the parent compound as a function of time is described by:

$$R_p = R_{p,o} f^{\left(\frac{\varepsilon_{\text{bulk}}}{1000}\right)} \quad (3)$$

where R_p is the isotope ratio of the parent compound at any time, $R_{p,0}$ is its isotopic ratio at time zero (before any degradation), f is the fraction of parent compound remaining at a given time (i.e., C/C_0) (measured by GC/FID), and ε_{bulk} is the bulk enrichment factor. ε_{bulk} values were calculated by nonlinear regression using experimentally measured values of $\delta^{13}C$ and f.

Task 1 Details

Experiments with Minerals

Batch kinetic experiments were conducted at pH 7, 8, and 9 in 5 mL glass ampules containing either HEPES (pH 7 and 8) or CHES (pH 9) buffers (50 mM). Mineral mass loadings were (in g L^{-1}): FeS: 10; GR-Cl: 10; GR-SO_4: 25; pyrite: 77; magnetite: 20; and goethite: 4. One experiment with TCE was done at a pyrite mass loading of 400 g L^{-1}. Surface area loadings were (in m^2 L^{-1}): FeS: 20.1; GR-Cl: 210; GR-SO_4: 93; pyrite: 578; magnetite: 1800; and goethite: 296. For one TCE experiment with a pyrite mass loading of 400 g/L, the pyrite surface area loading was 3000 m^2 L^{-1}. Initial PCE and TCE aqueous concentrations ranged from 15-30 µM, except for one experiment (see above) where the initial TCE concentration was approximately 7.5 mM. In each ampule, the aqueous phase volume was 6.5 mL and the gas phase volume was approximately 1.25 mL. Ampules were prepared in an anaerobic chamber containing approximately 96% N_2 and 4% H_2, with a catalytic O_2 removal system (Coy Products, Grass Lake, MI). After preparation, ampules were temporarily covered with polyvinylidene chloride film (Saran™ Wrap) that was secured with a short piece of plastic tubing (Barbash and Reinhard, 1989), then taken out of the chamber and spiked with PCE or TCE stock solution prepared in N_2-sparged methanol. Ampules were then immediately sealed using a methane/oxygen flame while kept anaerobic with the Saran™ Wrap cover, and placed in a constant temperature chamber at 25°C in the dark on a rocking platform shaker (Labquake, Cole Parmer Instrument Company). At regular intervals, ampules were centrifuged, broken open, and sampled.

Treatment of Kinetic Data

As discussed below, only certain experimental conditions showed significant transformation of PCE or TCE in the time scale of our experiments. In these cases, we fit data for aqueous concentration of PCE or TCE versus time to a pseudo-first-order rate model, adjusted the resulting rate constants to those that would be measured in a headspace-free system (Burris et al. 1996), then divided them by surface area concentration. Mass recoveries of PCE or TCE reaction products (Tables 1 and 2) were calculated as follows:

$$\text{Mass Recovery (\%)} = \frac{M_{\text{p, aq, t}} + M_{\text{p, g, t}}}{M_{\text{r, aq, 0}} + M_{\text{r, g, 0}}} \times 100\% \quad (4)$$

where $M_{p,\,aq,\,t}$ and $M_{p,\,g,\,t}$ equal the moles of a product in the aqueous and gas phases at the last sampling time (given in Tables 1 and 2), and $M_{r,\,aq,\,0}$ and $M_{r,\,g,\,0}$ equal the moles of reactant (PCE or TCE) in the aqueous and gas phases at time zero. The same approach was used to calculate mass recoveries of unreacted PCE and TCE. Dimensionless Henry's Law constants (PCE: 0.612; TCE: 0.404; *cis*-DCE: 0.221; acetylene: 0.932; ethylene: 9.013; acetaldehyde: 0.00322; ethanol: 0.000204) were used to convert measured aqueous concentrations to masses, based on the aqueous and gas phase volumes. These values (for 25 ^{o}C) were obtained by averaging data from Nirmalakhandan and Speece (1988), Howard and Meylan (1997), and Bierwagen and Keller (2001). Acetate was assumed to be nonvolatile.

Experiments with Pure and Mixed Cultures

All culture microcosms were prepared in 1 L Pyrex™ bottles modified by a glassblower (G. Finkenbeiner Inc., Waltham, MA) to accommodate a septum stopper (Bellco Biotechnology). A reduced anaerobic basal salts medium (BS medium) was prepared according to Sung et al. (2003). After the medium was boiled and cooled, the pH was adjusted to 7.2 with 2.52 g/L $NaHCO_3$ under a stream of N_2/CO_2 (80%/20%). A vitamin solution, trace metals (Hurst et al., 2002), 0.2 mM L-cysteine, and 0.5 mM Na_2S were added from sterile anaerobic solutions. The electron donors were (all 5 mM): lactate (BDI), acetate (BB1) and pyruvate (*Sm*). Cultures were inoculated using a 1:50 dilution ratio. Serum bottle microcosms were sealed with sterilized Teflon-lined rubber stoppers (West Pharmaceutical Services) and aluminum seals. Initial concentrations of PCE and TCE in the microcosm experiments were approximately 117 µM and 108 µM, respectively. Microcosms were prepared in duplicate and incubated in the dark at room temperature. All microcosm manipulations were performed under a stream of sterile N_2/CO_2 gas.

Task 2 and 3 Details

Microcosm Setup

Solid and liquid samples were collected from three sites, including an anaerobic zone of an aquifer located adjacent to the closed landfill at the Norman Landfill Environmental Research Site (U.S. Geological Survey Toxic Substances Hydrology Research Program), Norman, Oklahoma (Norman Landfill or L), a pond in Brandt Park, Norman, Oklahoma (Duck Pond or DP), and two permeable reactive barriers containing mulch ("biowalls") at AAFB, Altus, Oklahoma. There have been no reports of PCE or TCE contamination at the first two sites, while the sampling areas at AAFB intersect TCE plumes (Kennedy et al., 2006; Lu et al., 2008). Two AAFB samples (AAFB 12 and AAFB 14) were from a biowall section that had been modified by addition of magnetite to promote formation of FeS upon microbial sulfate reduction (Parsons Corporation, 2006).

Norman Landfill (L) soil samples were obtained from approximately 2 m below the ground surface near the No. 35 multilevel well (Cozzarelli et al., 2000) using a Geoprobe® (Geoprobe Systems, Kansas) and ground water was obtained approximately 3.5 m below the ground surface from the same well using a peristaltic pump. DP sediments were taken from the top 3-8 cm of the near shore sediment with a sterile spatula. Duck Pond water was collected in autoclaved 2L Pyrex® medium bottles at the sediment sampling site. AAFB biowall samples were obtained

using a Simco earthprobe® (Simco Drilling Equipment Inc. IA) from 3.5-6.2 m deep and approximately 1.5 m south of Well MP 1 (microcosms AAFB-8, AAFB-9 and AAFB-10) inside the biowall in the OU1 area (see map in Lu et al. (2008) and from 2.7-5.0 m deep and about 0.9 m east of Well BB04 inside the biowall downgradient of Building 506 in the SS-17 area (microcosms AAFB-12 and AAFB-14) (see map of the area around building 506 in Kennedy et al. (2006). In order to prevent oxidation and loss of fine particles during the sampling process, biowall samples were frozen *in-situ* with liquid nitrogen injected into the ground via a steel tube, extracted from the ground frozen, and then stored on dry ice in a cooler until transport to the laboratory. Ground water at AAFB was pumped from 4.6 m below the ground surface from Wells MP1 and BB05W. All solid and liquid samples were flushed with sterile N_2/CO_2 and stored in the dark at 4°C before use.

Microcosms were prepared in an anaerobic chamber (Coy Laboratory Products Inc., Michigan). Buffered site water (100 mL containing 25 mM HEPES (pH 7.2) or TAPS (pH 8.2) and 20 g wet sediment or solids were added to 160 mL serum bottles. Experiments were done at pH 7.2 and 8.2 to include the range of pH values found in natural waters. HEPES and TAPS are generally considered suitable for biological systems, and we are not aware of any reports of HEPES or TAPS acting as electron donors for bacteria or exhibiting side effects such as toxicity to dehalogenating bacteria. Strict pH control was required since pH can strongly affect the rates of abiotic reductive dechlorination of PCE and TCE (Hwang and Batchelor, 2000; Butler and Hayes, 2001; Lee and Batchelor, 2002b; and Maithreepala and Doong, 2005). Microcosms were either "unamended" (U), which were not preincubated with electron donors or acceptors before spiking with PCE or TCE and represented baseline geochemical conditions; "amended" (A), which were preincubated with electron acceptors and/or donors in order to increase microbial activity and stimulate reactive mineral formation before spiking with PCE or TCE; or "killed" (K), which were amended and preincubated as described above, then treated by boiling water bath and antibiotics to kill bacteria prior to addition of PCE or TCE. Microcosm conditions are summarized in Table 3.

Except for those that were unamended, microcosms were set up to stimulate iron reduction (IR), sulfate reduction (SR), or methanogenesis (Meth). Electron donors and acceptors were added to the microcosms to increase both the concentrations of potentially reactive biogenic minerals and microbial activity. Duck Pond and Landfill aquifer microcosms were amended with amorphous Fe(III) gel (50 mM) (Cornell and Schwertmann, 2003), $FeSO_4$ (30 mM), or no electron acceptor in order to establish iron reducing, sulfate reducing, or methanogenic conditions, respectively. For AAFB microcosms, only sulfate reducing conditions were stimulated, since this most closely represented site conditions, where dissolved sulfate in the ground water is high (1.4-12.5 mM). Acetate (20 mM), lactate (40 mM), and ethanol (15 mM) were added as electron donors for iron reducing, sulfate reducing, and methanogenic conditions, respectively. While it is possible that the use of different electron donors affected the rate and/or extent of dechlorination in the microcosms, the choice of each electron donor was made to be certain to stimulate microorganisms known to be capable of iron reduction, sulfate reduction, or methanogenesis, respectively.

In order to prevent methanogenic bacteria present in soil and sediment samples from competing for electron donors and preventing the establishment of iron or sulfate reduction, 1 mM 2-bromo-

ethanosulfonic acid was added to the sulfate and iron reducing microcosms before adding electron acceptors and/or donors. This concentration was chosen because it is lower than concentrations reported to inhibit dechlorinating bacteria (2-3 mM) (Loffler et al., 1997; Chiu and Lee, 2001), but was still sufficient to inhibit methane production. After addition of these amendments, microcosms were preincubated until terminal electron acceptors were consumed in the sulfate and iron reducing microcosms or formation of methane leveled off in the methanogenic microcosms.

Then, the solid phase geochemistry was analyzed, microcosms were spiked with PCE or TCE, and monitored for abiotic and microbial transformation. Experiments with PCE were done for all microcosm conditions; experiments with TCE were done for selected conditions (Table 3). Sediments from one microcosm were imaged by SEM to visualize the morphology and surface conditions of biogenic minerals. The images (Figure 2), show rod-shaped bacteria (Figure 2(a) and (b) and nano- to micrometer scale crystalline precipitates (Figure 2(b) that could be FeS, Fe_3S_4, and/or FeS_2.

After preparation, microcosms were sealed with sterilized thick butyl rubber stoppers and aluminum crimp seals, removed from the anaerobic chamber and flushed with sterile cotton filtered N_2. Microcosms (except unamended ones) were preincubated until the desired terminal electron accepting process was established. We determined this by monitoring Fe(II) (aq), sulfate, and methane, for iron reducing (IR), sulfate reducing (SR), and methanogenic (Meth) conditions, respectively. During preincubation, microcosms were stored upside down at room temperature in the dark.

After preincubation, some microcosms were killed by placement in a boiling water bath for 15 minutes a total of three times at three day intervals. Then, 100 μg/mL of the wide spectrum antibiotics kanamycin and chloramphenicol were added to completely inhibit microbial metabolism (Wu et al., 2000). Both sulfate reduction and methane production were inhibited in the killed microcosms for up to 155 days.

After this procedure, butyl rubber septa were replaced with autoclaved Teflon-lined butyl rubber septa (West Pharmaceutical Services, Kearney, Nebraska) inside the anaerobic chamber. Ten milliliters of saturated PCE or TCE stock solution were then spiked into the microcosms to yield total concentration (mass in the aqueous plus gas phases divided by aqueous volume) of 24-103 μM (PCE) or 92-130 μM (TCE) in standards containing no solid phase. At the same time, an additional 5 mM of electron donor was spiked into the microcosms to support microbial reductive dechlorination. After preincubation with electron donors and acceptors (or without preincubation for unamended microcosms), one microcosm for each condition was sacrificed for geochemical analysis using techniques summarized below, and the results are summarized in Table 4. Each geochemical parameter was measured in duplicate. Dissolved Fe(II), sulfate, and methane were also measured to determine whether the desired redox conditions had been established.

All amended microcosms were prepared in triplicate, and unamended and killed microcosms were prepared in duplicate. Except if noted otherwise, reported concentrations, percent remaining values, and product recoveries are means of values measured in replicate microcosms; uncertainties are standard deviations of the mean. For brevity, microcosms conditions in Tables

3 and 4 and throughout the discussion below are given in abbreviated form. As an example, the abbreviation "DP-Meth-pH 8.2-TCE" is used hereafter for Duck Pond sediments preincubated under methanogenic conditions at pH 8.2 and spiked with TCE.

Geochemical Analysis

Sulfate was quantified using a Dionex ion chromatograph (IC) with an Ion Pac AG 11 guard column (4 × 50 mm) and an Ion Pac AS 11 anion analytical column (4 × 250 mm), coupled with an ED 50 conductivity detector. Solid phase S(-II) was measured using a method adapted from Ulrich et al. (1997) and described in Shao and Butler (2007). FeS was assumed to be equal to the molar concentration of solid phase S(-II), measured as cited above. After S(-II) measurement, the remaining solid was reduced by 1 M Cr(II)-HCl solution for 72 hrs to quantify Cr(II) reducible or Cr(II) extractable sulfur (CrES), which includes S(0), polysulfides, and pyrite (Canfield et al., 1986, Huerta-Diaz et al., 1993).

Ferrous iron species were measured by ferrozine assay as described in Lovley and Phillips (1987). For soluble Fe(II), the supernatant of the centrifuged solid/water slurry was acidified with anaerobic 0.5 N HCl at a 1:1 volume ratio prior to Fe(II) measurement. Sequential extractions were then performed to quantify different Fe(II) species in the solid phase (Heron et al., 1994). Five milliliters of solid/water slurry was collected and extracted with 1 M $MgCl_2$ for 5 hours to quantify weakly bound Fe(II) (Gibbs, 1973; Tessier et al., 1979). Extraction with 0.5 N HCl was used to quantify total solid phase Fe(II), including FeS and non-sulfur Fe(II) (Lovley and Phillips, 1987). Non-sulfur solid phase Fe(II) species are referred to as "surface associated Fe(II)". Strongly bound Fe(II) was calculated by subtracting weakly bound Fe(II) from surface associated Fe(II) (Shao and Butler, 2007). Total organic carbon (TOC) in the solid phase was measured with a TOC-5000 analyzer (Shimadzu Corp.) with a solid-sample module (SSM-5050) following the protocols provided by the manufacturer.

To assess the effect of heat treatment on abiotic mineral species that could potentially react with PCE and TCE, the solid phase mineral fractions described above were analyzed for two microcosm conditions (DP-IR-pH 8.2 and AAFB-8-SR-pH 7.2) before and after heat treatment by boiling water bath for 20 minutes. While heat treatment did not significantly affect the concentration of FeS, strongly bound Fe(II), or CrES (as evidenced by overlapping 95% confidence intervals for the concentration of these species before and after heat treatment), it did significantly lower the concentration of weakly bound Fe(II) in the one microcosm (DP-IR-pH 8.2) for which this species was above detection limits (Table 5). Specifically, for DP-IR-pH 8.2, weakly bound Fe(II) decreased by 37% upon heat treatment. While we considered the possibility that this decrease in weakly bound Fe(II) in the killed microcosms could cause us to underestimate the abiotic contribution to PCE or TCE reductive dechlorination, our conclusions about the relative importance of abiotic and microbial reductive dechlorination are in fact based on several lines of evidence—mainly analysis of reaction kinetics and product recoveries in live microcosms. Thus, the 37% decrease in weakly bound Fe(II) upon heat treatment in one representative microcosm (Table 5) does not change our overall conclusions.

For certain microcosms, we identified the more abundant minerals in the solid phase after preincubation by XRD using a Rigaku DMAX® x-ray Diffractometer (Table 4). Solid/liquid

samples were centrifuged at a relative centrifugal force of 1260 × g for 10 min and the solid was then freeze-dried under vacuum. Transfer to and from the freeze dryer was done in a glass tube with a custom vacuum valve to prevent exposure to the air. Freeze dried samples were then placed in the XRD sample holder inside the anaerobic chamber and mixed with petroleum jelly to retard the diffusion of oxygen to the sample. Quartz was the major mineral identified by XRD in the Landfill and Duck Pond solids and the two solid samples from AAFB that were analyzed (AAFB-12-SR-pH 7.2 and AAFB-14-SR-pH 7.2). We used the Hanawalt search/match method (Jenkins and Snyder, 1996), to identify minor mineral species by XRD. First, the peaks associated with quartz were eliminated from the sample pattern. Then the d-spacing value of the strongest peak in the remaining pattern was compared to the d-spacing values of the strongest peaks for iron minerals likely to be present in the natural environment. If a match was found, the sample pattern was searched for the other representative peaks for that mineral (i.e., the second or third strongest peaks). If these additional peaks were matched, then we concluded that that mineral was present in our sample. The whole XRD pattern associated with that mineral was then eliminated and the process restarted with the strongest peak in the remaining XRD pattern. If, however, no match was found for the original strongest peak not associated with quartz, that peak was ignored and the process restarted with the next strongest peak in the sample pattern. All minor mineral species identified in the microcosms using this approach are given in Table 4. In general, only unreactive Fe(III) oxides were identified, with the exception of one microcosm (L-SR-pH 8.2), where mackinawite was identified and two microcosms (AAFB-SR-12-pH 7.2 and AAFB-SR-14-pH 7.2) where magnetite was identified. As stated above, magnetite was added to the biowall area from which the solids used to construct these microcosms were obtained. Other potentially reactive minerals were below XRD detection limits.

One microcosm (DP-SR-pH 8.2) was analyzed using SEM with a JEOL JSM-880 High Resolution instrument. This microcosm was chosen because of the high concentration of FeS formed under sulfate reducing reactions (Table 4). The SEM sample was prepared using the method by Herbert and coworkers (Herbert et al., 1998) except that ethanol and not acetone was used for sample dehydration.

Calculation of Total Concentrations

Task 2 and 3 microcosms contained three phases: gas, aqueous, and solid. Concentrations discussed below and used in calculations "total concentrations" are equal to the sum of the aqueous, solid, and gas phase masses divided by the aqueous volume. Kinetic parameters were calculated assuming rapid equilibrium of PCE or TCE among the phases relative to kinetic transformation, and kinetic transformation in the aqueous phase only; the approach is described below.

Aqueous concentrations of PCE, TCE, and their dechlorination products ($C_{i,aq}$) were calculated from measured gas concentrations ($C_{i,g}$) using Henry's Law:

$$C_{i,aq} = \frac{C_{i,g}}{H_i} \tag{5}$$

where H_i is the dimensionless Henry's Law constant for species i. Henry's Law constants used in these calculations are given in Table 6. Total concentrations ($C_{i,T}$), defined here as the sum of the masses of species i in the gas, aqueous, and solid phases, divided by the volume of the aqueous phase, were calculated using the approach in Hwang and Batchelor (2000):

$$C_{i,T} = C_{i,aq}\left(1 + K_{i,s} + H_i \frac{V_g}{V_{aq}}\right) = C_{i,aq}F_i \qquad (6)$$

where $K_{i,s}$ is the solid-liquid partition coefficient, V_g and V_{aq} are volumes of the gas and aqueous phases (50 and 110 mL, respectively), and the partitioning factor (F_i) is defined as $\left(1 + K_{i,s} + H_i(V_g / V_{aq})\right)$. $K_{i,s}$ was calculated as follows (Hwang and Batchelor, 2000):

$$K_{i,s} = K_{i,d}\frac{m_s}{V_{aq}} \qquad (7)$$

where $K_{i,d}$ is the solid/water distribution coefficient and m_s is the mass of the solid phase in the microcosm (20 g). $K_{i,d}$ was estimated from the empirical relationship $K_{i,d} = K_{i,oc}f_{oc}$ (Karickhoff et al., 1979), where $K_{i,oc}$ is the solid phase organic matter/water distribution coefficient, and f_{oc} is the weight fraction of organic matter in the solid (i.e., total organic carbon or TOC, Table 4). $K_{i,oc}$ was estimated from published octanol/water partition coefficients ($K_{i,ow}$) (Howard and Meylan, 1997, Mackay et al., 2006) using two empirical equations: (1) for chlorinated aliphatics: $LogK_{i,oc} = 0.57LogK_{i,ow} + 0.66$ (Schwarzenbach et al., 2003); and (2) for ethylene and acetylene: $LogK_{i,oc} = -0.58LogS_i + 4.24$ (Doucette, 2000), where S_i is the aqueous solubility in μM, obtained from Howard and Meylan (1997) and Yalkowsky and He (2003) (Table 6). Estimated $K_{i,oc}$ values are given in Table 6.

Calculation of Observed Product Recoveries

Observed abiotic and biotic product recoveries (R) (Table 3) were calculated by summing the total concentrations of biotic products (i.e., TCE (for PCE), DCE isomers, VC and ethylene) or abiotic products (acetylene, and, except for Altus AFB microcosms, ethylene) by the total concentration of the reactant (PCE or TCE) at time zero ($C_{r,T,0}$):

$$R(\%) = \frac{\sum C_{p,T}}{C_{r,T,0}} \times 100\% = \frac{\sum C_{p,aq}F_p}{C_{r,T,0}} \times 100\% \qquad (8)$$

For the live AAFB microcosms, the kinetic data (as shown in Figure 3) indicate that, with the possible exceptions of AAFB-12-SR-pH 7.2-PCE and AAFB-14-SR-pH 7.2-PCE, the majority of ethylene was produced microbially, as evidenced by no-codetection of acetylene, and co-detection of VC. Therefore, we included ethylene in the biotic product recoveries (Table 3) for all live AAFB microcosms, except AAFB-12-SR-pH 7.2-PCE and AAFB-14-SR-pH 7.2-PCE. Because it was unclear if ethylene came from abiotic or microbial dechlorination in AAFB-12-

SR-pH 7.2-PCE and AAFB-14-SR-pH 7.2-PCE, we calculated neither abiotic nor microbial product recoveries for these microcosms (Table 3).

For AAFB killed microcosms, low concentrations of ethylene were observed even when VC was not detected. Thus, ethylene (and, when detected, acetylene) was included in the abiotic product recoveries for killed AAFB microcosms (Table 3).

Correction of Rate Constants for Partitioning among the Gas, Aqueous, and Solid Phases

Mass normalized rate constants (i.e., rate constants divided by mass loading) for PCE or TCE transformation by FeS, adjusted to or measured in a zero-headspace system (k_m), were taken from this study (Table 7) or the literature (Butler and Hayes, 1999, 2001; Zwank, 2004). The mass loadings of FeS in Zwank (2004) were estimated from the concentrations of reagents used to synthesize FeS. Rate constants for similar pH values were averaged, yielding the following k_m values ($Lg^{-1}d^{-1}$): PCE at pH 7-7.3: 2.41×10^{-4}; PCE at pH 8-8.3: 1.22×10^{-3}; TCE at pH 7.3: 7.28×10^{-4}; and TCE at pH 8-8.3: 1.95×10^{-3}. Then, we used the approach in Hwang and Batchelor (2000) to correct rate constants to account for partitioning of PCE or TCE among the gas, aqueous, and solid phases ($k_{m,corr}$):

$$k_{m,corr} = \frac{k_m}{F_i} \qquad (10)$$

where F_i is defined above, and the subscript "i" corresponds to the reactant (PCE or TCE). While V_g and V_{aq} were the same in all our microcosms, $K_{i,s}$ was not, since f_{oc} varied among the microcosms. Values of $k_{m,corr}$ for the case where f_{oc}=0, and therefore $K_{i,s}$ is zero are reported in Table 6. We then multiplied the values in Table 6 by the term $(1 + H_i(V_g / V_{aq})) / F_i$ to yield $k_{m,corr}$ values appropriate for the f_{oc} values of each microcosm. These values of $k_{m,corr}$ were used to estimate half lives for abiotic PCE and TCE transformation based on FeS mass loadings in the microcosms. These values are discussed in the Results and Accomplishments section.

Results and Accomplishments

Results and accomplishments are discussed below by Task.

Distinguishing Abiotic and Biotic Transformation by Stable Carbon Isotope Fractionation (Task 1).[4]

The objective of this Task was "to assess whether stable (i.e., non-radioactive) carbon (C) isotope fractionation can be used to distinguish between abiotic and biotic reductive dechlorination of TCE and PCE". We hypothesized that the greater extent of isotope fractionation generally observed for abiotic versus biotic reductive dechlorination of PCE and TCE was due to rate control by the bond cleavage step (step 3, equation 1) for abiotic reactions, and rate control (or partial rate control) by non-fractionating steps for microbial reactions. This suggestion is reasonable considering the very slow rates of mineral mediated transformation of PCE and TCE (Sivavec et al., 1995; Sivavec et al., 1996; Sivavec and Horney, 1997; Butler and Hayes, 1999; Hwang and Batchelor, 2001; Butler and Hayes, 2001; Weerasooriya and Dharmasena, 2001; Lee and Batchelor, 2002a; Lee and Batchelor, 2002b, Maithreepala and Doong, 2005), which would make rate control by mass transport or surface complexation unlikely. To test our hypothesis and meet our objective, we studied both abiotic and microbial reductive dechlorination and performed kinetic and isotope analysis in well defined model systems. Since preliminary experiments with a variety of mineral species (iron sulfide (FeS), magnetite, pyrite, sulfate green rust (GR-SO_4), chloride green rust (GR-Cl), and goethite treated with HS^- or Fe^{+2}) showed that FeS was the most reactive mineral in abiotic PCE and TCE dechlorination, we chose FeS as a model abiotic system for comparison with microbial reactions. Reaction of PCE and TCE with a number of the other minerals listed above were then studied further (see below). We compared results for FeS to several bacterial systems including those converting PCE and TCE to *cis*-DCE and a consortium converting PCE and TCE to ethylene. Based on our results and those of others, we provide an explanation for differences in ε_{bulk} values for abiotic and microbial reductive dechlorination of PCE and TCE.

Abiotic Reductive Dechlorination and Isotope Fractionation

Figure 4 shows that PCE and TCE were degraded following pseudo first order kinetics at pH 7, 8, and 9 (PCE), and pH 8 and 9 (TCE) in the presence of FeS. Surface area normalized pseudo first order rate constants (k_{SA} values), adjusted to equal those that would be measured in a zero-headspace system (Burris et al., 1996) are reported in Table 7. For TCE at pH 7, degradation was too slow to calculate a rate constant, so no value of k_{SA} is reported in Table 7 and no line showing a pseudo first order fit is shown in Figure 4. Dechlorination of PCE and TCE by FeS was strongly pH-dependent with faster rates at higher pH values, in agreement with previously reported results (Butler and Hayes, 2001).

Solution pH also affected isotope fractionation for PCE and TCE transformation by FeS, quantified by the difference in ε_{bulk} values (Table 7) and illustrated by the change in $\delta^{13}C$ with f

[4] The information discussed in this section was reported in Liang et al. (2007) and Liang et al. (2009, in press).

(Figure 5). The magnitude of isotope fractionation decreased (i.e., ε_{bulk} values became less negative) with increasing pH for both PCE and TCE. Acid/conjugate pairs such as $\equiv FeOH_2^+/\equiv FeOH$ (Butler and Hayes, 1998) and $\equiv Fe^{III}OFe^{II+}/\equiv Fe^{III}OFe^{II}OH^0$ (Charlet et al., 1998; Liger et al., 1999; Danielsen and Hayes, 2004) have been proposed to exist at reactive mineral surfaces. As discussed in greater detail elsewhere (Huskey, 1991; Elsner et al., 2005), the susceptibility of a bond containing a particular isotope to cleavage (and therefore fractionation) depends in part on its molecular vibrations in the transition state. Assuming the transition state consists of an activated complex between the mineral surface and PCE or TCE, pH-dependent changes in the chemical composition of the mineral surface could affect the transition state structure, molecular vibrations, and isotope fractionation. By "transition state structure" we mean the lengths and angles of partially broken and partially formed bonds in the transition state.

Our ε_{bulk} value for PCE dechlorination by FeS at pH 7 (-30.2 ± 4.3‰) is quite different than that measured by Zwank (2004) at an initial pH of 7.3 (-14.7‰). This difference may be due to the presence of 4 mM dissolved Fe(II) (added as $FeCl_2$) in Zwank's experiments. Addition of dissolved Fe(II) would increase non-sulfide Fe(II) at the FeS surface, both weakly bound (i.e., $MgCl_2$ extractable) and strongly bound (i.e., 0.5 N HCl extractable) (Shao and Butler, 2007), which might have influenced ε_{bulk} values. The different ε_{bulk} values could also be due to the presence of HEPES buffer in our experiments, compared to Zwank's unbuffered experiments. Since TCE dechlorination by FeS at pH 7 did not proceed to a great enough extent to calculate an ε_{bulk} value (Figure 4), we cannot fairly compare our results to Zwank's results for TCE obtained pH 7.3 (-9.6‰) (Zwank, 2004). Our values at pH 8 and 9, are, however, significantly more negative, perhaps for the reasons described above.

Zwank (2004) found more isotope fractionation for PCE versus TCE dechlorination by FeS, which he attributed to different transition state compositions for PCE and TCE. Our experiments showed the same trend at pH 9, but the opposite trend at pH 8, although ε_{bulk} values for PCE and TCE at pH 8 and 9 are similar (Table 7). ε_{bulk} values could not be compared at pH 7 because the TCE reaction proceeded too slowly at this pH in our experiments to measure an ε_{bulk} value.

Biotic Reductive Dechlorination and Isotope Fractionation

Plots of C/C_0 versus time for microbial transformation of PCE and TCE are shown in Figure 6. Microbial dechlorination took place solely by hydrogenolysis, as evidenced by the good mass recovery (generally >80%) of hydrogenolysis products (Figure 6). ε_{bulk} values for microbial dechlorination are reported in Table 7 and plots of $\delta^{13}C$ versus *f* are shown in Figure 5. Our measured ε_{bulk} values for dechlorination by *Sm* are similar to most previously reported values (Zwank, 2004; Nijehuis et al., 2005), but less negative than the value of -16.4 ± 1.5‰ reported by Lee et al. (2007) for TCE.

Table 7 and Figure 5 also show a greater magnitude of isotope fractionation for microbial TCE dechlorination compared to PCE dechlorination for all cultures, as found in previous studies (Slater et al., 2001; Zwank, 2004). For *Sm*, this trend was explained by different values of "commitment to catalysis" for PCE and TCE (Zwank, 2004). The commitment to catalysis equals the rate of step 3 divided by the reverse of step 2 (equation 1). Different commitments to catalysis would reflect different affinities of PCE and TCE for the dehalogenase enzyme.

Comparison of Abiotic Versus Biotic Microcosms

Isotope fractionation of PCE and TCE during abiotic transformation was consistently stronger than fractionation during biotic transformation (Table 7, Figure 5). To understand why, we calculated additional isotope parameters for the abiotic and biotic systems. While ε_{bulk} values represent the overall isotope fractionation for an entire molecule, the kinetic isotope effect for carbon (KIE_C) equals the rate constant for cleavage of a ^{12}C-Cl bond divided by that for a ^{13}C-Cl bond (i.e., $^{12}k/^{13}k$), and thus represents isotope effects resulting from C-Cl bond cleavage. We calculated values of the "apparent" kinetic isotope effect for carbon ($AKIE_C$) from ε_{bulk} values using the approach described in Elsner et al. (2005) and Zwank et al. (2005a). This approach considers two factors: (1) the presence of C atoms at positions in a molecule that are non-reactive (i.e., C atoms with no potential for bond cleavage) and (2) the presence of different isotopes at more than one equally reactive position in a molecule (intra-molecular competition). These two factors can result in dilution or enhancement of the $AKIE_C$ and can be accounted for using the following equation (Zwank et al., 2005a):

$$\frac{1}{\mathrm{AKIE_C}} = \frac{z \cdot n \cdot \varepsilon_{\mathrm{bulk}}}{x \cdot 1000} + 1 \qquad (11)$$

where n is the number of C atoms in the molecule, x is the number of C atoms with the potential for bond cleavage, and z is the number of C atoms having equal reactivity.

We then compared our calculated $AKIE_C$ values with theoretical KIE_C values for C-Cl bond cleavage to determine whether the rate limiting processes in the overall transformation reaction involved bond cleavage (step 3 in equation 1) or other steps. Assuming bond cleavage is rate limiting, the $AKIE_C$ and KIE_C values should be the same (Elsner et al., 2005). We used a KIE_C value of 1.03, estimated by Semiclassical Streitwieser limits (Huskey, 1999) and assuming 50% bond cleavage in the transition state (Elsner et al., 2004b; Elsner et al., 2005). The term "semiclassical" means this parameter was calculated using a combination of classical and quantum mechanical assumptions (Huskey, 1999). While the extent of bond cleavage in the transition state is not known, this value provides a consistent basis for comparison of our biotic and abiotic experiments. The lower and upper limits of the KIE_C using Semiclassical Streitwieser limits are 1.00 (for 0% bond cleavage in the transition state) and ~1.057 (for 100% bond cleavage in the transition state) (Elsner et al., 2004b).

The most commonly proposed mechanism for hydrogenolysis involves a rate limiting carbon-halogen bond cleavage step that takes place concurrent with electron transfer (Castro and Kray, 1963). For PCE hydrogenolysis, x=2 and z=2, since both C atoms are identical chemically and therefore have equal potential for bond cleavage. For TCE hydrogenolysis, x=1 and z=1, since the lengths and therefore strengths of the C-Cl bonds vary with C position (Riehl et al., 1994; Yokoyama et al., 1995), and thus the two C atoms have different potentials for cleavage. Additional evidence for the unequal reactivity of the two C atoms in TCE is the preponderance of *cis* 1,2-DCE and not 1,1-DCE, as the TCE hydrogenolysis product.

While biotic reductive dechlorination took place entirely by hydrogenolysis, abiotic reductive dechlorination of PCE and TCE occurred by both hydrogenolysis and reductive β-elimination, as evidenced by detection of the products of both reaction pathways, specifically *cis*-DCE and, for PCE, TCE (hydrogenolysis), and acetylene (reductive β-elimination). PCE and TCE reductive β-elimination yields acetylene via short-lived dichloroacetylene (for PCE) and chloroacetylene (for TCE) intermediates (Roberts et al., 1996). Due to problems quantifying acetylene, we don't report or illustrate our reductive β-elimination product yields, but a previous study found that the major pathway for PCE and TCE transformation by FeS was reductive β-elimination and not hydrogenolysis (Butler and Hayes, 1999). Consistent with this, we calculated TCE hydrogenolysis yields of 12.7 % at pH 8 and 2.6 % at pH 9 using the method of Fennelly and Roberts (1998), confirming that hydrogenolysis was a minor pathway for TCE. We could not quantify PCE hydrogenolysis yields without acetylene concentration values, since the TCE from PCE hydrogenolysis can transform to acetylene via reductive β-elimination (Butler and Hayes, 1999).

Two mechanisms are possible for reductive β-elimination, each with different x and z values for equation 11. (Regardless of pathway or mechanism, n=2 for both PCE and TCE.) It was previously proposed that, as for hydrogenolysis, reductive β-elimination of PCE and TCE by FeS involves an initial rate limiting C-Cl cleavage step (Butler and Hayes, 1999). We refer to this as "mechanism 1" below. Another mechanism involving simultaneous carbon-halogen bond cleavage and C-C bond formation, referred to below as "mechanism 2", is also well known for nucleophiles like sulfide (Ramasamy et al., 1978; Baciocchi, 1983; Curtis and Reinhard, 1994; Perlinger et al., 1996; Miller et al., 1998). For reductive β-elimination by mechanism 1, x and z for PCE and TCE are identical to those for hydrogenolysis. For mechanism 2, x=2 for PCE and TCE since both C-Cl bonds are broken in the rate limiting step, and z=1, since there is no intramolecular competition (Zwank et al., 2005a). $AKIE_C$ values for reductive β-elimination were calculated first assuming mechanism 1, then mechanism 2. All values of n, x, and z and the resulting values of $AKIE_C$ are summarized in Table 7.

We first observed that the $AKIE_C$ values for microbial PCE and TCE reductive dechlorination were generally less than the theoretical KIE_C of ~1.03 for C-Cl bond cleavage. This could be due to rate limitation by one or more non-fractionating processes (i.e., steps 1, 2, 4, and/or 5 in equation 1), rather than C-Cl bond cleavage. On the other hand, TCE dechlorination by *Sm*, and PCE and TCE dechlorination by BDI, had $AKIE_C$ values closer to the theoretical value than did the other cultures (Table 7), suggesting that the rate of PCE or TCE dechlorination by these cultures is more strongly influenced by the rate of C-Cl bond cleavage (equation 1, step 3).

Table 7 shows that most $AKIE_C$ values for abiotic PCE and TCE reductive β-elimination calculated assuming mechanism 1 are near the top or outside the theoretical range of KIE_C values for C-Cl bond cleavage calculated using Semiclassical Streitwieser limits (Elsner et al., 2004b) (i.e., 1.00-1.057). While $AKIE_C$ values calculated assuming mechanism 2 are within this range (Table 7), comparison of these values to the theoretical KIE_C for a single C-Cl bond cleavage is not valid since other bond breaking and formation steps are also involved in a concerted mechanism like mechanism 2. Specifically, the strong driving force for formation of an additional C-C bond (i.e., the triple bond in the reactive chloroacetylene and dichloroacetylene intermediates that yield acetylene), likely influences the theoretical KIE_C for mechanism 2, since

atomic mass (i.e., ^{12}C or ^{13}C) affects the driving force for bond formation as well as bond cleavage.

Despite uncertainty about the mechanism of reductive β-elimination of PCE and TCE by FeS, the $AKIE_C$ values for PCE and TCE transformation by this pathway probably lie between those calculated assuming mechanisms 1 and 2. And it is noteworthy that these values are generally significantly larger than those for microbial dechlorination of PCE and TCE (Table 7), suggesting that fractionating processes such as C-Cl bond cleavage, and not mass transport steps like diffusion and surface complex formation, limit the rate of abiotic reductive dechlorination. This is consistent with the slow rate of FeS mediated PCE and TCE transformation (half-lives on the order of months (Figure 4), for which mass transport and reactive complex formation are likely to be much faster than bond cleavage and associated electron transfer.

Measurement of Kinetic and Isotope Parameters for Other Reactive Minerals

Next, we measured isotope parameters for other minerals shown to be reactive with chlorinated solvents. We did a series of batch experiments with the following minerals: chloride green rust (GR-Cl), sulfate green rust (GR-SO_4), pyrite, magnetite, and Fe(II) or S(-II) treated goethite. Plots of concentration versus time for transformation of PCE and TCE by GR-Cl, pyrite, GR-SO_4, and magnetite are shown in Figures 7 (PCE) and 8 (TCE), and mass recoveries of reactants and products and, in some cases, surface area normalized pseudo first order rate constants, are given in Tables 1 (PCE) and 2 (TCE). There was little transformation of either PCE or TCE by Fe(II) and S(-II)-treated goethite over 7-8 months (Tables 1 and 2); therefore these reactions are not illustrated in Figures 7 and 8. Surface area normalized rate constants were calculated only in cases where sufficient transformation of PCE or TCE (at least 15-20%) had occurred by the end of the experiment (Tables 1 and 2). Even for reactions that were too slow to calculate rate constants, appearance of reaction products (Tables 1 and 2) is evidence that some reductive dechlorination of PCE and TCE took place in the presence of all mineral systems that were studied.

Two main pathways have been proposed for abiotic reductive dechlorination of PCE and TCE (Figure 1): (1) hydrogenolysis, or replacement of a chlorine by a hydrogen in sequence to produce TCE (for PCE), *cis*-DCE, VC and ethylene, and (2) reductive β-elimination that forms acetylene via the short-lived intermediate chloroacetylene (Roberts et al., 1996). The main reaction products for PCE and TCE transformation by all minerals are consistent with the reductive β-elimination pathway (Tables 1 and 2). Detection of *cis*-DCE under some conditions (Tables 1 and 2) indicates that hydrogenolysis is a minor pathway. Since we detected no VC under any conditions, we conclude that the ethylene detected (Tables 1 and 2) formed by acetylene hydrogenation (Arnold and Roberts, 2000; Jeong et al., 2007).

The most reactive minerals with both PCE and TCE under the conditions of these experiments were GR-Cl and pyrite, and faster disappearance of TCE than PCE was observed for both minerals (Figures 7 and 8; Tables 1 and 2). The observed reactivities of PCE and TCE with GR-Cl are similar to those reported by Maithreepala and Doong (2005), who found 67% of PCE and 79% of TCE remaining after reaction with GR-Cl for 35 days (the GR-Cl surface area loading was not reported), although the relative reactivity reported by Maithreepala and Doong (2005)

(PCE>TCE) differs from the results reported here (Figures 7 and 8; Tables 1 and 2). Small differences in surface composition may affect the relative rates of PCE and TCE transformation by different minerals.

Like this study, Lee and Batchelor (2002a) also found that TCE was transformed faster than PCE by pyrite, although their reported surface area normalized rate constants for PCE and TCE are closer together than those reported here (Tables 1 and 2). In their experiments, the pyrite surface area loadings and initial concentrations of PCE and TCE may have resulted in a limitation of reactive surface sites (Lee and Batchelor, 2002a) that could have limited the reaction rate for PCE, TCE, or both.

Weerasooriya and Dharmasena (2001) reported much faster transformation of TCE than in this study (their data indicate a TCE half life of approximately 1 day at pH 8 for 2 m^2 L^{-1} pyrite (Weerasooriya and Dharmasena, 2001). Their more rapid TCE transformation may have been caused by different impurities in the pyrite used for TCE transformation, since transition metal impurities in pyrite can catalyze contaminant transformation reactions (Carlson et al. 2003).

Although the reactions of PCE and TCE with GR-SO_4, magnetite, and Fe(II)- and S(-II)-treated goethite were too slow to calculate rate constants (Tables 1 and 2), mass recovery data for these experiments can in some cases be used to compare the reactivities of the different minerals with PCE and TCE, since amount of PCE or TCE removed and the yields of reaction products are proportional to rates. For GR-SO_4, total product yields were approximately 17% for PCE after 111 days and approximately 6% for TCE after 148 days. (Product yields were calculated by summing the mass recoveries of reaction products in Tables 1 and 2.) Lee and Batchelor (2002b) found a greater extent of PCE and TCE disappearance in the presence of GR-SO_4 (30-40% over approximately two months) than in this study. The difference might be explained by a higher GR-SO_4 surface area loading (604 m^2/L in Lee and Batchelor (2002b) compared to 92 m^2/L used in these experiments). Comparing the total product yields for PCE and TCE transformation by GR-SO_4 (Tables 1 and 2) suggests that, unlike our results for GR-Cl and pyrite, PCE was more reactive with GR-SO_4 than was TCE. Lee and Batchelor (2002b) also found significantly faster transformation of PCE than TCE by GR-SO_4. Comparing the intrinsic reactivity of GR-SO_4 with GR-Cl and pyrite is not possible since we could not calculate a surface area normalized rate constant for reaction of PCE and TCE with GR-SO_4 due to the slow reaction. It is likely that faster rates of PCE and TCE transformation would be observed at higher GR-SO_4 surface area loadings; thus the surface area normalized rate constants for PCE and TCE transformation by GR-SO_4 could be similar to those for GR-Cl and pyrite.

The extent of PCE and TCE transformed by magnetite over approximately 3 months was similar to that reported by Lee and Batchelor (2002a), but TCE disappearance in this study was significantly slower than that found by Sivavec and Horney (1997), who reported a half life for TCE reaction with magnetite of 19 days. This difference may be due to different magnetite synthesis methods, which Sivavec and Horney do not report. As was the case for pyrite, Lee and Batchelor (2002a) report a slightly larger rate constant for PCE versus TCE transformation by magnetite. In this study, we also found more PCE than TCE was transformed by magnetite over 141-148 days (i.e., less unreacted PCE versus TCE remained after that time) (Tables 1 and 2), suggesting greater reactivity of magnetite with PCE versus TCE. Unlike for GR-SO_4, however,

quantitative comparison of product yields for PCE and TCE is not possible due to uncertainties in trace product measurements (Tables 1 and 2). As with GR-SO_4, we could not calculate surface area normalized rate constants for reaction of PCE and TCE with magnetite, so we cannot compare the intrinsic reactivity of magnetite to that of GR-Cl, pyrite, or GR-SO_4. Considering the very high surface area loadings used for magnetite experiments (Tables 1 and 2), however, it is unlikely that surface area limited the reaction rate, and magnetite appears to be significantly less reactive with PCE and TCE than the other minerals discussed so far.

There was no significant difference in the amount of PCE or TCE removed or total product yields (<2%) for Fe(II)- and S(-II) treated goethite after 222-233 days (Tables 1 and 2). This slow PCE or TCE transformation is in contrast to the high reactivity of Fe(II)-treated goethite with carbon tetrachloride and hexachloroethane reported under similar conditions (Elsner et al., 2004a; Shao and Butler, 2007). For S(-II)-treated goethite, the estimated quantity of FeS formed (approximately 0.06 g L^{-1} based on the reaction stoichiometry for Fe(III) oxide reductive dissolution and FeS formation (Pyzik and Sommer 1981), was significantly lower than the FeS mass loading in other experiments at similar pH (Table 7, Figure 4) and was probably inadequate to cause significant transformation of PCE and TCE in the time scale of these experiments.

The particularly low total mass recovery for TCE transformation by pyrite (Table 2) led us to hypothesize that additional non-volatile or water soluble reaction products, such as acetate, ethanol, and acetaldehyde (Glod et al., 1997), had formed in this experimental system. In order to identify these products and improve the total mass recovery, an additional batch experiment was performed using a much higher initial TCE concentration (7.5 mM) to make it possible to detect these products using analytical methods with significantly higher detection limits. In this experiment, after 18 days, approximately 16% of TCE had disappeared, and the following products were detected (in decreasing order of concentration): acetate, *cis*-DCE, ethanol, acetaldehyde, and ethylene (Table 2). Although the reaction did not proceed to a great extent for the higher initial concentration of TCE (high $[TCE]_0$) (probably due to the much higher ratio of TCE to pyrite surface area for the high $[TCE]_0$ experiment (Table 2), the total mass recovery was much higher (Table 2), indicating that the newly detected reaction products (acetate, ethanol, and acetaldehyde) likely account for the missing mass in the pyrite/low $[TCE]_0$ experiment (Table 2). In addition to hydrogenation to ethylene, acetylene produced by reductive β-elimination can be oxidized to acetaldehyde and acetic acid in the presence of some transition metals (Moggi and Albanesi, 1991) and aldehydes such as acetaldehyde can be reduced to the corresponding alcohol (which, for acetaldehyde, is ethanol) by catalytic hydrogenation or chemical reductants (Morrison and Boyd, 1983). Thus, the products detected in the pyrite/high $[TCE]_0$ experiment (Table 2) are consistent with initial reductive β-elimination of TCE to acetylene. (*cis*-DCE, which comes from TCE hydrogenolysis, was a minor product.) It is possible that similar products could form during the transformation of PCE by pyrite, but this must be confirmed experimentally.

ε_{bulk} values and plots of $\delta^{13}C$ versus fraction remaining are shown for the reaction of TCE with GR-Cl and pyrite in Figure 9. (These are the only experimental mineral systems other than FeS for which there was enough transformation of the parent compound to accurately calculate ε_{bulk} values.) Significantly stronger isotope fractionation was observed for TCE dechlorination by FeS at pH 8 (ε_{bulk} = - 33.4 ± 1.5‰) (Table 7). A significantly less negative value for TCE dechlorination by FeS (-9.6‰) was also reported by Zwank (2004) for somewhat different

conditions (4 mM dissolved Fe(II); no pH buffer; initial pH=7.3). Considering the relatively long half lives for the reactions discussed here (tens to hundreds of days), it is unlikely that mass transport (e.g., diffusion of contaminants to the surface, complexation with the surface, or diffusion of products away from the surface) limited the overall rate of TCE transformation and "diluted" (Zwank et al. 2005b) the isotope fractionation associated with bond cleavage in our experiments. According to Zwank et al. (2005b), assuming rate limitation by surface electron transfer and not mass transport to reactive surface sites, a more negative ε_{bulk} value suggests a greater extent of C-Cl bond cleavage in the transition state. Thus, we conclude that the less negative ε_{bulk} values for TCE transformation by GR-Cl and pyrite (Figure 9) compared to that for TCE transformation by FeS under the same conditions (Figure 4) is due to a smaller extent of bond cleavage in the transition state. Different transition state structures for TCE transformation by GR-Cl, pyrite, and FeS could result from different modes of interaction between TCE and the mineral surfaces (Zwank et al. 2005b). For example, TCE could coordinate with surface iron atoms (Arnold and Roberts, 2000), with the disulfide groups in pyrite (as has been postulated for carbon tetrachloride transformation by pyrite (Kriegman-King and Reinhard, 1994), or with no surface atoms (i.e., no covalent bonding between TCE and the mineral surface) in the case of outer-sphere electron transfer.

Correlation of Geochemical Parameters with Abiotic Reductive Dechlorination; Validation at DoD Field Sites (Tasks 2 and 3)[5]

Our objectives under Tasks 2 and 3 were "to identify the geochemical conditions most strongly correlated with high rates of abiotic PCE and TCE reductive dechlorination in well-defined microcosm studies (Task 2); and (3) to validate and apply our findings at DoD field sites contaminated with PCE or TCE (Task 3)". We also sought to compare the relative importance of microbial and abiotic transformation of PCE and TCE under a variety of geochemical conditions. We assessed the importance of microbial and abiotic reductive dechlorination by analysis of reaction products and reaction kinetics, utilization of killed controls, comparison of observed half lives to those of laboratory studies using pure minerals, and stable carbon isotope analysis. To study a range of geochemical conditions, we set up anaerobic microcosms using aquifer solids from three locations, and then incubated them with different terminal electron acceptors to generate reactive Fe(II) and S(-II) minerals and also to stimulate general microbial activity. Sequential extractions were used to characterize the microcosm solid phase geochemistry. Because we collected an analyzed data for both Tasks 2 and 3 together, they are discussed together below. Kinetic data for the microcosms is reported in Table 3 and geochemical data is reported in Table 4.

Relative Importance of Abiotic and Biotic Reductive Dechlorination

Normalized concentrations of PCE and TCE versus time were plotted for all the microcosm conditions (Figure 10) and time courses for representative microcosms, which also show normalized concentrations of detected reaction products, were also plotted (Figure 11). Normalized concentrations for antibiotic/heat killed microcosms along with their live counterparts prepared under the same conditions, as well as time courses for all live AAFB microcosms, are shown in Figures 12 and 3, respectively. Evidence from these figures indicates

[5] The information in this section was reported in Dong et al., 2009, in press.

that in most cases, reductive dechlorination of PCE and TCE in the microcosms took place primarily by microbial transformation by indigenous dechlorinating bacteria rather than abiotic transformation by reactive minerals. This evidence includes: (1) slow rates and a small extent of PCE transformation in killed microcosms compared to the amended and unamended microcosms prepared under the same conditions (Figure 12); (2) a lag time followed by a rapid pseudo-zero-order (i.e., straight line or constant slope) disappearance of PCE or TCE that is characteristic of microbial transformations, rather than an initial pseudo-first-order reaction characteristic of abiotic reactions (Figures 3, 10, 11, and 12); (3) near quantitative accumulation of PCE and TCE hydrogenolysis products, such as TCE (for PCE), *cis* 1,2-DCE, and VC, for all microcosms where there was significant transformation of PCE or TCE (Figure 11) (two possible exceptions to this trend, AAFB-12-SR-pH 7.2-PCE and AAFB-14-SR-pH 7.2-PCE, are discussed further below); and (4) the rapid transformation of PCE or TCE after the initial lag period, compared to the relatively slow abiotic transformation of these compounds. For instance, using previously reported mass-normalized rate constants for PCE and TCE transformation by FeS that were corrected for partitioning among the gas, aqueous, and solid phases (Table 6), we estimated that the half lives for PCE or TCE transformation by the FeS present in our microcosms would be 900-5,000 days (PCE) or 500-1,000 days (TCE) at the highest FeS mass loading (approx. 0.9 g/L) and a median fraction organic carbon (f_{oc}) value of 0.002 (Table 4). (Longer half lives are for pH ≈ 7; shorter half lives are for pH ≈ 8.) While other reactive minerals could have also contributed to abiotic PCE and TCE transformation in the microcosms, their mass loadings and reactivity are likely to be at least the same order of magnitude as those for FeS, so abiotic reactions alone cannot account for the rapid transformation of PCE and TCE following the lag period (Figure 10).

To quantify the extent of microbial and abiotic PCE and TCE transformation, we calculated product recoveries for both processes by dividing the summed total concentrations of abiotic or microbial dechlorination products at the last sampling time (see Table 3, column 2) by the initial total concentration of PCE or TCE, and multiplying by 100 % (Lee and Batchelor 2002a). Calculation details are described above and abiotic and microbial product recoveries are reported in Table 3. While product recoveries are not constant with time, their calculation allows comparison of the relative importance of abiotic versus microbial PCE and TCE transformation among microcosms sampled at approximately the same time. For some live AAFB microcosms, we were not able to distinguish whether the ethylene detected in the microcosms came from microbial hydrogenolysis of VC or from abiotic hydrogenation of acetylene (e.g., Jeong et al. (2007); in these cases, product recoveries were not calculated.

Table 3 shows that abiotic product recoveries were never significantly higher than 1%. Considering only live microcosms, there were two conditions where the abiotic product recovery exceeded the microbial product recovery, one for PCE transformation (DP-IR-pH 8.2; Figure 11d, Table 3), and one for TCE transformation (L-IR-pH 8.2; Figure 11f, Table 3). For these microcosms, both abiotic and microbial transformation were slow (close to 100% of the PCE or TCE remained after approximately 100 days (Table 3), but abiotic products accumulated to a greater extent than did microbial products, suggesting that abiotic processes could be more important for PCE or TCE transformation in subsurface environments under conditions where dechlorinating bacteria are not active. The high pH (8.2) of these microcosms may have inhibited the activity of dechlorinating bacteria. In five other live microcosms (DP-Meth-pH 8.2-PCE; L-IR-pH 8.2-PCE; L-SR-pH 7.2-PCE; L-SR-pH 8.2-TCE; and L-Meth-pH 8.2-TCE), the abiotic

and microbial product recoveries were relatively close to each other (within a factor of 10). Four of these five were incubated at pH 8.2, providing additional evidence that, at least in some cases, higher pH values may not be optimal for growth of dechlorinating bacteria. In all other samples, microbial product recoveries were much higher than abiotic product recoveries.

We considered the possibilities that our low abiotic product recoveries could be due to microbial transformation of abiotic dechlorination products (e.g., acetylene). To test this possibility, we spiked acetylene into the Duck Pond and Landfill microcosms at a total concentration of approximately 2 μM, which was close to the highest concentration of acetylene observed in our microcosms. Figure 13 shows that acetylene was transformed within approximately 2-4 days in the Duck Pond microcosms, but remained essentially constant after more than 40 days in all the Landfill microcosms. We then treated the three Duck Pond microcosms showing the fastest acetylene transformation in a boiling water bath for 15 min and respiked them with acetylene. Following this, no acetylene transformation was observed, indicating that acetylene transformation was microbial, not abiotic. Microbial fermentation of acetylene has been reported previously (Schink, 1985). Despite the loss of abiotically-generated acetylene via microbial transformation in the Duck Pond microcosms, however, there are still several lines of evidence (discussed above) indicating the greater involvement of microbial versus abiotic transformation of PCE and TCE in the microcosms. Consumption of acetylene by indigenous microorganisms cannot account for the low abiotic product recoveries observed for almost every microcosm condition (Table 3), including the Landfill microcosms, where acetylene transformation was not observed (Figure 13).

Two possible exceptions to the trend of higher microbial versus abiotic product recoveries are AAFB-12-SR-pH 7.2-PCE and AAFB-14-SR-pH 7.2-PCE (Table 3, Figures 3(d) and (e). In neither case could we determine if the abundant ethylene in these microcosms came from abiotic or microbial processes, or some combination of both. The existence of a lag phase before the onset of pseudo-zero-order PCE disappearance (Figures 3(d) and (e) and the inhibition of PCE disappearance in killed controls (Figure 12), however, are consistent with a greater role for microbial PCE dechlorination in these microcosms.

Isotope Fractionation during Reductive Dechlorination

Stable carbon isotope fractionation is another tool that may provide information about the predominant process for PCE or TCE transformation, i.e., abiotic or microbial. Several recent articles describe in detail the principles of isotope analysis for environmental applications (Elsner et al., 2005). While a range of ε_{bulk} values has been reported for both abiotic and microbial transformation of PCE and TCE, the range of reported ε_{bulk} values for abiotic PCE transformation in batch systems is generally more negative than that for microbial PCE transformation, shown in Table 7 and Figures 5 and 9, as well as other references (Bloom et al., 2000; Slater et al., 2001, 2002, 2003; Schuth et al., 2003; Zwank, 2004; Nijenhuis et al., 2005; Cichocka et al., 2007, 2008; Lee et al., 2007). Thus, very large (in magnitude), negative ε_{bulk} values are suggestive of abiotic PCE transformation while very small (in magnitude), negative ε_{bulk} values are suggestive of microbial PCE transformation. The limitation of this approach lies in the exceptions; specifically, negative ε_{bulk} values that are intermediate in magnitude have been reported for both abiotic and microbial PCE transformation. As just one example, an ε_{bulk} value of -14.7‰ was reported for

abiotic transformation of PCE by FeS (Zwank, 2004), while a more negative value of -16.7‰ was reported for microbial transformation of PCE (Cichocka et al., 2008). Thus, intermediate ε_{bulk} values such as these are of less value in assessing the predominant reaction pathway for PCE transformation (abiotic or microbial), than are very large or small (in magnitude) values. Also, interpretation of ε_{bulk} values must always be done with caution and in conjunction with other lines of evidence such as those described above (e.g., analysis of reaction order and reaction products). Finally, ε_{bulk} values for abiotic and microbial transformation of TCE are typically closer together than are those for PCE (illustrated in Table 7 and also discussed by Zwank (2004), making isotope fractionation less useful for differentiating abiotic and microbial transformation of TCE versus PCE.

Plots of $\delta^{13}C$ versus fraction PCE or TCE remaining (C/C_0) for all microcosms for which significant PCE or TCE transformation took place are plotted in Figure 14. ε_{bulk} values were calculated using the Rayleigh equation (Mariotti et al., 1981). For PCE, ε_{bulk} values for the Duck Pond and all but one AAFB microcosm showed weak isotope fractionation (these ε_{bulk} values ranged from -0.71 to -3.1‰), which is typical of microbial reductive dechlorination of PCE (shown in Table 7 of this report as well as other references (Bloom et al., 2000; Slater et al., 2001; Nijenhuis et al., 2005; Cichocka et al., 2007, 2008), and therefore consistent with the other evidence for microbial dechlorination discussed above. Significantly stronger isotope fractionation was measured in the remaining AAFB microcosm (AAFB-14-SR-pH 7.2-PCE; ε_{bulk} = -8.5‰) and the Landfill microcosms incubated under methanogenic conditions (ε_{bulk} = -10.68 and -16.78‰ for pH 7.2 and 8.2, respectively); thus the isotope data from these microcosms is less useful in distinguishing abiotic from microbial dechlorination. While the first two of these ε_{bulk} values are less negative than previously reported ranges for abiotic PCE dechlorination, and therefore presumably due to microbial dechlorination, the third value (for L-Meth-pH 8.2-PCE (ε_{bulk} = -16.78‰) is close to reported values for both microbial PCE transformation (ε_{bulk} = -16.7‰) (Cichocka et al., 2008) and abiotic PCE transformation (ε_{bulk} = -14.7‰) (Zwank, 2004). The remaining evidence (discussed above) is, however, consistent with microbial reductive dechlorination for these microcosms.

For TCE, ε_{bulk} values for Duck Pond microcosms incubated with different terminal electron acceptors at pH 8.2 equaled -10.1, -19.4, and -20.9‰ for methanogenic, sulfate reducing, and iron reducing conditions, respectively. The first of these values is within the range of previously reported values for microbial TCE reductive dechlorination (see Table 7 in this report as well as Hunkeler et al., 1999; Sherwood Lollar et al., 1999; Bloom et al., 2000; Slater et al., 2001; Zwank, 2004; Lee et al., 2007). The second two are more negative than previously reported ε_{bulk} values for microbial dechlorination of TCE, but they are close to the value of -18.9‰ recently reported by Cichocka et al. (2007). We are reluctant, therefore to interpret these second two ε_{bulk} values as indicative of abiotic reductive dechlorination of TCE. In addition, the remaining evidence for these microcosms (low abiotic and high biotic product recoveries (Table 3) and a lag period before the start of TCE degradation (Figures 10d and 11e) is consistent with microbial and not abiotic reductive dechlorination.

Influence of Geochemical Parameters on Abiotic Reductive Dechlorination

While microbial transformation of PCE and TCE was typically faster than abiotic transformation in our microcosms, it is possible that abiotic dechlorination may ultimately transform more PCE and TCE under certain conditions, for example where the activity of dechlorinating bacteria is low (e.g., Figures 11a, d, and f), for microbial communities that do not completely dechlorinate PCE or TCE, or for soils or sediments that are amended to generate significantly higher mass loadings of reactive minerals or significantly higher pH values as part of a remediation strategy. For this reason, we analyzed our kinetic and geochemical data to see if there was a relationship between the concentration of one or more geochemical parameters and abiotic product recoveries. Because a number of studies indicate that abiotic reductive dechlorination is a surface and not aqueous phase process (Erbs et al., 1999; Kenneke and Weber, 2003), we considered only solid-associated geochemical species in this analysis. Geochemical data are reported in Table 4 and illustrated in Figure 15. The arrows in Figure 15 indicate those microcosms where no abiotic PCE or TCE reaction products were detected; this occurred under only three conditions (L-U-pH 7.2, DP-Meth-pH 7.2, and L-Meth-pH 7.2). These three conditions were either unamended (no electron donors or acceptors added), or amended to produce methanogenic conditions (Figure 15). Table 4 and Figure 15 show that such microcosms typically had lower concentrations of potentially reactive Fe(II) and S(-II) mineral fractions (presumably due to the absence of iron and sulfate reduction that leads to formation of Fe(II) and S(-II) minerals) than did microcosms incubated under iron reducing or sulfate reducing conditions, suggesting the importance of freshly precipitated Fe(II) and S(-II) minerals in abiotic PCE and TCE dechlorination. It is not possible from Table 4 and Figure 15 to identify which mineral fraction is most reactive with respect to PCE and TCE abiotic reductive dechlorination, but Table 3 shows similar abiotic product recoveries for microcosms incubated under both iron reducing and sulfate reducing conditions, indicating that both non-sulfur-bearing and sulfur-bearing Fe(II) mineral fractions likely contribute to the slow abiotic reductive dechlorination of PCE and TCE observed in most microcosms.

Conclusions

Task 1 experiments showed that ε_{bulk} values were more negative for PCE and TCE reductive dechlorination by FeS, and for TCE reductive dechlorination by GR-Cl and pyrite, than by three dechlorinating cultures isolated from different locations. Together with the literature to date, these results suggest that isotope fractionation is one tool that can be used, in conjunction with other tools such as microbial, geochemical, and reaction product analysis, to provide evidence about the predominant PCE or TCE transformation pathway at a contaminated site, i.e., abiotic or biotic. There is too much variability and overlap in ε_{bulk} values for different minerals and different microbial cultures, however, for isotope fractionation to be a stand alone tool for distinguishing abiotic and microbial reductive dechlorination of PCE or TCE.

Another application of Task 1 results involves use of stable C isotope fractionation to distinguish PCE and TCE reductive dechlorination from non-fractionating processes such as advection, dispersion, and sorption (Slater et al., 2000; Sherwood Lollar et al., 2001). Use of an erroneously small (i.e., less negative) ε_{bulk} value for this purpose would result in overestimation of contaminant degradation. Our reported ε_{bulk} values for abiotic PCE and TCE degradation are more negative than those for previously studied systems and should be considered when evaluating the performance of in situ remediation technologies that involve abiotic transformation of PCE and TCE by abiotic minerals. Handling of ε_{bulk} values from in situ remediation applications involving flow through porous media must always account for the effects of dispersion and dilution on isotope parameters (e.g., van Breukelen, 2007).

Abiotic transformation of PCE and TCE in the microcosm experiments in Tasks 2 and 3 was typically much slower than microbial reductive dechlorination due to the very slow abiotic transformation of PCE and TCE by reactive minerals that were present at concentrations typically below 1 g/L. Under field conditions, the mass loadings of both reactive minerals and bacteria would potentially be higher than in the batch studies conducted here where microcosms contained a low mass loading of solids (approx. 150 g soil/L) compared to a saturated aquifer (e.g., approx. 2000 g soil/L). Further testing will be needed to assess the relative contribution of abiotic and microbial reductive dechlorination under such conditions at a variety of contaminated sites. In one such study, Shen and Wilson (2007) recently assessed the relative contributions of abiotic and microbial transformation of TCE in column studies using Altus Air Force Base OU1 biowall materials (samples AAFB-8, -9, and -10 were obtained from the OU1 biowall, see Materials and Methods) and concluded that the predominant TCE transformation process was abiotic.

Tasks 2 and 3 showed that bacteria capable of dechlorinating PCE or TCE were present under almost all microcosm conditions, and microbial PCE and TCE dechlorination had a typical half life (after the lag phase) of 10 days (Figure 10). Such half lives are shorter than those reported in most studies of abiotic transformation of PCE and TCE by minerals (Butler and Hayes, 1999, 2001; Sivavec and Horney, 1996, 1997; Lee and Batchelor 2002a, 2002b), even for conditions where mass loadings of reactive minerals were much higher than those in the microcosms studied here (Table 4). From this we conclude that microbial processes have the potential for the most rapid transformation of PCE and TCE in the field and should be exploited for this purpose where appropriate. Abiotic processes also have the potential to contribute to the transformation of PCE

and TCE in cases where significantly higher mass loadings of reactive minerals are generated in situ as part of a remediation technology or where the activity of dechlorinating bacteria is low (e.g., Figures 11a, 11d and 11f). Abiotic processes can also play a significant role in cases where complete microbial degradation of PCE or TCE to ethene does not occur (e.g., Figure 11b), since mineral-mediated dechlorination of *cis*-DCE and VC to ethane, ethylene, and/or acetylene has been shown (Lee and Batchelor, 2002a, 2002b). Under these conditions, although slow, abiotic processes may significantly contribute to the complete transformation of PCE and TCE to benign products at contaminated sites.

References

Arnold, W. A., A. L. Roberts. Pathways and Kinetics of Chlorinated Ethylene and Chlorinated Acetylene Reaction with Fe (0) Particles. *Environmental Science and Technology* **2000**, *34*, 1794-1805.

Atkinson, R. J., A. M. Posner, J. P. Quirk. Adsorption of Potential Determining Ions at the Ferric Oxide-aqueous Electrolyte Interface. *Journal of Physical Chemisrty* **1967**, *71*, 550-558.

Baciocchi, E. 1,2-Dehalogenations and Related Reactions, in Patai, S.; Rappoport, Z Eds., *The Chemistry of Halides, Pseudo-Halides and Azides*, Supplement D to the Chemistry of Functional Groups, 1983, Wiley: New York, pp. 161-201.

Bagley, D. M., J. M. Gossett. Tetrachloroethylene Transformation to Trichloroethylene and *cis*-1,2-Dichloroethylene by Sulfate-reducing Enrichment Cultures. *Applied and Environmental Microbiology* **1990,** *56*, 2511-2516.

Barbash, J. E., M. Reinhard. Abiotic Dehalogenation of 1, 2-dichloroethane and 1, 2-Dibromoethane in Aqueous Solution Containing Hydrogen Sulfide. *Environmental Science and Technology* **1989**, *23*, 1349-1358.

Bierwagen, B. G., A. A. Keller. Measurement of Henry's Law Constant for methyl *tert*-butyl ether Using Solid-phase Microextraction. *Environmental Toxicology and Chemistry* **2001**, *20*, 1625-1629.

Bloom, Y., R. Aravena, D. Hunkeler, E. Edwards, S. K. Frape. Carbon Isotope Fractionation During Microbial Dechlorination of Trichloroethene, *cis*-1, 2-dichloroethene, and Vinyl Chloride for Assessment of Natural Attenuation. *Environmental Science and Technology* **2000**, *34*, 2768-2772.

Bossert, I. D., M. M. Haeggblom, Y. Y. Young. In *Dehalogenation, Microbial Processes and Environmental Application: Microbial Ecology of Dehalogenation.* Kluwer Academic Publishers, **2003**, 33-52.

Bouwer, E. J., P.L. McCarty. Transformations of 1- and 2-carbon Halogenated Aliphatic Organic Compounds Under Methanogenic Conditions. *Applied and Environmental Microbiological* **1983,** *45*, 1286-1294.

Burris, D. R., C. A. Delcomyn, M. H. Smith, A. L. Roberts. Reductive Dechlorination of Tetrachloroethylene and Trichloroethylene Catalyzed by Vitamin B_{12} in Homogeneous and Heterogeneous Systems. *Environmental Science and Technology* **1996**, *30*, 3047-3052.

Butler, E. C., K. F. Hayes. Effects of Solution Composition and pH on the Reductive Dechlorination of Hexachloroethane by Iron Sulfide. *Environmental Science and Technology* **1998**, *32*, 1276-1284.

Butler, E. C., K. F. Hayes. Kinetics of the Transformation of Trichloroethylene and Tetrachloroethylene by Iron Sulfide. *Environmental Science and Technology* **1999**, *33*, 2021-2027.

Butler, E. C., K. F. Hayes. Factors Influencing Rates and Products in the Transformation of Trichloroethylene by Iron Sulfide and Iron Metal. *Environmental Science and Technology* **2001**, *35*, 3884-3891.

Canfield, D. E.; R. Raiswell, J. T. Westrich, C. M. Reaves, R. A. Berner. The Use of Chromium Reduction in the Analysis of Reduced Inorganic Sulfur in Sediments and Shales. *Chemical Geology* **1986**, *54*, 149-155.

Carlson, D. L., M. M. McGuire, A. L. Roberts, D. H. Fairbrother. Influence of Surface Composition on the Kinetics of Alachlor Reduction by Iron Pyrite. *Environmental Science and Technology* **2003**, *37*, 2394-2399.

Castro, C. E.; W. C. Kray, Jr. The Cleavage of Bonds by Low Valent Transition Metal Ions. The Homogeneous Reduction of Alkyl Halides by Chromous Sulfate. *Journal of the American Chemical Society* **1963**, *85*, 2768-2773.

Charlet, L.; E. Silvester, E. Liger. N-compounds Reduction and Actinide Immobilization in Surficial Fluids by Fe(II): the Surface $\equiv Fe^{III}OFe^{II}OH°$ Species, as Major Reductant. *Chemical Geology* **1998**, *151*, 85-93.

Cichocka, D., M. Siegert, G. Imfeld, J. Andert, K. Beck, G. Diekert, H.-H. Richnow, I. Nijenhuis. Factors Controlling the Carbon Isotope Fractionation of Tetra- and Trichloroethene During Reductive Dechlorination by *Sulfurospirillum sp*. and *Desulfitobacterium sp*. Strain PCE-S. *FEMS Microbiology and Ecology* **2007,** *62*, 98-107.

Cichocka, D., G. Imfeld, H.-H. Richnow, I. Nijenhuis. Variability in Microbial Carbon Isotope Fractionation of Tetra- and Trichloroethene Upon Reductive Dechlorination. *Chemosphere* **2008**, *71*, 639-648.

Cornell, R. M., Schwertmann, U. *The Iron Oxides: Structure, Properties, Reactions, Occurrences and Uses*. 2nd ed., 2003. Wiley-VCH Verlag GmbH & Co. KGaA, Weinheim, pp. 441, 525-540.

Cozzarelli, J. M., J. M. Suflita, G. A. Ulrich, S. H. Harris, M. A. Scholl, J. L. Schlottmann, and S. Christenson. Geochemical and Microbiological Methods for Evaluating Anaerobic Processes in an Aquifer Contaminated by Landfill Leachate. *Environmental Science and Technology*, **2000**, *34*, 4025-4033.

Curtis, G. P.; Reinhard, M. Reductive Dehalogenation of Hexachloroethane, Carbon Tetrachloride, and Bromoform by Anthrahydroquinone Disulfonate and Humic Acid, *Environmental Science and Technology* **1994**, *28*, 2393-2402.

Danielsen, K. M. and K. M. Hayes. pH Dependence of Carbon Tetrachloride Reductive Dechlorination by Magnetite. *Environmental Science and Technology,* **2004**, *38*, 4745-4752.

Dayan, H., T. Abrajano, N. C. Sturchio, L. Winsor. Carbon Isotopic Fractionation During Reductive Dehalogenation of Chlorinated Ethenes by Metallic Iron. *Organic Geochemistry* **1999**, *30*, 755-763.

Dong, Y., X. Liang, L. R. Krumholz, R. P. Philp, E. C. Butler. The Relative Contributions of Abiotic and Microbial Processes to the Transformation of Tetrachloroethylene and Trichloroethylene in Anaerobic Microcosms. *Environmental Science and Technology* **2009**, in press, DOI: 10.1021/es801917p.

Doong, R. and H. Chiang. Transformation of Carbon Tetrachloride by Thiol Reductants in the Presence of Quinine Compounds. *Environmental Science and Technology,* **2005**, *39*, 7460-7468.

Doucette, W. J., Soil and Sediment Sorption Coefficients. In *Handbook of Property Estimation Methods for Chemicals: Environmental and Health Sciences*, Boethling, R. S., D. Mackay, Eds. CRC Press LLC: Boca Raton, Florida, 2000; pp 141-188.

Elsner, M., R. P. Schwarzenbach, and S. B. Haderlein, Reactivity of Fe(II)-bearing Minerals Toward Reductive Transformation of Organic Contaminants. *Environmental Science and Technology*, **2004a**, *38*, 799-807.

Elsner, M., S. B. Haderlein, T. Kellerhals, S. Luzi, L. Zwank, W. Angst, R. P. Schwarzenbach. Mechanisms and Products of Surface-mediated Reductive Dehalogenation of Carbon

Tetrachloride by Fe(II) on Goethite. *Environmental Science and Technology* **2004b**, *38*, 2058-2066.

Elsner, M., L. Zwank, D. Hunkeler, R. P. Schwarzenbach. A New Concept Linking Observable Stable Isotope Fractionation to Transformation Pathways of Organic Pollutants. *Environmental Science and Technology* **2005**, *39*, 6896-6916.

Erbs, M., H. C. Bruun Hansen, and C. E. Olsen. Reductive Dechlorination of Carbon Tetrachloride using Iron(II) Iron(III) Hyrdoxide Sulfate (Green Rust). *Environmental Science and Technology*, **1999**, *33*, 307-311.

Fennelly, J. P., A. L. Roberts. Reaction of 1, 1, 1-trichloroethane with Zero-valent Metals and Bimetallic Reductants. *Environmental Science and Technology* **1998**, *32*, 1980-1988.

Gibbs, R. J., Mechanisms of Trace Metal Transport in Rivers. Science 1973, 180, 71-73.

Glod, G., U. Brodmann, W. Angst, C. Holliger, R. P. Schwarzenbach. Cobalamin-mediated Reduction of *cis*- and *trans*-dichloroethene, 1,1-dichloroethene, and Vinyl Chloride in Homogeneous Aqueous Solution: Reaction Kinetics and Mechanistic Considerations. *Environmental Science and Technology* **1997**, *31*, 3154-3160.

Hanoch, R. J., H. Shao, and E. C.Butler. Transformation of Carbon Tetrachloride by Bisulfide Treated Goethite, Hematite, Magnetite, and Kaolinite. *Chemosphere* **2006**, *63*, 323-334.

Herbert, R. B., Jr., S. G. Benner, A. R. Pratt, D. W. Blowes. Surface Chemistry and Morphology of Poorly Crystalline Iron Sulfides Precipitated in Media Containing Sulfate-reducing Bacteria. *Chemical Geology* **1998**, *144*, 87-97.

Heron, G., C. Crouzet, A. C. Bourg, and T. H. Christensen. Speciation of Fe(II) and Fe(III) in Contaminanted Aquifer Sediments Using Chemical Extraction Techniques. *Environmental Science and Technology*, **1994**, *28*, 1698-1705.

Howard, P. H., W. M. Meylan. *Physical Properties of Organic Chemicals*. CRC, Lewis Publishers: Boca Raton, Florida, 1997; p 51-284.

Huerta-Diaz, M. A., R. Carignan, A. Tessier. Measurement of Trace Metals Associated with Acid Volatile Sulfides and Pyrite in Organic Freshwater Sediments. *Environmental Science and Technology* **1993,** *27*, 2367-2372.

Hunkeler, D., R. Aravena. Evidence of Substantial Carbon Isotope Fractionation Among Substrate, Inorganic Carbon and Biomass During Aerobic Mineralization of 1, 2-Dichloroethane by Xanthobacter Autotrophicus. *Applied and Environmental Microbiology* **2000**, *66*, 4870-4876.

Hunkeler, D., R. Aravena, B. J. Butler. Monitoring Microbial Dechlorination of Tetrachloroethene (PCE) in Groundwater Using Compound-specific Stable Carbon Isotope Ratios: Microcosm and Field Studies. *Environmental Science and Technology* **1999**, *33*, 2733-2738.

Hurst, C. J., R. L. Crawford, G. R. Knudsen, M. J. McInerney, L. D. Stetzenbach. *Manual of Environmental Microbiology*; ASM Press Washington, D.C. 2002; p 62.

Huskey, W. P. In *Enzyme Mechanism from Isotope Effects*; Cook, P.F.; Ed.; CRC Press: Boca Raton, FL, 1991; pp 37-69.

Hwang, I.; Batchelor, B., Reductive dechlorination of tetrachloroethylene by Fe(II) in cement slurries. *Environmental Science and Technology* **2000**, *34*, 5017-5022.

Hwang, I., B. Batchelor. Reductive Dechlorination of Tetrachloroethylene in Soils by Fe (II)-Based Degradative Solidification/stabilization. *Environmental Science and Technology* **2001**, *35*, 3792-3797.

JCPDS, 1990. Powder Diffraction File, Inorganic Volume, Swarthmore, Pennsylvania.

Jenkins, R., R. Snyder. *Introduction to X-ray Powder Diffractometry*. John Wiley & Sons, Inc.: New York, New York, 1996; Vol. 138, p 335-339.

Jeong, H. Y., H. Kim, K. F. Hayes. Reductive Dechlorination Pathways of Tetrachloroethylene and Trichloroethylene and Subsequent Transformation of Their Dechlorination Products by Mackinawite (FeS) in the Presence of Metals. *Environmental Science and Technology* **2007**, *41*, 7736-7743.

Kang, Y. S., S. Risbud, J. F. Rabolt, P. Stroeve. Synthesis and Characterization of Nanometer-Size Fe_3O_4 and γ-Fe_2O_3 Particles. *Chemistry of Materials* **1996**, *8*, 2209-2211.

Karickhoff, S. W.; Brown, D. S.; Scott, T. A., Sorption of hydrophobic pollutants on natural sediments. *Water Research* **1979**, *13*, 241-248.

Kennedy, L. G., J. W. Everett, J. Gonzales. Assessment of Biogeochemical Natural Attenuation and Treatment of Chlorinated Solvents, Altus Air Force Base, Altus, Oklahoma. *Journal of Contaminant Hydrology* **2006**, *83*, 221-236.

Kenneke, J. F., E. J. Weber. Reductive Dehalogenation of Halomethanes in Iron- and Sulfate-Reducing Sediments. 1. Reactivity Pattern Analysis. *Environmental Science and Technology* **2003**, *37*, 713-720.

Klausen, J., S. P. Troeber, S. B. Haderlein, and R. P. Schwarzenbach. Reduction of Substituted Nitrobenzenes by Fe(II) in Aqueous Mineral Suspensions. *Environmental Science and Technology* **1995**, *29*, 2396–2404.

Kriegman-King, M. R. and M. Reinhard. Reduction of Hexachloroethane and Carbon Tetrachloride at Surfaces of Biotite, Vermiculite, Pyrite, and Marcasite, in R. Baker, Ed., *Organic Substances and Sediments in Water*, **1991**, Vol. 2, Processes and Analytical, Lewis Publishers, Inc., Chelsea, Michigan, pp. 349-364.

Kriegman-King, M. R., M. Reinhard. Transformation of Carbon Tetrachloride by Pyrite in Aqueous Solution. *Environmental Science and Technology* **1994**, *28*, 692-700.

Lee, P. K. H., M. E. Conrad, L. Alvarez-Cohen. Stable Carbon Isotope Fractionation of Chloroethenes by dehalorespiring Isolates. *Environmental Science and Technology* **2007**, *41*, 4277-4285.

Lee, W. and B. Batchelor. Abiotic Reductive Dechlorination of Chlorinated Ethylenes by Iron-bearing Soil Minerals. 1. Pyrite and Magnetite. *Environmental Science and Technology* **2002a**, *36*, 5147-5154.

Lee, W. and B. Batchelor. Abiotic Reductive Dechlorination of Chlorinated Ethylenes by Iron-bearing Soil Minerals 2. Green rust. *Environmental Science and Technology* **2002b**, *36*, 5348-5354.

Liang, X., Y. Dong, T. Kuder, L. R. Krumholz, R. P. Philp, E. C. Butler. Distinguishing Abiotic and Biotic Transformation of Tetrachloroethylene and Trichloroethylene by Stable Carbon Isotope Fractionation. *Environmental Science and Technology* **2007**, 41, 7094-7100.

Liang, X., R. P. Philp, E. C. Butler. Kinetic and Isotope Analyses of Tetrachloroethylene and Trichloroethylene Degradation by Model Fe(II)-Bearing Minerals, *Chemosphere* **2009**, in press, DOI: 10.1016/j.chemosphere.2008.11.042.

Liger, E., L. Charlet, P. V. Cappellen. Surface catalysis of uranium(VI) reduction by iron(II). *Geochim. Cosmochim. Acta* **1999**, *63*, 2939-2955.

Lovley, D. R., E. J. P. Phillips. Rapid Assay for Microbially Reducible Ferric Iron in Aquatic Sediments. *Applied and Environmental Microbiology* **1987**, 53, 1536-1540.

Lu, X., J. T. Wilson, H. Shen, B. M. Henry, D. Kampbell. Remediation of TCE-contaminated Groundwater by a Permeable Reactive Barrier Filled with Plant Mulch (Biowall). *Journal of*

Environmental Science and Health, Part A: Environmental Science and Engineering **2008,** *43*, 24-35.

Luijten, M. L. G. C., J. de Weert, H. Smidt, H. T. S. Boschker, W. M. de Vos, G. Schraa, and A. J. M. Stams. Description of *Sulfurospirillum halorespirans* sp. nov., an Anaerobic, Tetrachloroethene-respiring Bacterium, and Transfer of *Dehalospirillum multivorans* to the genus *Sulfurospirillum* as *Sulfurospirillum multivorans* comb. nov. *International Journal of Systematic and Evolutionary Microbiology* **2003**, *53*, 787-793.

Mackay, D., W. Y. Shiu, K.-C. Ma, K.-C., S. C. Lee. *Handbook of Physical-Chemical Properties and Environmental Fate for Organic Chemicals*. 2nd ed.; CRC Press LLC: Boca Raton, FL, 2006; Vol. II, p 1063-1115.

Maithreepala, R. A., R. Doong, R. Enhanced Dechlorination of Chlorinated Methanes and Ethenes by Chloride Green Rust in the Presence of Copper (II). *Environmental Science and Technology* **2005**, *39*, 4082-4090.

Mariotti, A., J. C. Germon, P. Hubert, P. Kaiser, R. Letolle, A. Tardieux, P. Tardieux. Experimental Determination of Nitrogen Kinetic Isotope Fractionation: Some Principles; Illustration for the Denitrification and Nitrification Processes. *Plant Soil* **1981**, *62*, 413-430.

McCormick M. L., E. J. Bouwer, and P. Adriaens. Carbon Tetrachloride Transformation in a Model Iron-reducing Culture: Relative Kinetics of Biotic and Abiotic Reactions, *Environmental Science and Technology* **2001**, *36*, 403-410.

Miller, P. L., D. Vasudevan, P. M. Gschwend, A. L. Roberts. Transformation of Hexachloroethane in a Sulfidic Natural Water," *Environmental Science and Technology* **1998**, *32*, 1269-1275.

Moggi, P., G. Albanesi. Transition Metal Phosphomolybdates as Catalysts for the Gas Phase Hydration of Acetylene to Acetaldehyde and Acetic Acid. *Reaction Kinetics and Catalysis Letters* **1991**, *44*, 375-380.

Morrison, R. T., R. N. Boyd, R. N. *Organic Chemistry*, 4th Ed., 1983. Allyn and Bacon, Inc., Boston, pp. 753-754.

Neumann, A., G. Wohlfarth,G. Diekert. Purification and Characterization of Tetrachloroethene Reductive Dehalogenase from *Dehalospirillum multivorans*. *Journal of Biological Chemistry* **1996**, *271*, 16515-16519.

Nijenhuis, I., J. Andert, K. Beck, M. Kastner, G. Diekert, H. Richnow. Stable Isotope Fractionation of Tetrachloroethene During Reductive Dechlorination by *sulfurospirillum multivorans* and *desulfitobacterium* sp. strain PCE-S and Abiotic Reactions with Cyanocobalamin. *Applied and Environmental Microbiology* **2005**, *71*, 3413-3419.

Nirmalakhandan, N. N., R. E. Speece. QSAR Model for Predicting Henry's Constant. *Environmental Science and Technology* **1988**, *22*, 1349-1357.

O'Leary, M. H., C. P. Yapp. Equilibrium Carbon Isotope Effect on a Decarboxylation Reaction. *Biophys. Res. Commun*. **1978**, *80*, 155-160.

O'Loughlin, E. J., K. M. Kemner, D. R. Burris. Effects of Ag^{I}, Au^{III}, and Cu^{II} on the Reductive Dechlorination of Ccarbon Tetrachloride by Green Rust. *Environmental Science and Technology* **2003**, *37*, 2905-2912.

Parsons Corporation., *Construction Closeout Report Bark Mulch Trench Interim Corrective Action for In-situ Anaerobic Bioremediation of Chlorinated Solvents in Ground Water Altus Air Force Base, Oklahoma. Prepared for AAFB Air Education and Training Command and the Air Force Center for Environmental Excellence, Brooks City-Base, Texas*. Contract No. F41624-01-D-8544, Delivery Order No. 0025; Parsons, Denver, CO.: May 2006.

Pecher, K., S. B. Haderlein, and R. P. Schwarzenbach. Reduction of Polyhalogenated Methanes by Surface-bound Fe(II) in Aqueous Suspensions of Iron Oxides, *Environmental Science and Technology*, **2002**, *36***,** 1734-1741.

Perlinger, J. A., W. Angst, R. P. Schwarzenbach. Kinetics of the Reduction of Hexachloroethane by Juglone in Solutions Containing Hydrogen Sulfide," *Environmental Science and Technology* **1996**, *30*, 3408-3417.

Pyzik, A. J., S. E. Sommer. Sedimentary Iron Monosulfides: Kinetics and Mechanisms of Formation. *Geochim. Cosmochim. Acta* **1981**, *45*, 687-698.

Ramasamy, K., S. L. Kalyanasundaram, P. Shanmugam. Debromination of *vic*-dibromides Using Sodium Hydrogen Telluride Reagent," *Synthesis* **1978**, 311-312.

Refait, P. H., M. Abdelmoula, J.-M. R. Génin. Mechanisms of Formation and Structure of Green Rust One in Aqueous Corrosion of Iron in the Presence of Chloride Ions. *Corrosion Science* **1998**, *40*, 1547-1560.

Rickard, D. T. The Chemistry of Iron Sulfide Formation at Low Temperatures. *Stockholm Contr. Geol*. **1969**, *20*, 67–95.

Riehl, J.-F., D. G. Musaev, K. Morokuma. An *ab initio* Molecular Orbital Sudy of the Unimolecular Dissociation Reactions of di- and Trichloroethylene. *Journal of Chemical Physics* **1994**, *101*, 5942-5956.

Ritalahti, K. M., F. E. Löffler, E. E. Rasch, S. S. Koenigsberg. Bioaugmentation for Chlorinated Ethene Detoxification: Bioaugmentation and Molecular Diagnostics in the Bioremediation of Chlorinated Ethene-contaminated Sites. *Industrial Biotechnology* **2005**, *1*, 114-118.

Roberts, A. L., L. A. Totten, W. A. Arnold, D. R. Burris, T. J. Campbell. Reductive Elimination of Chlorinated Ethylenes by Zero-valent Metals. *Environmental Science and Technology* **1996**, *30*, 2654-2659.

Schink, B. Fermentation of Acetylene by an Obligate Anaerobe, *Pelobacter acetylenicus. Archiv. Microbiol.* **1985**, *142*, 295–301.

Scholz-Muramatsu, H., A. Neumann, M. Messmer, E. Moore, G. Diekert. Isolation and Characterization of Dehalospirillum Multivorans gen. nov., sp. nov., a Tetrachloroethene-Utilizing, Strictly Anaerobic Bacterium. *Archives of Microbiology* **1995**, *163*, 48-56.

Schüth, C., M. Bill, J. A. C. Barth, G. F. Slater, R. M. Kalin. Carbon Isotope Fractionation During Reductive Dechlorination of TCE in Batch Experiments with Iron Samples from Reactive Barriers. *Journal of Contaminant Hydrology* **2003**, *66*, 25-37.

Schwarzenbach, R. P., P. M. Gschwend, D. M. Imboden. *Environmental Organic Chemistry* 2nd ed.; John Wiley & Sons, Inc.: Hoboken, NJ, 2003; p 276-330.

Schwertmann, J., R. Cornell. *Iron oxides in the laboratory: Preparation and characterization*; VCH publishers. New York, **1991**; pp 111-116.

Shao, H., E. C. Butler, E. C. The Influence of Iron and Sulfur Mineral Fractions on Carbon Tetrachloride Transformation in Model Anaerobic Soils and Sediments. *Chemosphere* **2007**, *68*, 1807-1813.

Shen, H., J. T. Wilson. Trichloroethylene Removal from Groundwater in Flow-through Columns Simulating a Permeable Reactive Barrier Constructed with Plant Mulch. *Environmental Science and Technology* **2007**, *41*, 4077-4083.

Sherwood Lollar, B., G. F. Slater, J. Ahad, B. Sleep, J. Spivack, M. Brennan, P. Mackenzie. Contrasting Carbon Isotope Fractionation During Biodegradation of Trichloroethylene and Toluene: Implications for Intrinsic Bioremediation. *Organic Geochemistry* **1999**, *30*, 813-820.

Sherwood Lollar, B., G. F. Slater, B. Sleep, M. Witt, G. M. Klecka, M. Harkness, J. Spivack. Stable Carbon Isotope Evidence for Intrinsic Bioremediation of Tetrachloroethene and Trichloroethene at Area 6, Dover Air Force Base. *Environmental Science and Technology* **2001**, *35*, 261-269.

Siivola, J., R.A. Schmid. List of Mineral Abbreviations. In *Metamorphic Rocks: A Classification and Glossary of Terms. Recommendations of the International Union of Geological Sciences Subcommission on the Systematics of Metamorphic Rocks*; Douglas, F.; Desmons, J., Eds; Cambridge University Press: New York, 2007; pp 93-110.

Sivavec, T. M., D. P. Horney, S. S. Baghel. Reductive Dechlorination of Chlorinated Ethenes by Iron Metal and Iron Sulfide Minerals. In *Emerging Technologies in Hazardous Waste Management VII*, ACS Special Symposium; American Chemical Society: Atlanta, GA, **1995**; pp 42-45.

Sivavec, T. M., D. P. Horney, S. S. Baghel. U.S. Patent Number 5,575,927, **1996**.

Sivavec, T. M., D. P. Horney. Reductive Dechlorination of Chlorinated Solvents by Zero-valent Iron, Iron Oxide and Iron Sulfide Minerals. In Book of Abstracts, 211th ACS National Meeting, New Orleans, Louisiana, 1996.

Sivavec, T. M. and Horney, D. P. Reduction of Chlorinated Solvents by Fe(II) Minerals. *Preprints of Papers Presented at the 213th ACS National Meeting*, April 13-17, **1997**, San Francisco, California, Vol 37 (1), pp. 115-117.

Slater, G. F., B. Sherwood Lollar, E. Edwards, B. Sleep, M. Witt, G. M. Klecka, M. R. Harkness, J. L. Spivack. Carbon Isotopic Fractionation of Chlorinated Ethenes During Biodegradation: Field Applications. In *Natural Attenuation Considerations and Case Studies, Second International Conference on Remediation of Chlorinated and Recalcitrant Compounds, Monterrey, California, May 22-25, 2000*, Wickramanayake, G. B.; Gavaskar, A. R.; Kelley, M. E., Eds., Batelle Press: Columbus, OH, **2000**; pp 17-24.

Slater, G. F., B. Sherwood Lollar, R. A. King, S. F. O'Hannesin. Isotopic Fractionation During Reductive Dehalogenation of Trichloroethene by Zerovalent Iron: Influence of Surface Treatment. *Chemosphere* **2002**, *49*, 587-596.

Slater, G. F., B. Sherwood Lollar, B. E. Sleep. Variability in Carbon Isotopic Fractionation During Biodegradation of Chlorinated Ethenes: Implication for Field Applications. *Environmental Science and Technology* **2001**, *35*, 901-907.

Slater, G. F., B. Sherwood Lollar, S. Lesage, S. Brown. Carbon Isotope Fractionation of PCE and TCE During Dechlorination by Vitamin B_{12}. *Groundwater Monit. Remed.* **2003**, *4*, 59-67.

Stone, A.T. Adsorption of Organic Reductants and Subsequent Electron Transfer on Metal Oxide Surfaces, in *Geochemical Processes at Mineral Surfaces*; Davis, J. A. and Hayes, K.F., Eds.; American Chemical Society: Washington, DC, 1986; pp. 446 - 461.

Sung, Y., K. M. Ritalahti, R. A. Sanford, J. W. Urbance, S. J. Flynn, J. M. Tiedje, F. E. Loeffler. Characterization of Two Tetrachloroethene-reducing, Acetate-oxidizing Anaerobic Bacteria and Their Description as *Desulfuromonas michiganensis* sp. nov. *Applied and Environmental Microbiology* **2003**, *69*, 2964-2974.

Taylor, R. M., B. A. Maher, P. G. Self. Magnetite in Soils: I. The Synthesis of Single-domain and Superparamagnetic Magnetite. *Clay Miner*. **1987**, *22*, 411-422.

Tessier, A., P. G. Campbell, and M. Bisson. Sequential Extraction Procedure for the Speciation of Particulate Trace Metals. *Analytical Chemistry*, **1979**, *51*, 844-850.

Ulrich, G.A., L. R. Krumholz, and J. M. Suflita. A Rapid and Simple Method for Estimating Sulfate Reduction Activity and Quantifying Inorganic Sulfides. *Applied and Environmental Microbiology*, **1997**, *63*, 1627-1630.

van Breukelen, B. M. Quantifying the Degradation and Dilution Contribution to Natural Attenuation of Contaminants by Means of an Open System Rayleigh Equation. *Environmental Science and Technology* **2007**, *41*, 4980-4985.

VanStone, N. A., R. M. Focht, S. A. Mabury, B. Sherwood Lollar. Effect of Iron Type on Kinetics and Carbon Isotopic Enrichment of Chlorinated Ethylenes During Abiotic Reduction on Fe(0). *Ground Water*, **2004**, *42*, 268-276.

Vieth, A., J. Müller, G. Strauch, M. Kastner, M. Gehre, R. U. Mechenstock, H. H. Richnow. *In-situ* Biodegradation of Tetrachloroethene and Trichloroethene in Contaminated Aquifers Monitored by Stable Isotope Fractionation. *Isotope Environ. Health Stud*. **2003**, *39*, 113-124.

Weerasooriya, R. and B. Dharmasena. Pyrite Assisted Degradation of Trichoroethene (TCE). *Chemosphere*, **2001**, *42*, 389-396.

Wu, Q., K. R. Sowers, H. D. May. Establishment of a Polychlorinated Biphenyl-dechlorinating Microbial Consortium, Specific for Doubly Flanked Chlorines, in a Defined, Sediment-free Medium. *Applied and Environmental Microbiology* **2000**, *66*, 49-53.

Yalkowsky, S. H., Y. He. *Handbook of Aqueous Solubility Data*. CRC Press LLC: Boca Raton, FL, 2003; pp 22-29.

Yokoyama, K., G. Fujisawa, A. Yokoyama. The Mechanism of the Unimolecular Dissociation of Trichloroethylene $CHCl{=}CCl_2$ in the Ground Electronic State. *Journal of Chemical Physics* **1995**, *102*, 7902-7909.

Zhu, X. D., S. R.Castleberry, M. Nanny, and E. C. Butler. Effects of pH and Catalyst Concentration on Photocatalytic Oxidation of Aqueous Ammonia and Nitrite in Titanium Dioxide Suspensions, *Environmental Science and Technology,* **2005**, *39*, 3784 –3791.

Zwank, L. Assessment of the Fate of Organic Groundwater Contaminants Using Their Isotopic Signatures. 2004. PhD thesis, Swiss Federal Institute of Technology (ETH), Zurich, Switzerland.

Zwank, L., M. Berg, M. Elsner, T. Schmidt, R. P. Schwarzenbach, S. B. Haderlein. New Evaluation Scheme for Two-dimensional Isotope Analysis to Decipher Biodegradation Processes: Application to Groundwater Contamination by MTBE. *Environmental Science and Technology* **2005a**, *39*, 1018-1029.

Zwank, L., M. Elsner, A. Aeberhard, R. P. Schwarzenbach, S. B. Haderlein. Carbon Isotope Fractionation During Reductive Dehalogenation of Carbon Tetrachloride at Iron (hydr)oxide and Iron Sulfide Minerals. *Environmental Science and Technology* **2005b**, *39*, 5634-5641.

Table 1. Surface Area Normalized Pseudo-first-order Rate Constants, Products, and Mass Recoveries, for PCE Transformation by Chloride Green Rust (GR-Cl**), Pyrite, Sulfate Green Rust (**GR-SO_4**), Magnetite, Fe(**II**)-treated Goethite, and S(-**II**)-treated Goethite at pH 8.**

Mineral (Surface area loading)	Time (days)	k_{SA} (L m^{-2} d^{-1}) [a]	Products	Mass Recovery (%)[a]
GR-Cl (210 m^2 L^{-1})	417	$(5.6 \pm 1.4) \times 10^{-6}$	acetylene	52.25 ± 0.53
			ethylene	22.46 ± 0.23
			TCE	0.8559 ± 0.0086
			PCE remaining	56.32 ± 0.57
			total	131.8 ± 1.3
Pyrite (578 m^2 L^{-1})	253	$(1.6 \pm 1.0) \times 10^{-6}$	ethylene	0.422 ± 0.054
			cis-DCE	2.72 ± 0.14
			TCE	3.400 ± 0.082
			PCE remaining	78.3 ± 2.1
			total	84.8 ± 2.3
GR-SO_4 (93 m^2 L^{-1})	111	NC [b]	acetylene	10.5 ± 1.3
			ethylene	6.35 ± 0.92
			PCE remaining	99.7 ± 1.1
			total	116.5 ± 3.4
Magnetite (1800 m^2 L^{-1})	141	NC	acetylene	3.8 ± 6.2
			ethylene	18 ± 29
			PCE remaining	82.6 ± 4.1
			total	104 ± 40
Fe(II)-treated goethite (296 m^2 L^{-1})	222	NC	acetylene	0.198 ± 0.030
			ethylene	0.863 ± 0.034
			PCE remaining	95.3 ± 5.9
			total	96.3 ± 6.0
S(-II)-treated goethite (296 m^2 L^{-1})	233	NC	acetylene	0.034 ± 0.011
			ethylene	1.014 ± 0.072
			PCE remaining	100.2 ± 7.1
			total	101.2 ± 7.2

[a] Uncertainties are 95% confidence intervals calculated by propagation of error; [b]NC: not calculated due to slow reaction.

Table 2. Surface Area Normalized Pseudo-first-order Rate Constants, Products, and Mass Recoveries, for TCE Transformation by Chloride Green Rust (GR-Cl), Pyrite, Sulfate Green Rust (GR-SO_4), Magnetite, Fe(II)-treated Goethite, and S(-II)-treated Goethite at pH 8.

Mineral (Surface area loading)	Time (days)	k_{SA} (L m^{-2} d^{-1}) [a]	Products	Mass Recovery (%)[a]
GR-Cl (210 m^2 L^{-1})	275	$(2.92 \pm 0.61) \times 10^{-5}$	acetylene	68 ± 18
			ethylene	10.9 ± 1.6
			cis-DCE	3.03 ± 0.51
			TCE remaining	19.7 ± 2.6
			total	101 ± 23
Pyrite/low $[TCE]_0$ [c] (578 m^2 L^{-1})	92	$(6.4 \pm 1.5) \times 10^{-5}$	ethylene	1.44 ± 0.81
			cis-DCE	6.67 ± 0.19
			TCE remaining	4.1 ± 3.2
			total	12.2 ± 4.2
Pyrite/high $[TCE]_0$ [d] (3000 m^2 L^{-1})	18	NC [b]	ethylene	0.0146 ± 0.0015
			cis-DCE	1.32 ± 0.23
			acetaldehyde	0.1661 ± 0.0067
			ethanol	0.462 ± 0.019
			acetate	10.90 ± 0.45
			TCE remaining	83.7 ± 4.4
			total	96.6 ± 5.1
GR-SO_4 (93 m^2 L^{-1})	148	NC	acetylene	4.237 ± 0.053
			ethylene	1.94 ± 0.23
			TCE remaining	103.8 ± 5.7
			total	110.0 ± 6.0
Magnetite (1800 m^2 L^{-1})	131	NC	acetylene	2.86 ± 0.87
			ethylene	3.9 ± 1.4
			TCE remaining	92.3 ± 2.3
			total	99.1 ± 4.6
Fe(II)-treated goethite (296 m^2 L^{-1})	222	NC	acetylene	0.01363 ±
			ethylene	1.046 ± 0.067
			TCE remaining	103.6 ± 2.7
			total	104.7 ± 2.7
S(-II)-treated goethite (296 m^2 L^{-1})	233	NC	acetylene	0.201 ± 0.027
			ethylene	0.979 ± 0.073
			TCE remaining	106.96 ± 0.76
			total	108.14 ± 0.86

[a] Uncertainties are 95% confidence intervals calculated by propagation of error; [b] NC: not calculated due to slow reaction; [c] $[TCE]_0$ = 30 μM; [d] $[TCE]_0$ = 7.5 mM.

Table 3. Summary of Results for the Microcosm Experiments[a]

Microcosm ID[b]	Time (days) (PCE/TCE)	Percent remaining (%)		Abiotic product recovery (%)		Microbial product recovery (%)	
		PCE	TCE	PCE	TCE	PCE	TCE
Unamended Microcosms							
DP-U-pH 7.2	107/102	2.26±0.87	94.0±3.9	0	0.097±0.023	90.7±7.2	5.3±3.5
L-U-pH 7.2	107/102	90.1±2.0	98.77±0.42	0	0	7.6±7.3	1.032±0.078
AAFB-8-U-pH 7.2	59	0	–[c]	NC[d]	–	119.02±0.24	–
AAFB-9-U-pH 7.2	74	0	–	NC	–	112.1±6.7	–
AAFB-10-U-pH 7.2	77	0	–	NC	–	122.9±3.1	–
AAFB-12-U-pH 7.2	75	0	–	NC	–	104.5142±0.0012	–
AAFB-14-U-pH 7.2	54	0	–	NC	–	98.52±0.37	–
Amended Microcosms							
DP-IR-pH 7.2	27	0	–	0.73±0.45	–	88.5±7.0	–
DP-IR-pH 8.2	98/79	104.7±5.7	0.607±0.030	0.76±0.30	0.456±0.017	0.496±0.084	98.31±0.78
DP-SR-pH 7.2	33	0	–	0.147±0.029	–	101.7±2.6	–
DP-SR-pH 8.2	79/31	67.3±1.6	0	0.23±0.17	0.102±0.035	11.9±1.1	111.4±1.1
DP-Meth-pH 7.2	35	0.88±0.63	–	0	–	97.2±1.5	–
DP-Meth-pH 8.2	96/83	83±12	4.72	0.21±0.17	0.49	1.53±0.44	106.2
L-IR-pH 7.2	98	86±16	–	0.84±0.73	–	17±10	–
L-IR-pH 8.2	98/102	81.6±8.1	98.4±2.5	1.270±0.058	1.80±0.39	2.0±2.8	0.62±0.10
L-SR-pH 7.2	107	72±12	–	0.76±0.44	–	7.6±9.1	–
L-SR-pH 8.2	98/102	85±35	104.8±6.5	0.62±0.29	0.591±0.011	21±28	1.86±0.17
L-Meth-pH 7.2	93	2.9±3.5	–	0	–	73.1±4.9	–
L-Meth-pH 8.2	93/102	1.9±2.3	74.9±19.9	0	1.072±0.065	104±10	7.6±2.9
AAFB-8-SR-pH 7.2	17	0	–	NC	–	66.9±3.6	–
AAFB-9-SR-pH 7.2	51	0	–	NC	–	89.3±5.3	–
AAFB-10-SR-pH 7.2	54	0	–	NC	–	105.0±1.9	–
AAFB-12-SR-pH 7.2	74	0	–	NC	–	NC	–
AAFB-14-SR-pH 7.2	70	0	–	NC	–	NC	–
Killed Microcosms							
L-K-Meth-pH 7.2	53	77.9±3.2	–	0	–	0	–
L-K-Meth-pH 8.2	53	87.08±0.14	–	0	–	0	–
AAFB-8-K-U-pH 7.2	154	71.1±4.3	–	0.82±0.15	–	6.6±1.3	–
AAFB-9-K-U-pH 7.2	149	71.2±1.5	–	0.80±0.17	–	4.24±0.38	–

AAFB-10-K-U-pH 7.2	154	64.8±3.9	–	0.667±0.011	–	2.54±0.35	–
AAFB -12-K-U-pH 7.2	155	79.8±17.4	–	0.496±0.063	–	3.268±0.060	–
AAFB -14-K-U-pH 7.2	155	77.5±5.8	–	0.425±0.062	–	5.8±1.1	–

[a] Uncertainties are standard deviations of replicate microcosms. [b] Abbreviations: Duck Pond (DP), Norman Landfill (L), Altus AFB (AAFB), unamended (U), killed with heat-treatment and antibiotics (K), iron reduction (IR), sulfate reduction (SR) and methanogenesis (Meth). [c] __, samples were not set up under these conditions. [d] NC, not calculated.

Table 4. Geochemical Properties of the Microcosms[a]

Microcosm ID	FeS (g FeS/L)	Weakly bound Fe(II) (g Fe/L)	Strongly bound (g Fe/L)	CrES (g S/L)	TOC (g/g solid)	Iron Minerals Detected by XRD[b]
Unamended Microcosms						
DP-U-pH 7.2	$(5.10\pm0.68)\times10^{-2}$	$(2.76\pm0.23)\times10^{-3}$	$(1.28\pm0.11)\times10^{-1}$	$(1.23\pm0.17)\times10^{-1}$	$(9.6\pm1.7)\times10^{-4}$	—[c]
L-U-pH 7.2	$(5.23\pm0.40)\times10^{-3}$	$(3.3\pm4.0)\times10^{-4}$	$(1.25\pm0.10)\times10^{-1}$	$(6.40\pm0.72)\times10^{-3}$	$(2.6\pm1.8)\times10^{-4}$	—
AAFB-8-U-pH 7.2	$(1.45\pm0.15)\times10^{-1}$	$(2.04\pm0.57)\times10^{-3}$	$(1.49\pm0.46)\times10^{-1}$	$(8.4\pm1.1)\times10^{-2}$	$(2.27\pm0.52)\times10^{-2}$	—
AAFB-9-U-pH 7.2	$(4.66\pm0.87)\times10^{-2}$	$(4.2\pm1.9)\times10^{-4}$	$(8.8\pm5.0)\times10^{-2}$	$(7.5\pm1.6)\times10^{-2}$	$(2.30\pm0.68)\times10^{-2}$	—
AAFB-10-U-pH 7.2	$(6.9\pm3.8)\times10^{-2}$	$(2.42\pm0.54)\times10^{-3}$	$(1.08\pm0.66)\times10^{-1}$	$(8.7\pm2.5)\times10^{-2}$	$(1.9\pm1.1)\times10^{-2}$	—
AAFB-12-U-pH 7.2	$(2.9\pm1.5)\times10^{-2}$	$(1.43\pm0.28)\times10^{-2}$	$(2.3\pm1.4)\times10^{-1}$	$(1.24\pm0.27)\times10^{-2}$	$(1.54\pm0.41)\times10^{-2}$	—
AAFB-14-U-pH 7.2	$(5.95\pm0.69)\times10^{-2}$	$(1.48\pm0.34)\times10^{-2}$	$(9.2\pm3.4)\times10^{-2}$	$(1.27\pm0.31)\times10^{-2}$	$(1.51\pm0.15)\times10^{-2}$	—
Amended Microcosms						
DP-SR-pH 7.2	0.385±0.049	$(1.325\pm0.074)\times10^{-3}$	0.349±0.084	$(9.8\pm1.6)\times10^{-2}$	$(2.58\pm0.67)\times10^{-3}$	Ge, Lep, Fer
DP-SR-pH 8.2	0.44±0.14	$(5.1\pm1.8)\times10^{-5}$	1.31±0.70	1.291±0.065	$(1.11\pm0.28)\times10^{-3}$	Ge, Lep
DP-IR-pH 7.2	$(1.15\pm0.19)\times10^{-2}$	$(3.898\pm0.071)\times10^{-2}$	0.214±0.038	$(3.18\pm0.49)\times10^{-2}$	$(1.85\pm0.34)\times10^{-3}$	Ge
DP-IR-pH 8.2	$(7.5\pm1.1)\times10^{-3}$	$(5.21\pm0.71)\times10^{-2}$	0.203±0.042	$(3.70\pm0.30)\times10^{-2}$	$(2.86\pm0.53)\times10^{-3}$	Ge, Lep
DP-Meth-pH 7.2	$(6.9\pm2.1)\times10^{-2}$	$(8.2\pm5.9)\times10^{-4}$	$(8.9\pm7.2)\times10^{-2}$	$(5.06\pm0.70)\times10^{-2}$	$(1.8\pm1.5)\times10^{-3}$	Ge, Lep, Fer
DP-Meth-pH 8.2	$(5.45\pm0.77)\times10^{-2}$	$(4.7\pm1.3)\times10^{-4}$	$(6.8\pm2.3)\times10^{-2}$	$(3.81\pm0.64)\times10^{-2}$	$(1.76\pm0.35)\times10^{-3}$	Ge
L-SR-pH 7.2	0.223±0.022	$(5.68\pm0.47)\times10^{-3}$	0.71±0.10	0.431±0.024	$(5.8\pm1.1)\times10^{-4}$	Ge
L-SR-pH 8.2	0.885±0.028	$(1.3355\pm0.0012)\times10^{-3}$	1.085±0.036	$(7.2\pm1.6)\times10^{-2}$	$(8.6\pm2.2)\times10^{-4}$	Ge, Lep, Fer, Mgh, Mk
L-IR-pH 7.2	$(3.328\pm0.095)\times10^{-3}$	$(9.5\pm1.7)\times10^{-3}$	0.375±0.071	$(6.2\pm2.6)\times10^{-3}$	$(1.32\pm0.74)\times10^{-4}$	Lep
L-IR-pH 8.2	$(2.63\pm0.26)\times10^{-3}$	$(3.46\pm0.12)\times10^{-2}$	0.158±0.018	$(6.22\pm0.19)\times10^{-3}$	$(3.2\pm2.2)\times10^{-4}$	Ge, Lep, Fer
L-Meth-pH 7.2	$(1.85\pm0.13)\times10^{-2}$	$(3.7\pm2.3)\times10^{-3}$	$(7.9\pm4.8)\times10^{-2}$	$(1.06\pm0.31)\times10^{-2}$	BDL[d]	Ge, Lep
L-Meth-pH 8.2	$(1.85\pm0.14)\times10^{-2}$	$(2.64\pm0.11)\times10^{-3}$	$(8.94\pm0.81)\times10^{-2}$	$(9.3\pm2.3)\times10^{-3}$	$(1.20\pm0.25)\times10^{-4}$	Ge, Lep
AAFB-8-SR-pH 7.2	0.170±0.093	BDL	0.132±0.082	$(4.65\pm0.57)\times10^{-2}$	$(5.5\pm2.2)\times10^{-2}$	—
AAFB-9-SR-pH 7.2	0.115±0.023	BDL	$(4.0\pm1.2)\times10^{-2}$	$(8.22\pm0.78)\times10^{-2}$	$(3.6\pm2.2)\times10^{-2}$	—
AAFB-10-SR-pH 7.2	0.111±0.037	BDL	$(7.4\pm2.8)\times10^{-2}$	$(1.08\pm0.13)\times10^{-1}$	$(2.95\pm0.41)\times10^{-2}$	—
AAFB-12-SR-pH 7.2	0.141±0.099	BDL	0.20±0.15	$(4.4\pm1.4)\times10^{-2}$	$(2.3\pm1.2)\times10^{-2}$	Mag, Mgh, Aka
AAFB-14-SR-pH 7.2	0.159±0.013	BDL	$(2.41\pm0.35)\times10^{-2}$	$(2.07\pm0.31)\times10^{-2}$	$(1.57\pm0.40)\times10^{-2}$	Mag, Mgh, Aka

[a]All measurements, except for weakly bound Fe(II), were done with freeze dried solids and the results were corrected by water content to yield values correct for wet solids. [b] Aka: akaganeite, Fer: ferrihydrite, Ge: goethite, Lep: lepidocrocite, Mag: Magnetite, Mgh: maghemite, Mk: mackinawite (Siivola and Schmid (2007); [c]—, XRD analysis was not performed for this condition. [d] BDL, below detection limits of approx. 8×10^{-6} g/L. Uncertainties are standard deviations of triplicate samples from the same microcosm.

Table 5. Results of Geochemical Analyses Before and After Heat Treatment.

	DP-IR-pH 8.2 (g/L)		AAFB-8-SR-pH 7.2 (g/L)	
	Before	**After**	**Before**	**After**
FeS	0.112±0.014	0.1230±0.0046	0.292±0.046	0.357±0.087
Weakly bound Fe(II)	0.0199±0.0047	0.01253±0.00084	BDL[a]	BDL
Strongly bound Fe(II)	1.72±0.27	1.84±0.16	0.056±0.054	0.076±0.018
CrES	0.114±0.042	0.122±0.014	0.0247±0.0098	0.033±0.012

[a] Uncertainties are 95% confidence intervals of the mean of triplicate samples from the same microcosm.
[b] BDL means below detection limits.

Table 6. Physical-chemical and Kinetic Properties of Reactants and Products.

Compound	H_i [b] (Dimensionless)	$K_{i,ow}$ [c]	Solubility [d] (S_i, μM)	$K_{i,oc}$ (25ºC, L/Kg)	$k_{m,corr}$ (pH~7) ($Lg^{-1}day^{-1}$)[a]	$k_{m,corr}$ (pH~8) ($Lg^{-1}day^{-1}$)[a]
PCE	0.75	2.99		231.37	$(1.8\pm1.2)\times10^{-4}$	$(9.1\pm1.6)\times10^{-4}$
TCE	0.39	2.67		153.90	$(6.2\pm5.7)\times10^{-4}$	$(1.7\pm1.9)\times10^{-3}$
cis-DCE	0.34	1.86		52.33		
trans-DCE	0.40	2.08		69.62		
1,1-DCE	1.62	2.13		74.83		
VC	5.95	1.53		33.87		
Acetylene	0.93		1.86×10^{7}	4.35		
Ethylene	8.93		1.62×10^{6}	1.05		

[a] Calculated for the condition where f_{oc}=0. [b] H values are from Howard and Meylan (1997) and Mackay et al. (2006). [c] K_{ow} values are from Howard and Meylan (1997) and Mackay et al. (2006). [d] Solubility values are from Howard and Meylan (1997) and Yalkowsky and He (2003).

Table 7. Rate Constants, ε_{bulk} Values, and Apparent Kinetic Isotope Effects for Carbon ($AKIE_C$ values**)**

Compound	Conditions	k_{SA}[a](L m^{-2} d^{-1})	ε_{bulk} (‰)[b]	Mechanism of Reductive β-Elimination[c]	n[c]	x[c]	z[c]	$AKIE_C$[a]
PCE	FeS, pH 7	$(6.3 \pm 1.6) \times 10^{-5}$	-30.2 ± 4.3	1	2	2	2	1.0644 ± 0.0097
				2	2	2	1	1.0312 ± 0.0045
	FeS, pH 8	$(5.30 \pm 0.51) \times 10^{-4}$	-29.54 ± 0.83	1	2	2	2	1.0628 ± 0.0019
				2	2	2	1	1.03044 ± 000088
	FeS, pH 9	$(1.21 \pm 0.12) \times 10^{-3}$	-24.6 ± 1.1	1	2	2	2	1.0517 ± 0.0025
				2	2	2	1	1.0252 ± 0.0012
	BB1	NA[d]	-1.39 ± 0. 21	NA[d]	2	2	2	1.00278 ± 0.00043
	Sm	NA	-1.33 ± 0.13	NA	2	2	2	1.00266 ± 0.00027
	BDI	NA	-7.12 ± 0.72	NA	2	2	2	1.0145 ± 0.0015
TCE	FeS, pH 8	$(1.61 \pm 0.19) \times 10^{-4}$	-33.4 ± 1.5	1	2	1	1	1.0715 ± 0.0034
				2	2	2	1	1.0345 ± 0.0016
	FeS, pH 9	$(6.40 \pm 0.81) \times 10^{-4}$	-27.9 ± 1.3	1	2	1	1	1.0592 ± 0.0030
				2	2	2	1	1.0287 ± 0.0014
	BB1	NA[d]	-4.07 ± 0.48	NA[d]	2	1	1	1.0082 ± 0.0010
	Sm	NA	-12.8 ± 1.6	NA	2	1	1	1.0262 ± 0.0034
	BDI	NA	-15.27 ± 0.79	NA	2	1	1	1.0315 ± 0.0017

[a]Uncertainties are 95% confidence intervals calculated by propagation of error. For k_{SA} values, we assumed that the major error was from determination of rate constants, since errors from measurement of surface area and mass loading were typically less than 5%. [b]Uncertainties are 95% confidence intervals calculated from non-linear regression. [c]See text discussion. [d]NA means not applicable.

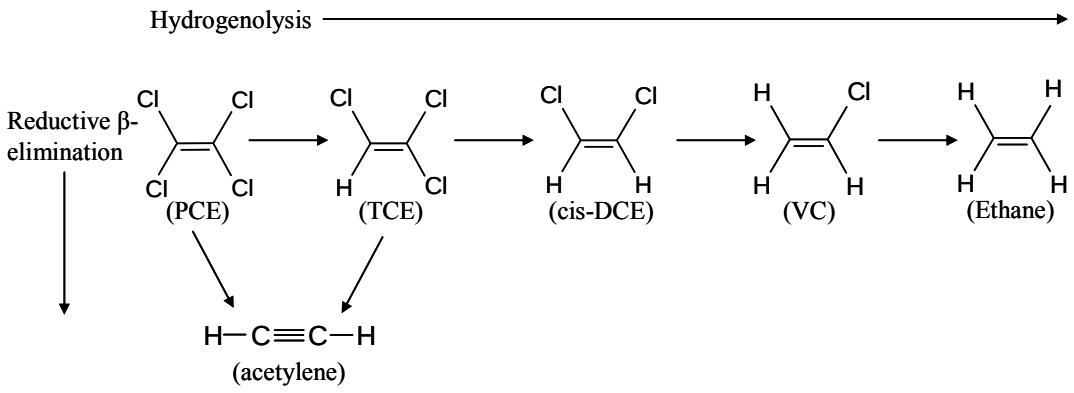

Figure 1. Pathways for Reductive Dechlorination of PCE and TCE.

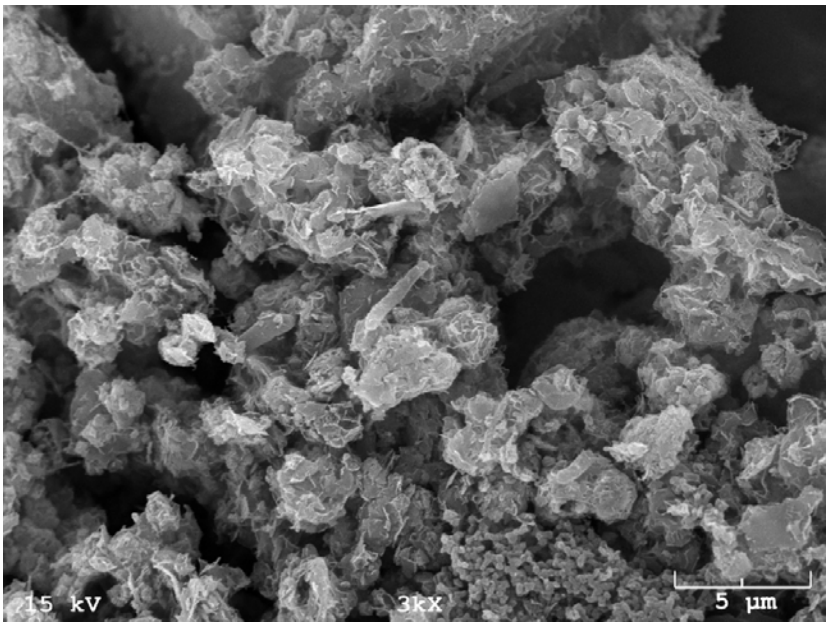

(a)

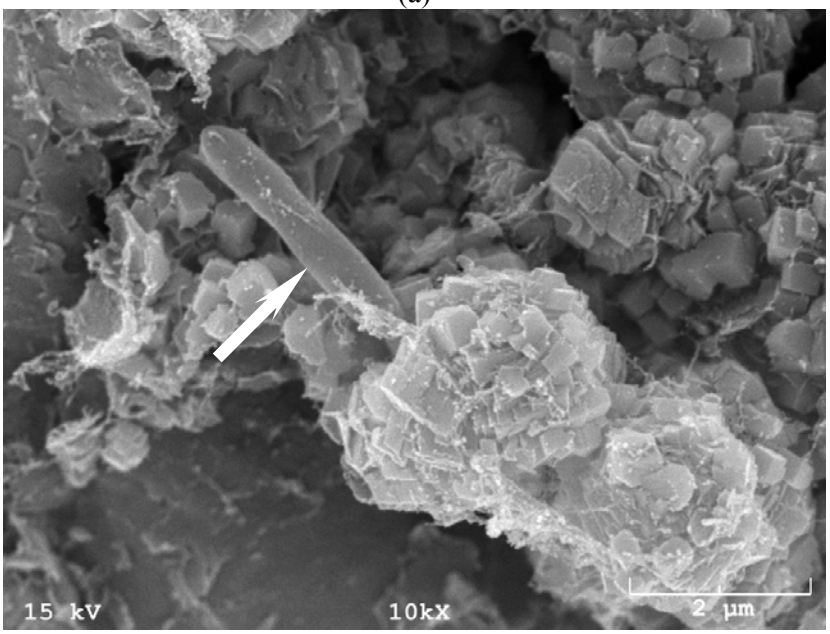

(b)

Figure 2. SEM Photomicrographs of Sediment from Sample DP-SR-pH 8.2. Cells Attached to the Surface of the Minerals are Indicated by Arrows. Crystalline Mineral Precipitates are Visible on the Right Side of Panel (b**).**

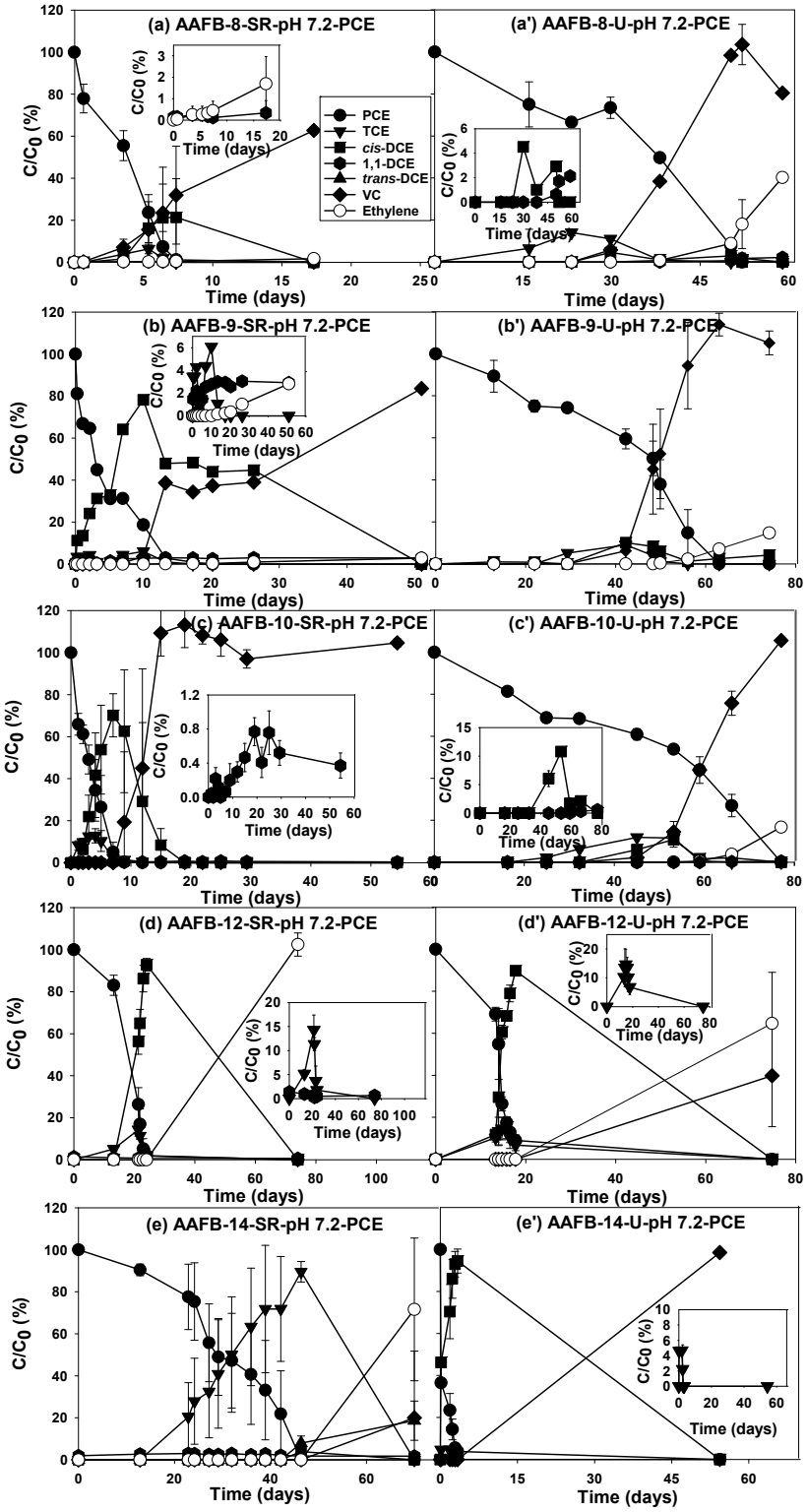

Figure 3. Normalized Concentrations of PCE and Reaction Products in Live AAFB Microcosms. Reactants and Products were Normalized by Dividing the Concentration at Any Time by the Concentration of the Reactant at Time Zero. The Insets Show Reaction Products with Low Concentrations. Error Bars are Standard Deviations of Triplicate Microcosms.

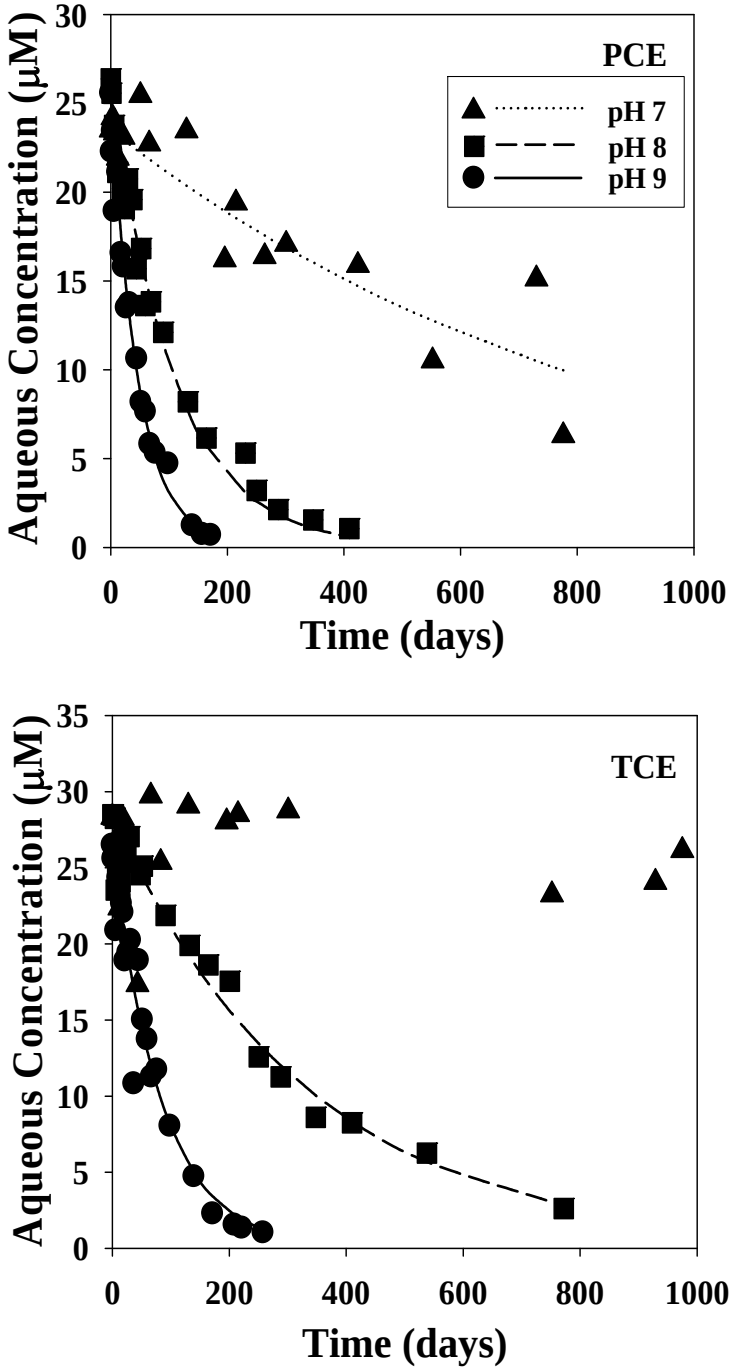

Figure 4. Abiotic Reductive Degradation of PCE and TCE in the Presence of FeS at Different pH values. Lines Represent a Pseudo First-order Model Fit.

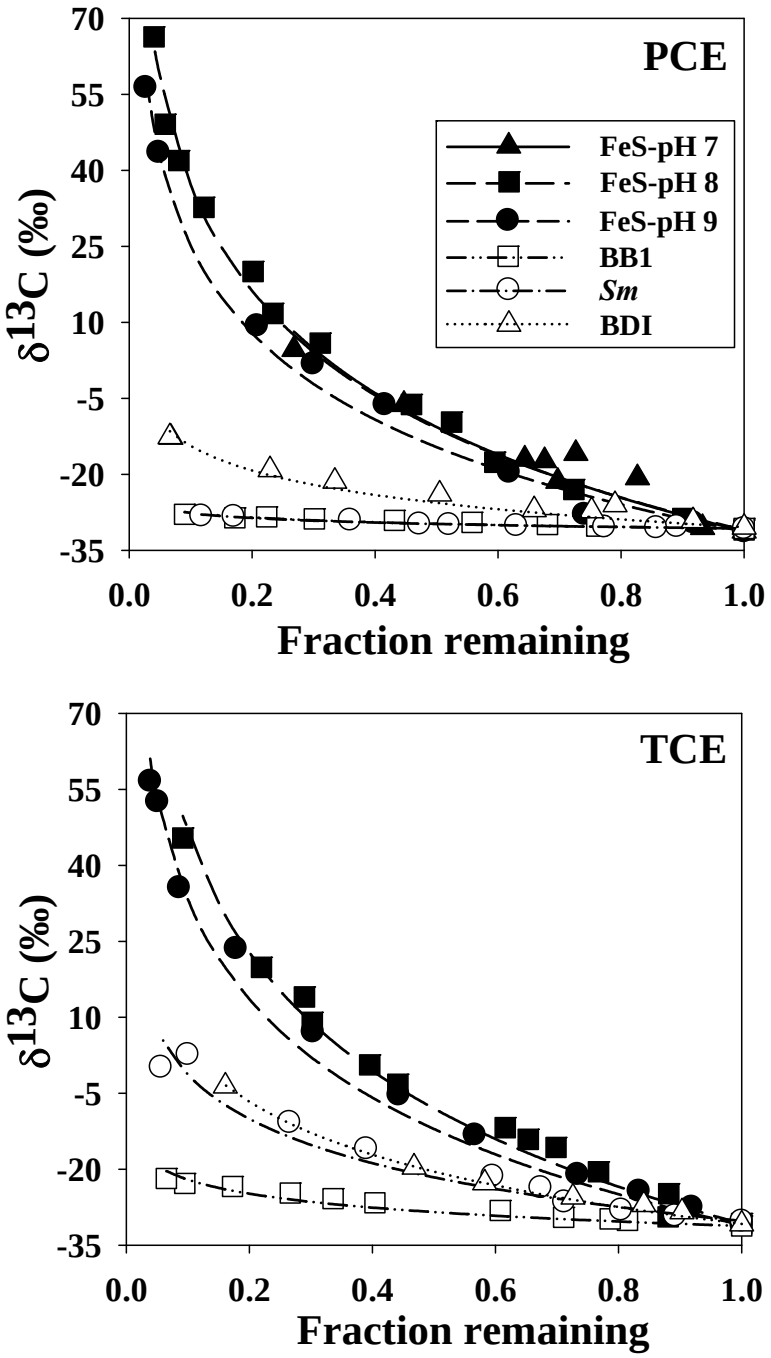

Figure 5. Isotope Fractionation During the Reductive Dechlorination of PCE and TCE by Abiotic and Biotic Microcosms. Lines Represent a Rayleigh Model Fit.

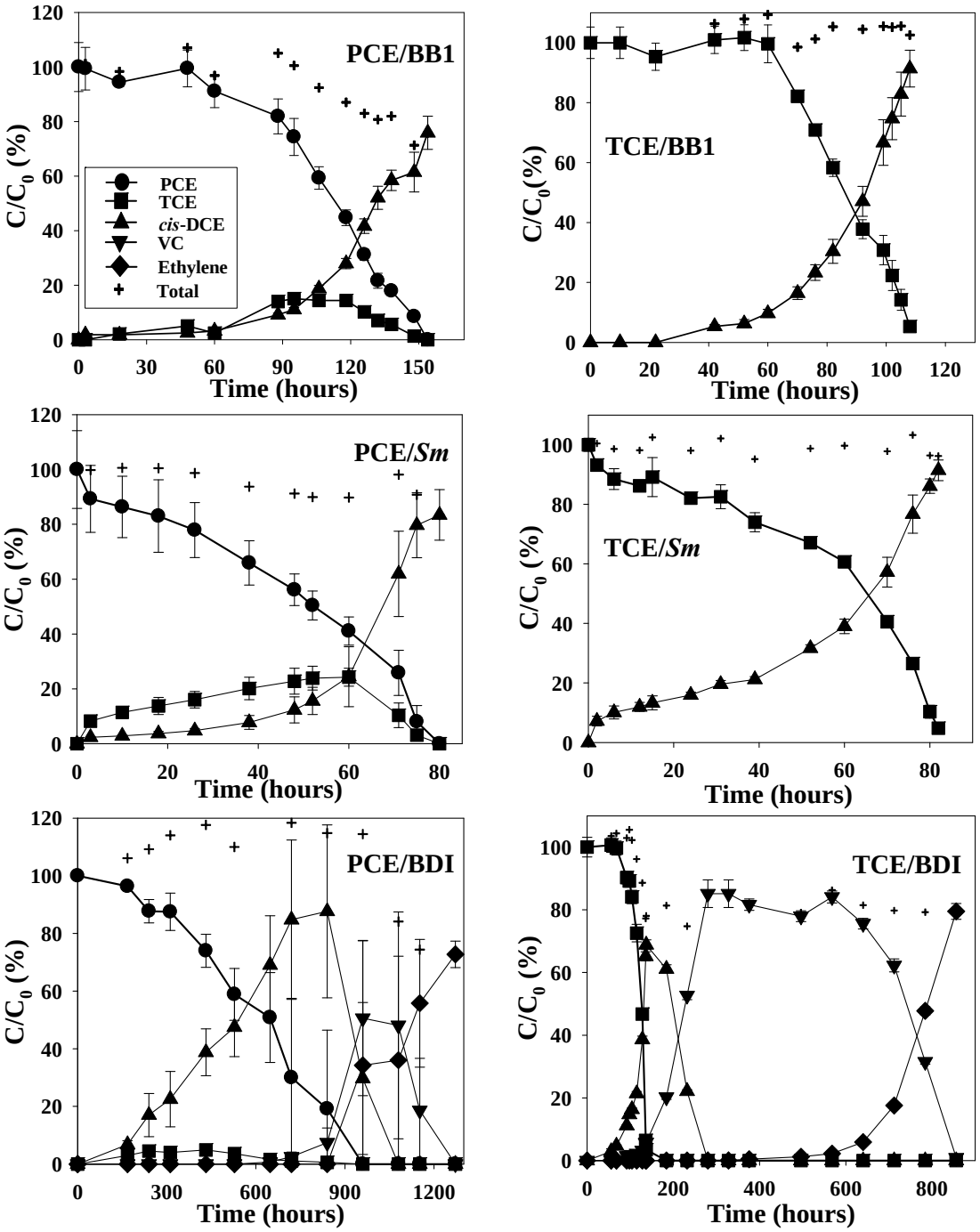

Figure 6. Microbial Reductive Degradation of PCE by (A) BB1, (B) *Sm*, and (C) BDI and TCE by (D) BB1, (E) *Sm*, and (F) BDI. Error Bars Represent 95 % Confidence Intervals for Mean Values from Three Microcosms.

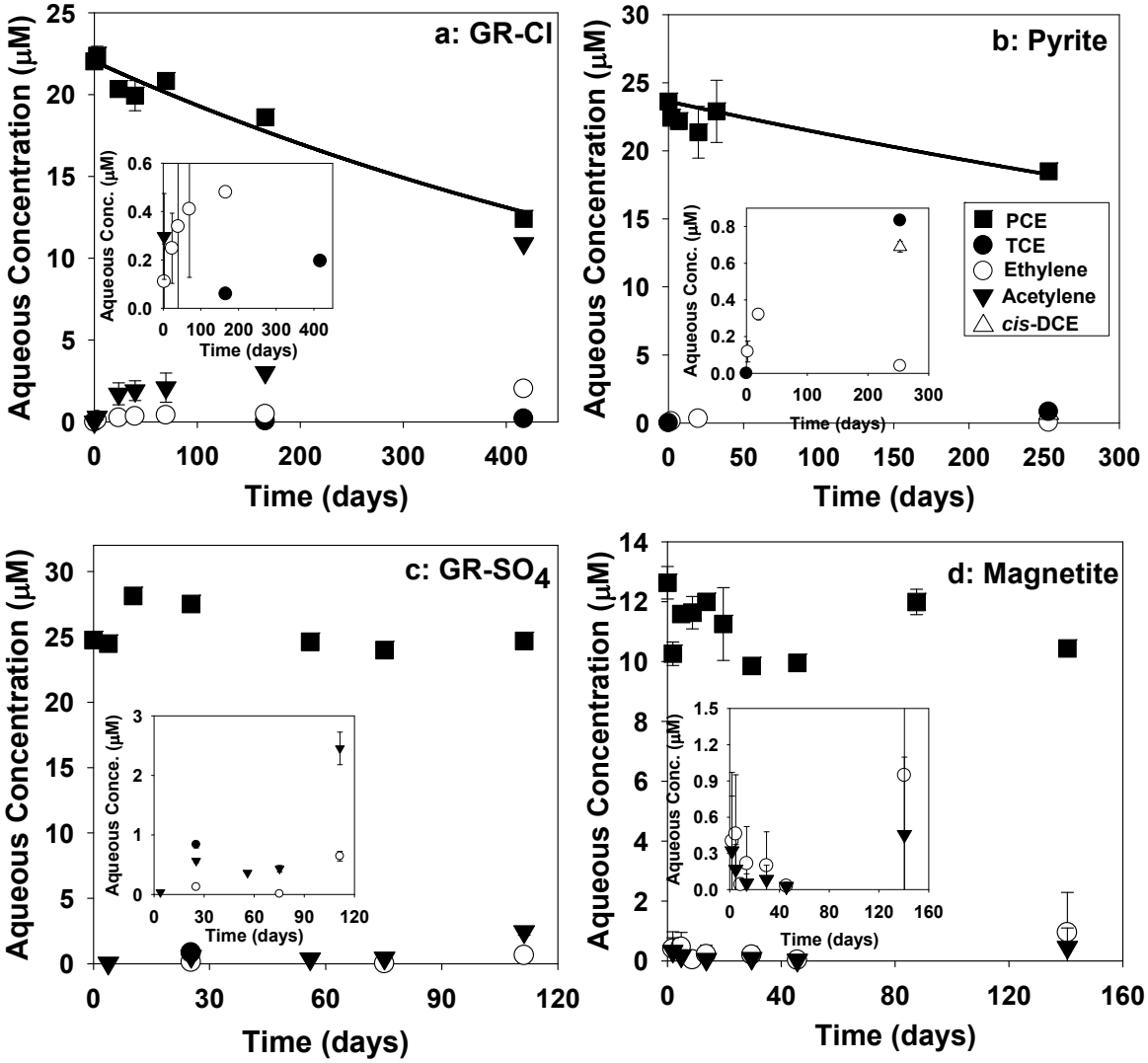

Figure 7. Abiotic Transformation of PCE in the Presence of Chloride Green Rust (GR-Cl**), Pyrite, Sulfate Green Rust (GR-**SO_4**), and Magnetite at pH 8. Lines Represent a Pseudo-first-order Model Fit. The Insets Show Reaction Products with Low Concentrations.**

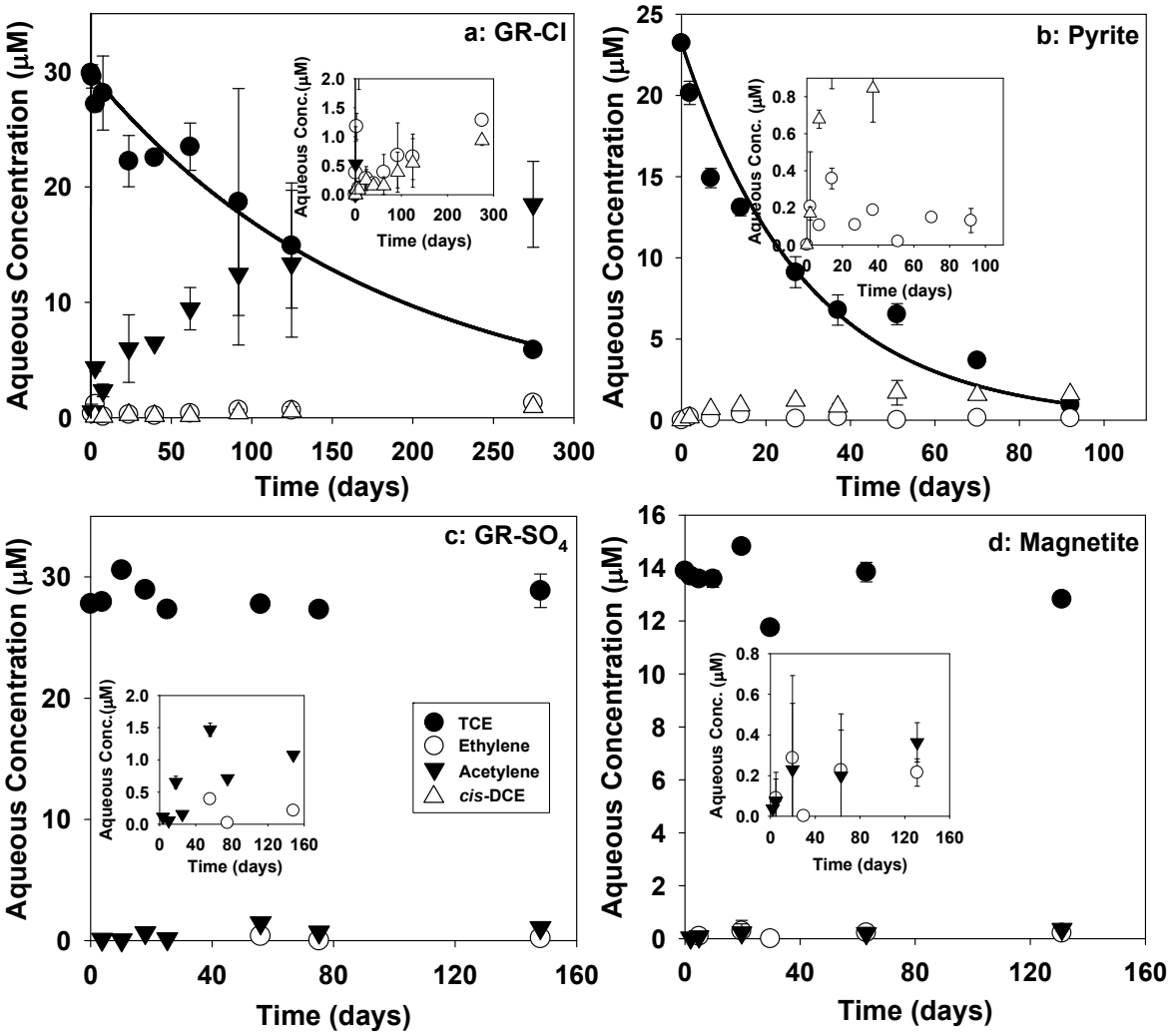

Figure 8. Abiotic Transformation of TCE in the Presence of Chloride Green Rust (GR-Cl**), Pyrite, Sulfate Green Rust (**GR-SO_4**), and Magnetite at pH 8. Lines Represent a Pseudo-first-order Model Fit. The Insets Show Reaction Products with Low Concentrations.**

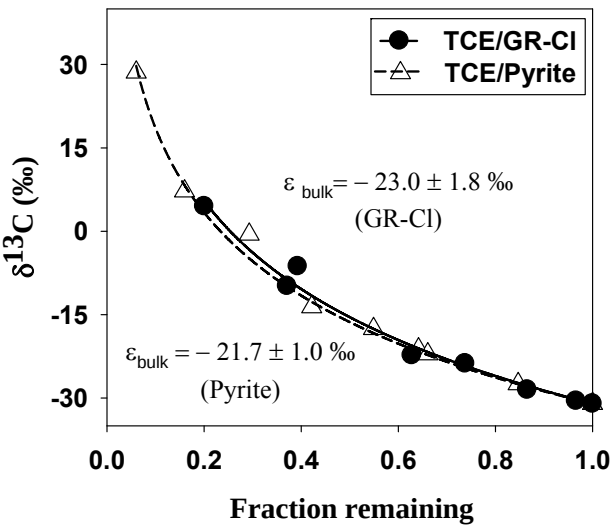

Figure 9. Carbon Isotope Fractionation During Abiotic Reductive Dechlorination of TCE by Chloride Green Rust (GR-Cl**) and Pyrite at pH 8. Lines Represent a Rayleigh Model Fit. Uncertainties are 95% Confidence Intervals Calculated by Nonlinear Regression.**

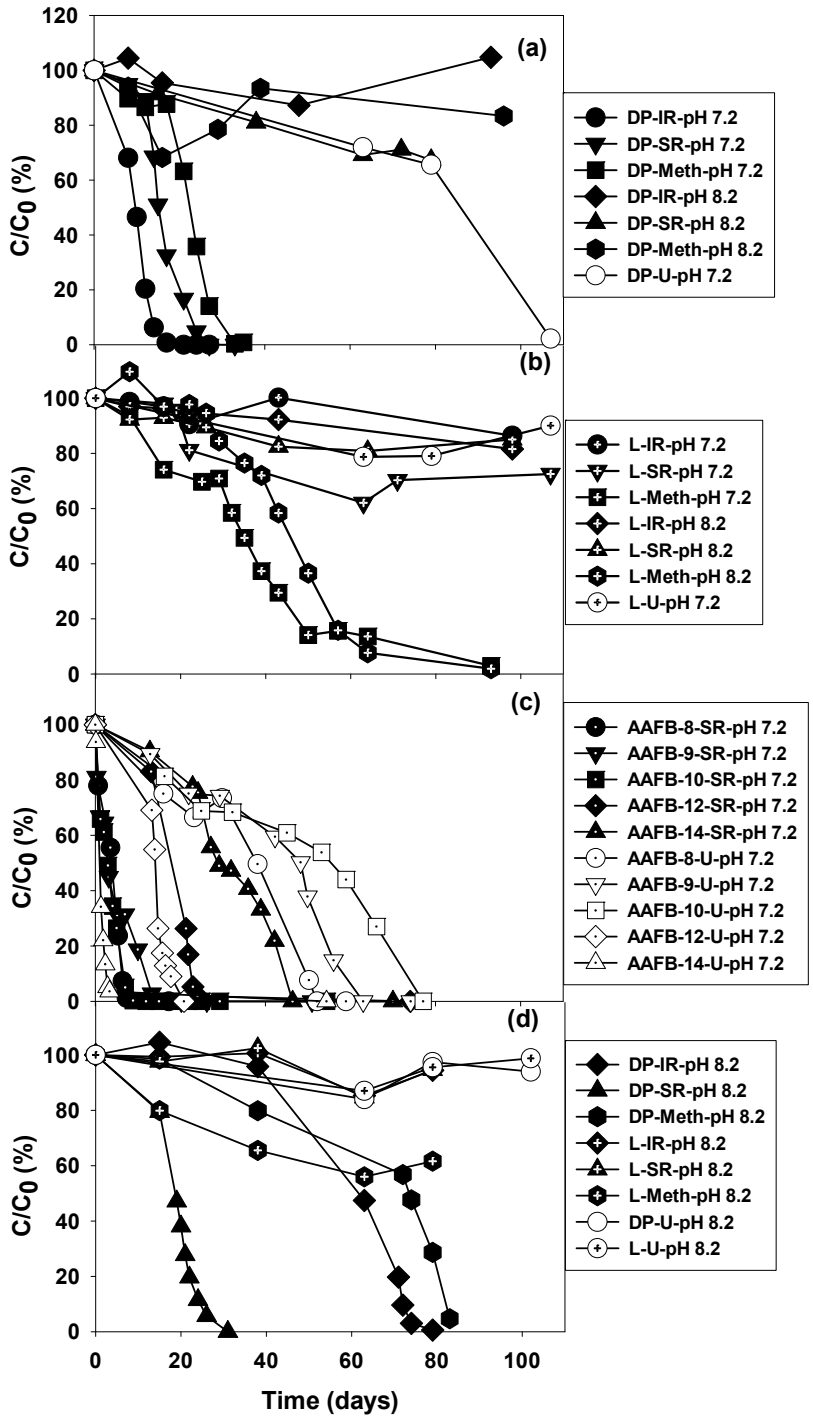

Figure 10. PCE Reductive Dechlorination in the Duck Pond (DP**) (**a**), Landfill (**L**) (**b**), and Altus AFB (**AAFB**) (**c**) Microcosms and TCE Reductive Dechlorination in Selected DP and L Microcosms (**d**), Under Iron Reducing (**IR**), Sulfate Reducing (**SR**), and Methanogenic (**Meth**) Conditions. Data Points are Averages of Samples from Duplicate or Triplicate Microcosms.**

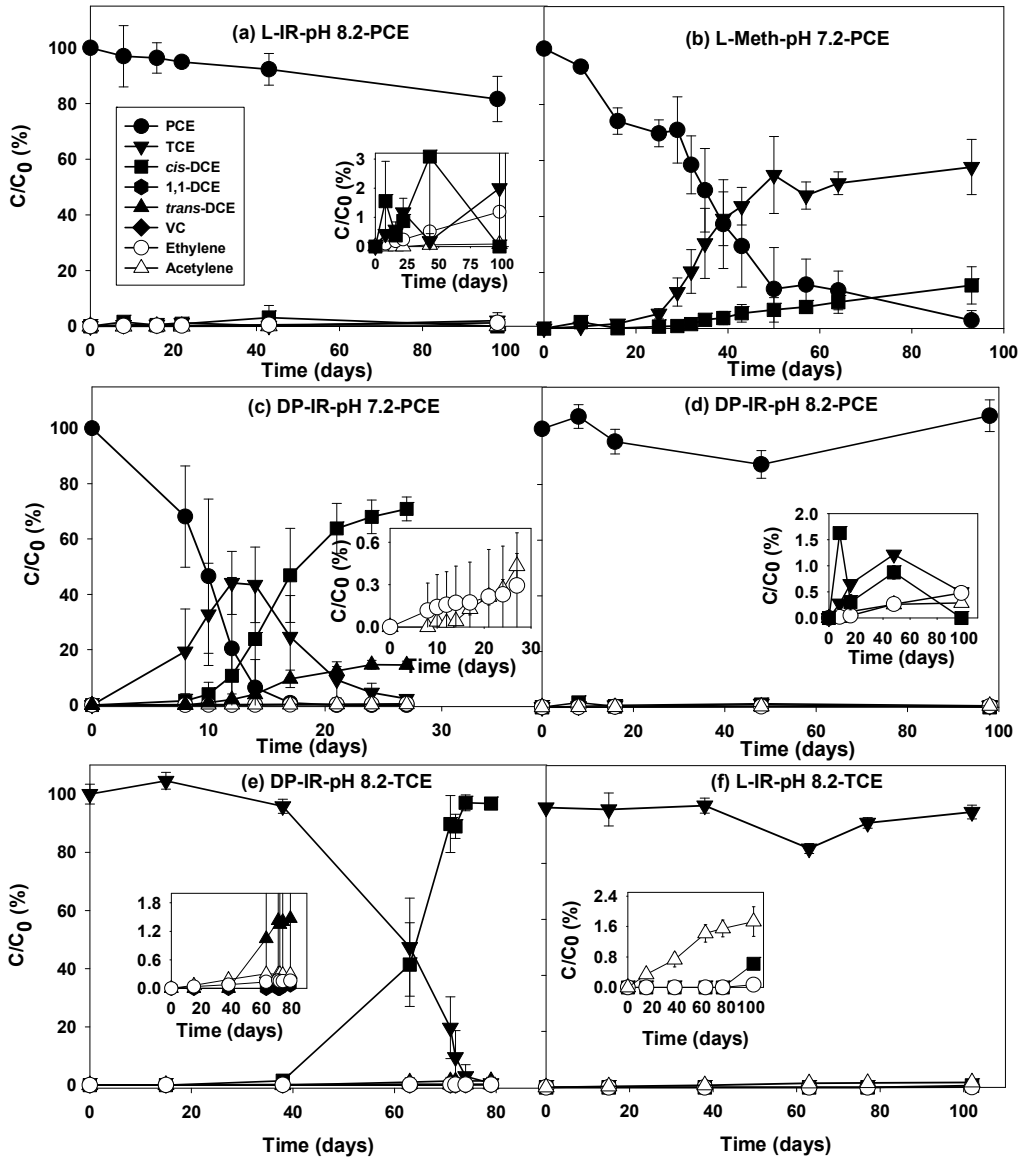

Figure 11. Normalized Concentrations of PCE (a-d**), TCE (**e-f**), and Reaction Products in Representative Microcosms. Reactants and Products Were Normalized by Dividing the Concentration at Any Time by the Concentration of the Reactant at Time Zero. The Insets Show Reaction Products with Low Concentrations. Error Bars are Standard Deviations of Triplicate Microcosms. To Better Show the Data Points, Parts of the Error Bars were Cut Off in the Insets for (**a**) and (**e**). In the Inset for (**e**), the Symbols for 1,1-DCE (**closed hexagons**) are Partially Covered with Ethylene (**open circles**) and Acetylene (**open triangles**).**

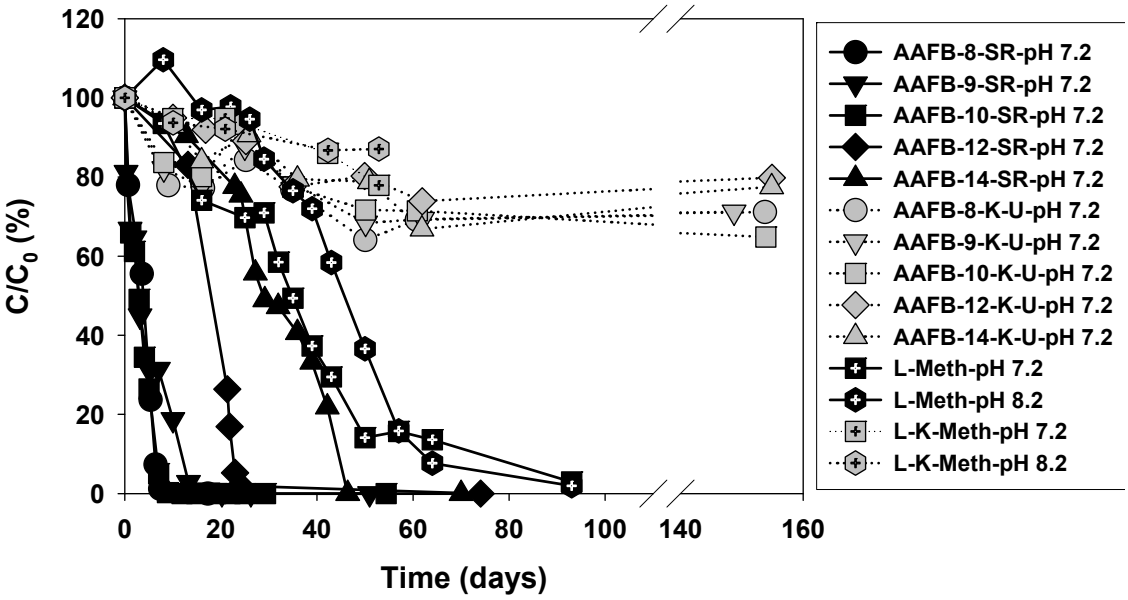

Figure 12. PCE Reductive Dechlorination in the Microcosms with (gray symbols**) and without (**black symbols**) Antibiotic and Heat Treatments.**

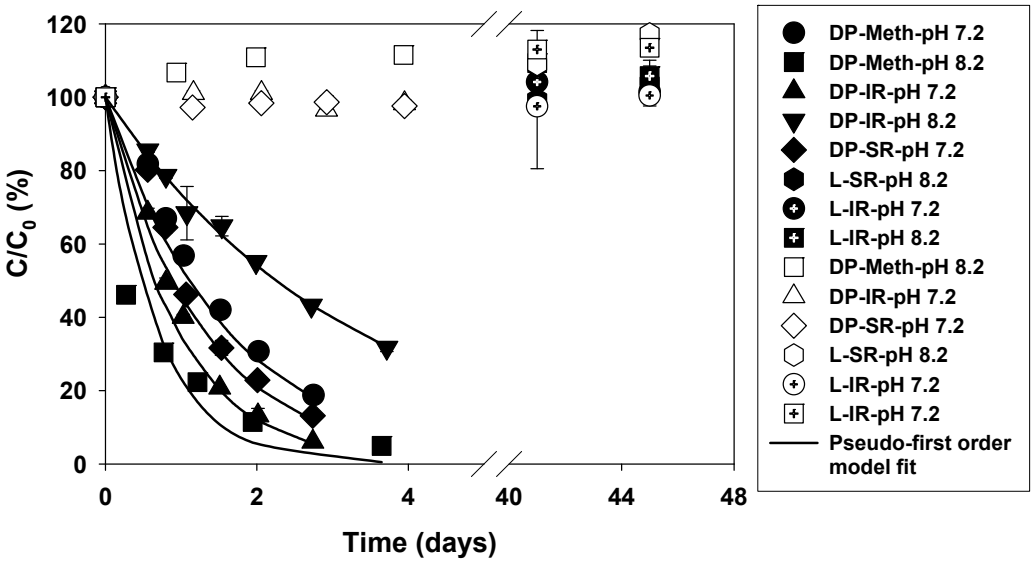

Figure 13. Acetylene Transformation in the Microcosms. Error Bars are Standard Deviations of the Means for Duplicate Measurements from the Same Microcosm.

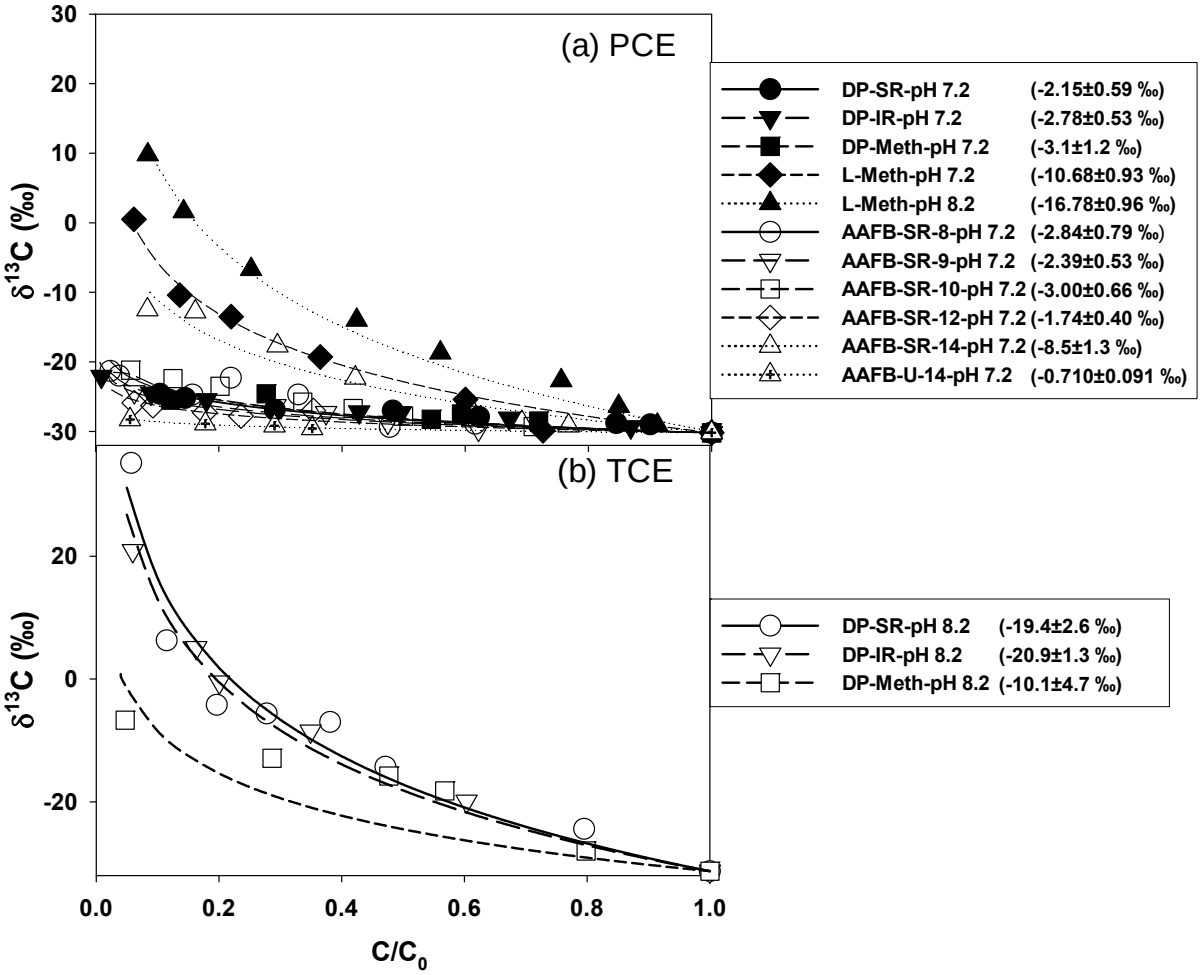

Figure 14. Isotope Fractionation of PCE (a) and TCE (b) in the Microcosms where PCE and TCE were Below Detection Limits at the End of experiment. The Values in Parentheses are Bulk Enrichment Factors (ε_{bulk} values). Data Points are Experimentally Measured Values, and Lines Represent a Fit to the Rayleigh Model. Uncertainties are 95 % Confidence Intervals.

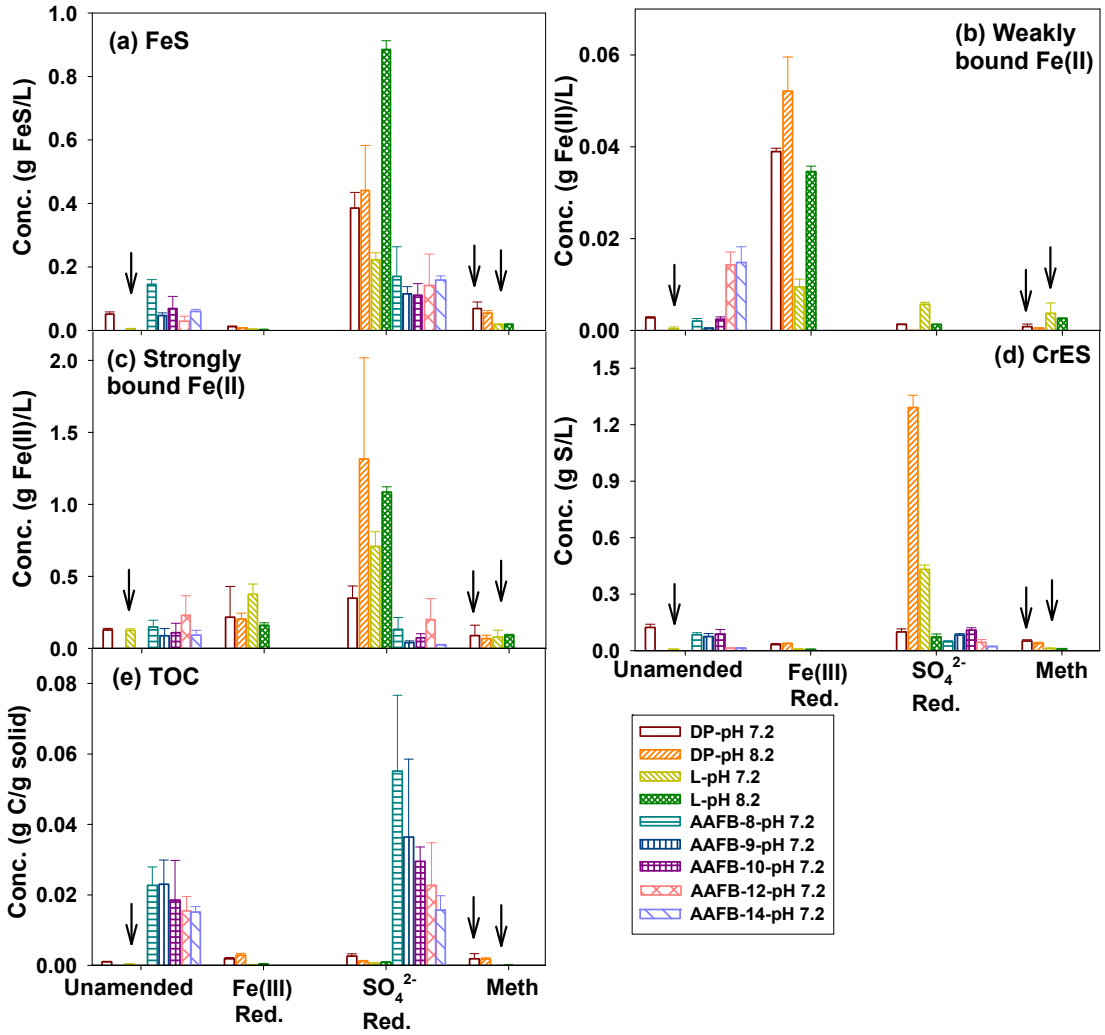

Figure 15. Geochemical analyses of the microcosms, including FeS (a**), weakly bound Fe(**II**) (**b**), strongly bound Fe(**II**) (**c**), chromium extractable sulfur (**CrES) (d) and TOC (e**), under unamended, iron reducing (**Fe[III] Red.**), sulfate reducing (**SO_4^{2-} Red.**) or methanogenic (**Meth**) conditions. Arrows indicate the microcosms where neither PCE nor TCE abiotic reductive dechlorination products were detected. Error bars are standard deviations of triplicate samples from the same microcosm.**

Appendix

List of Technical Publications

1. Articles in Peer-Reviewed Journals:

Published or in press

Liang, X., Dong, Y., Kuder, T., Krumholz, L. R., Philp, R. P., and Butler, E. C. Distinguishing Abiotic and Biotic Transformation of Tetrachloroethylene and Trichloroethylene by Stable Carbon Isotope Fractionation, *Environmental Science and Technology* **2007**, *40*, 7094-7100.

Dong, Y., Liang, X., Krumholz, L. R., Philp, R. P., Butler, E. C., The Relative Contributions of Abiotic and Microbial Processes to the Transformation of Tetrachloroethylene and Trichloroethylene in Anaerobic Microcosms. *Environmental Science and Technology* **2009**, in press, DOI: 10.1021/es801917p.

Liang, X., Philp, R. P., Butler, E. C. Kinetic and Isotope Analyses of Tetrachloroethylene and Trichloroethylene Degradation by Model Fe(II)-Bearing Minerals, *Chemosphere* **2009**, in press, DOI: 10.1016/j.chemosphere.2008.11.042.

2. Published Technical Abstracts:

Liang, X., Dong, Y., Kuder, T., Krumholz, L., Philp, R. P., and Butler, E. C. (2005), "Distinguishing abiotic and biotic reductive dechlorination of tetrachloroethylene by stable carbon isotope fractionation," SERDP/ESTCP Partners in Environmental Technology Technical Symposium & Workshop, 11/29/05-12/1/05, Washington, D. C.

Dong, Y, Liang, X., Kuder, T., Krumholz, L., Philp, R. P., and Butler, E. C. (2006), "Correlation of Geochemical Parameters with Rates of Abiotic Tetrachloroethylene (PCE) and Trichloroethylene (TCE) Reductive Dechlorination," SERDP/ESTCP Partners in Environmental Technology Technical Symposium & Workshop, 11/28/06-11/30/06, Washington, D. C.

Liang, X., Dong, Y., Kuder, T., Krumholz, L. R., Philp, R. P., Butler, E. C. (2007) "Identification of Reactive Geochemical Species Associated with Abiotic Tetrachloroethylene (PCE) and Trichloroethylene (TCE) Reductive Dechlorination in Well-Defined Microcosms," SERDP/ESTCP Partners in Environmental Technology Technical Symposium & Workshop, 12/4/07-12/6/07, Washington, D. C.